Università degli Studi di Ferrara

DOTTORATO DI RICERCA IN "SCIENZE DELL'INGEGNERIA"

CICLO XXXI

COORDINATORE Prof. Trillo Stefano

OPTIMIZATION OF HYBRID ENERGY PLANTS BY

ACCOUNTING FOR LIFE CYCLE ENERGY DEMAND

Settore Scientifico Disciplinare ING-IND/09

Tutore

Prof. Pier Ruggero Spina

_____

Dottorando

Dott. Hilal Bahlawan

_____

Cotutori

Prof. Mauro Venturini

Prof. Witold-Roger Poganietz

_____

Anni 2016/2018

Table of contents

Nomenclature

A	area	AB	auxiliary boiler
a	correction factor	ABS	absorption chiller
C	capital cost	AC	auxiliary chiller
c	coefficient	ASHP	air source heat pump
COP	coefficient of performance	CED	cumulative energy demand
E	energy	CHP	combined heat and power
EER	energy efficiency ratio	DP	dynamic programming
F	function	GWP	global warming potential
$fval$	fitness function value	GA	genetic algorithm
G	input or output flow of the life cycle inventory	GSHP	ground source heat pump
		HEP	hybrid energy plant
H	function	ICE	internal combustion engine
I	current		
Ind	Individual	ISO	international organization for standardization
k	time variable		
l	cost exponent	LCA	life cycle assessment
L	life cycle assessment scaling exponent	LCIA	life cycle impact assessment
N	last time step	LCI	life cycle inventory
P	power	load	ratio between actual power and nominal power
PE	primary energy consumption		
		ORC	organic rankine cycle
T	temperature	PV	photovoltaic
t	time	Sb	antimony
U	input or control variable	STC	solar thermal collector
V	volume	SOP	switch-on priority
W	work	TP	traditional plant
X	state	XSHP	generic heat pump
π	control policy		
η	efficiency	*Subscripts and superscripts*	
φ	incident radiant power	a	slope coefficient
ρ	density	amb	ambient
Acronyms		ABS	absorption chiller

IV

ASHP	air source heat pump	n	nuclear
av	average	nom	nominal
b	intercept coefficient	o	optical
best	best	op	operation
bio	biomass	out	outgoing
c	cooling	PV	photovoltaic panel
CHP	combined heat and power	ref	reference
cold	cooling	s	solar
cool	cooling	STC	solar thermal collector
diss	dissipation	sent	sent to the grid
el	electric	T	total
eq	equivalent	taken	taken from the grid
f	fossil	th	thermal
fuel	fuel	wa	wind
grid	grid	w	water
GSHP	ground source heat pump	XSHP	generic heat pump
in	entering	z	generic technology
max	maximum	*	optimal
min	minimum		

1. Introduction

According to the report of the *Impact Assessment of Energy Efficiency Directive* of the European Union [1], the energy used in the residential sector is responsible for approximately 40% of energy consumption and 36% of CO_2 emissions in the EU.

Governments of most nations around the world have pledged to limit carbon dioxide emissions and reduce primary energy consumption through an increase of efficiency in production, distribution and end-use and the utilization of renewable energy sources. In particular, the European Union has the goal of a 20% reduction of primary energy consumption by 2020 [2]: production, distribution and end-use of energy are identified as scopes of intervention. In order to achieve this goal, each Member State shall set an indicative national energy efficiency target, based on either primary or final energy consumption, primary or final energy savings, or energy intensity.

The Italian government set the goal of reducing the primary energy consumption in the residential sector of 103.8 GWh/year by 2020 which corresponds to 7.9% of the average annual energy consumption [3].

The expansion of the residential sector implies an increase of its energy consumption. Therefore, reduction of energy consumption and the use of energy from renewable sources in the buildings sector constitute important measures needed to reduce primary energy consumption and greenhouse gas emissions [4]. Reduced energy consumption and an increased use of energy from renewable sources also have an important part to play in promoting security of energy supply, technological developments and in creating opportunities for employment and regional development.

Moreover, the European Directive 2010/31/EU [5] "On the energy performance of buildings" requires national plans and measures from the Member States to increase the number of buildings which are more energy efficient with the aim of reducing both energy consumption and carbon dioxide emissions. In particular, all new buildings should be nearly zero-energy by 31 December 2020. In other words, buildings should be characterized by a high energy performance so that building energy demands can be covered to a very significant extent by energy from renewable sources produced on-site or nearby.

The dependence of renewable energy sources on weather and climate makes them intermittent and unpredictable energy sources [6]. Therefore, renewable energy systems such as wind turbines and solar thermal collectors will only be able to meet the energy demand for the time periods when the renewable energy sources (i.e. radiation and adequate wind speed) are available. Consequently, in

order to meet the energy demand during the periods when renewable energy is unavailable, an energy source is usually needed as a backup.

In addition to renewable energy systems, combined heat and power systems are broadly identified as friendly alternatives because of their energy-efficient and environmental benefits [7, 8]. In fact, these systems simultaneously produce heat and electricity, ensure high efficiency of energy use in buildings by recovering the waste heat and help to overcome energy related problems and environmental issues [9].

Energy production from engines is predictable and independent of climate. However, the use of these systems still have drawbacks such as environmental problems and high costs of operation and maintenance [6].

In view of the drawbacks related to both renewable and non-renewable energy sources, Hybrid Energy Plants (HEPs) can provide a further solution to overcome the limitations of a single source of energy. Generally, a HEP consists of a combination of two or more energy conversion systems which use different energy sources, that, when integrated, overcome the limitations that may be inherent in either [10]. HEPs have greater potential to provide higher quality and better reliability compared to a system based on a single source of energy.

A HEP is fed with a combination of different energy sources to cover building energy demands with the maximum efficiency. Several energy systems such as co-generators, electric chillers, absorption chillers, fuel cells, boilers, wind turbines, photovoltaic panels, solar thermal collectors, solar cooling systems and heat pumps could be integrated in a HEP depending on the availability of their primary energy resources.

In recent years, HEPs have gained a great deal of attention in scientific literature for the fulfilment of building's energy demands for primary energy saving and greenhouse gas emission reduction. Several authors have analyzed the combination of different technologies which use renewable, partially renewable and fossil energy sources. In [11], the authors studied the combination of a wood boiler, condensing boiler, heat pump, thermal and photovoltaic solar energy. Sontag and Lange [12] combined cogeneration with solar energy and wind energy. Moghaddam et al. [13] presented a model for scheduling a residential energy hub including a heat pump, boiler, absorption chiller, co-generator, electrical and thermal energy storage. A HEP composed of wind energy, solar energy, a fuel cell and a battery pack is designed in [14]. Lee et al. [15] studied an integrated renewable energy system composed of solar thermal collector, photovoltaic panel, ground source heat pump, electric chiller and gas fired boiler. Wu et al, [16] presented a study for the optimization of an integrated renewable

energy system composed of biomass co-generator, photovoltaic panel, heat pump and hot water storage. Mancarella [17] presented an overview of modelling approaches that are adopted to model multi-energy systems.

In this context, the integration of technologies powered by renewable energy sources may lead to increase the conversion efficiency and a significant reduction of the primary energy consumption and consequently the environmental impacts associated with the production of thermal, cooling and electrical energy demands of a building.

The promising energy and environmental benefits of HEPs for building applications are greatly dependent upon their design and operation strategy. In other words, due to the availability of different technologies, the key factors for the achievement of as high as possible primary energy saving and pollutants emissions reduction are the correct sizing of the HEP and the choice of the allocation strategy which allows the division of the energy demands among the various technologies composing the plant.

The sizing and operating optimization of a HEP must be based on the efficient matching between building energy demand and supply. Different environmental conditions determine different energy demands for space heating and space cooling. The integration with energy systems that use renewable energy raises additional problems during the analysis since they exhibit high geographical and temporal variability. Due to the number of variables involved and because of their multiple interrelations, the approaches and tools needed to model and to analyze the HEPs are of great complexity.

The optimal design of HEPs, which can be composed of renewable and non-renewable energy systems, is usually achieved by accounting for their environmental impacts during their useful life. However, this common approach, which only accounts for on-site environmental impacts, costs or primary energy consumption, may lead to burden shifting by ignoring the upstream life cycle of the HEP. In other words, in order to achieve an optimal design of the HEP, it is not sufficient to optimize on-site emissions because off-site emissions also need to be accounted for. In fact, energy production from renewable sources, such as photovoltaic panels, solar thermal collectors or wind turbines, is not associated with fossil fuel use and greenhouse gas emissions. However, a considerable amount of energy is consumed in the manufacturing, transporting and decommissioning of the different energy systems composing the HEP.

In other words, the energetic and environmental benefits associated with the use of HEPs should be compared with the impacts produced during the manufacturing, transporting and end of life phases by following a life cycle approach.

Given the complexity to deal with the number of variables involved, the multiple sources of energy that can be used (both renewable and non-renewable), the choice of energy converters (photovoltaic panels, solar thermal collectors, co-generators, heat pumps, etc…), the integration of Life Cycle Assessment (LCA) in system's design and the possible configuration and operation strategy that can be adopted, procedures ad guidelines are needed for the solution of such complex problem, i.e. the optimization of HEPs in order to achieve an optimal result in term of primary energy saving and consequently environmental impacts reduction over the life cycle of the plant.

1.1. Objectives of the thesis

Energy efficiency improvements lead to energy savings and produce direct environmental benefits. These benefits are achieved by two ways. First, by reducing the energy input requirements for the operation of the energy system and correspondingly the reduction of pollutants generated. Second, by considering the entire life cycle of energy resources and technologies, i.e. by reducing the energy consumption and environmental impacts during the different stages of the life cycle.

The aim of the research carried out was to develop original procedures and guidelines for the optimization of both sizing and operation of HEPs, which may be used for residential applications. The optimization is carried out with the aim of optimizing the exploitation of fossil and renewable energy sources throughout the life cycle of HEPs. In particular, the proposed research provides methods taking into account:

- The match between the energy demand and the energy supply in a residential building application;
- The variability of the conversion efficiencies, of the different technologies composing the HEP, as a function of external ambient conditions (i.e. ambient temperature and solar radiation);
- The variability of the conversion efficiencies of the energy systems as a function of the part load operating conditions;
- The variability of the efficiency as a function of the nominal capacity of the equipment, which is the power that the system must meet at design conditions;
- The nonlinearity associated with the optimization problem of HEPs;
- The quantification of the environmental impacts associated with the life cycle of the different energy systems and the integration of LCA in process systems design;

4

- The life cycle scaling problem, i.e. the non-linear relationship between the decision variables of the various technologies and the environmental impacts.

Therefore, the work of this thesis focuses on the development of original methods and procedures for the optimization of HEPs by accounting for the on-site and/or off-site energy consumption calculated throughout the various stages of the life cycle of the energy plant.

1.2. Outline of the thesis

Chapter 1 deals with HEPs in building with reference to the state of the art, then the main objectives of the work are summarized and presented.

Chapter 2 addresses general aspects of sustainable energy and environment and discusses energy efficiency and conservation issues. Chapter 2 also introduces the concept of multi-generation and hybridization and highlights their role in the transition away from fossil fuel based systems to cleaner and more sustainable future. An extensive review about: i) the latest models and techniques that are currently available to optimize the size and operation of HEPs, ii) the LCA of renewable and non-renewable energy systems for the quantification of off-site energy consumption and iii) the integration of LCA in process design and optimization, is also presented.

Chapter 3 focuses on the description of the different parts of the LCA methodology and deals with the act of setting up an LCA study as suggested by the International Organization for Standardization (ISO). In particular, it describes how to define the goal and scope of an LCA, how to construct a life cycle inventory model (i.e. how to draw a flowchart, collect data and perform the calculations), how to translate resource use and emissions into environmental impacts by conducting the life cycle impact assessment phase and finally how to analyze and present LCA results.

Chapter 4 presents energy technologies which can be used for the fulfillment of building's heating, cooling and electric energy demands. Renewable energy systems, partially renewable energy systems and systems powered by fossil fuel are taken into account. Chapter 4 also briefly presents, for each system, the working principles, the main characteristics and the different types available in the market.

Chapter 5, 6 and 7 are dedicated to the applications of methodologies presented in **Chapter 2** for the optimization of HEPs by accounting for on-site and off-site primary energy consumption. In particular, **Chapter 5** documents the development of a new methodology, called DP-DP method, for the optimization of both sizing and operation of HEPs. The optimization method is based on dynamic programming techniques. A case study consisting of a tower located in the north of Italy is considered to demonstrate the developed methodology. The HEP used for the fulfillment of the case study's

energy demands comprises a photovoltaic panel, a solar thermal collector, a ground source heat pump, an air source heat pump, a hot water storage, a combined heat and power system and an auxiliary boiler. The optimization problem is solved with the aim of minimizing only the on-site primary energy consumption (i.e. maximizing the energy efficiency of the different systems) without considering the entire life cycle of the plant. The effectiveness of the proposed methodology is demonstrated by a comparison with one of the most used optimization methodology, genetic algorithm.

Chapter 6 investigates the application of LCA methodology on energy systems which can be employed for residential applications. The methodology allows the calculation of the off-site primary energy consumption and environmental impacts, i.e. associated with the upstream life cycle of renewable and non-renewable energy systems. The second part also addresses the problem of LCA scaling of energy systems and presents a detailed procedure for the scaling of the life cycle inventory of the various systems and estimation of the environmental impacts of the considered technologies in a range of sizes. The scaling procedure allows to obtain impact curves which can be used for optimization purposes.

Chapter 7 describes the integration of LCA in optimization models used for the optimal design of energy conversion systems. The methodology is illustrated by an application to a HEP composed of a solar thermal collector, a ground source heat pump, an air source heat pump, air source heat pump, a hot water storage, a combined heat and power system, an absorption chiller, an auxiliary boiler and auxiliary chiller. The optimization problem is carried out by minimizing the primary energy consumption throughout the life cycle of the HEP. The on-site energy consumption is evaluated by using an optimization model based on a genetic algorithm and presented in Chapter 5, while the off-site energy consumption is evaluated by using the methodology of Chapter 6.

Finally, conclusions and future works are presented in **Chapter 8**.

2. A review on hybrid energy plants: optimization and life cycle assessment

Compared to traditional energy plants, HEPs are better options for construction of modern energy production plants that include economic, social and environmental benefits. The objective of this chapter is to help the readership obtaining an incisive overall understanding of issues related to optimization and LCA of HEPs. First the role of hybridization in energy efficiency improvement is discussed. Second, a comprehensive review of modeling, LCA, optimal sizing, energy management, operating and control strategies of HEPs is presented. The issue of LCA scaling and integration into systems design and optimization is also reviewed in the last section of this chapter.

2.1. Energy efficiency and sustainable development

Energy generation processes, such as generation of heating, cooling and electricity are polluting and harmful to the ecosystem and have serious implications for the environment. A strong relation exists between energy efficiency and environment since, an increase of energy efficiency normally leads to less resource utilization and pollution for the same services or products.

An increase of energy efficiency may help to overcome some of the limitations imposed on sustainable development by environmental emissions and their negative impacts. The efficient use of energy resources represents another factor that together with energy efficiency can reduce the energy demand and leading to the extension of the energy resources of a society.

The aim of sustainable energy is to design and develop sustainable energy systems, to substitute the damaging energy resources by more environmentally ones and to promote the use of energy resources in a sustainable manner, regardless of the nature of the resource (e.g. fossil fuels can be used, but the combustion must be completely clean by capturing CO_2).

Significant efforts have been made in energy-utilization efficiency improvement, resource recycling and reuse because of the limited nature of energy and other resources. Refuse and other solid wastes can be used to support fuel supplies, while recycling may extend the time of availability of the natural resources and is usually beneficial for the environment.

Several measures of energy efficiency and conservation, such as strict regulations and standards, incentive schemes to encourage energy saving investments, encouragement of cogeneration of heat and electricity and promotion of relevant research and development were applied. Indeed, the

improvement of energy efficiency provides a great potential for decreasing total world energy consumption and consequently energy-related environmental impacts. The potential for energy efficiency is significant during both energy production and consumption. Factors such as better energy efficiency, best technical-economical choice among options, adequate policy, proper energy management, recycling and energy recovery are the base of energy conservation practice. Energy conservation is the energy saving result of energy efficiency improvements and is indisputably beneficial to the environment, as a unit of energy not consumed equates to a unit of resources saved and a unit of pollution not generated (i.e., the production of thermal energy by using heat pumps contributes more than electrical heating systems to pollution reduction at power generation, and thus contributes to a better environment). Reduced energy consumption through energy saving programs is beneficial not only for consumers and utilities, but also for society as well. In particular, the reduction of primary energy consumption can lead to reduced emissions of greenhouse gases and other pollutants to environment [18].

Energy efficiency is a matter of better design, but at the same time is also a matter of economics. In other words, an energy system with higher energy efficiency is characterized by higher investment costs, while systems with lower energy efficiency have lower investment costs and higher primary energy consumption for the same useful effects; thus the life cycle costs are high. Therefore, for any particular energy system, in order to reduce the energy consumption, environmental impacts or/and costs, it is important to consider not only the useful life, but the entire life cycle of the system [18].

In order to encourage energy conservation in any society, energy policy has a leading role because it can create an adequate economic environment that eventually leads to savings and it may also impose regulations for proper energy management and promote recycling and energy recovery. Many countries have developed energy conservation programs to save energy, reduce the need for the new generation and to improve the environment. Moreover, in order to implement these programs in a beneficial manner, a comprehension of the type of the energy system used, the factors that influence the energy consumption and the type of end users is required.

2.2. Multi-generation and hybridization

A method to improve the efficiency of energy conversion technologies for better sustainability is multi-generation or poly-generation which refers to systems that fulfill several energy demands from one single or different kinds of primary energy sources. The purpose of this method is to improve the utilization of primary energy sources and reduce the wasted energy. In this way, less fuel is required to fulfill a given electrical and thermal energy demand in a single unit than is needed to generate the

same amount of both types of energy with separate conventional technologies (e.g., turbine-generator units and steam boilers).

Various options of multi-generating valuable energy products from a single primary energy source are developed. Some examples are co-generation of heat and power, tri-generation of power, heating and cooling, and multi-generation of hydrogen, oxygen, power, heating, cooling and desalination. Therefore, a multi-generation system combines several types of energy technologies and devices such as heat engines, heat pumps, refrigeration systems, hydrogen production technologies and desalination units. A gas turbine, for example, can be integrated with a solid oxide fuel cell to produce power and heat energy and improve fuel consumption. Compared to conventional systems for thermal, chemical and electrical energy production, the efficiency improvement and the corresponding decrease in fuel consumption by a multi-generation system, normally leads to large reductions in greenhouse gas emissions which can as large as 50 % in some cases.

The use of renewable energy resources is a key element of sustainable development and their integration could provide a cleaner energy system than conventional technologies. In fact, renewable energy resources have less environmental impact compared to other sources, they can provide reliable and sustainable supply, they cannot be depleted and they favor power system decentralization and enhance the flexibility of the system. Societies which are trying to attain sustainable development must devote much efforts to discover sustainable energy resources and to increase the energy efficiencies of processes utilizing the conventional and sustainable energy resources.

Renewable energy integration is considered to play a crucial role in sustainable energy and for the reduction of carbon emission in the future. Green energy from renewable energy source such as hydro, solar, wind, geothermal, wave and biomass can provide a more environmentally benign and sustainable society, increase energy security, reduce air, water and soil pollution and deforestation, reduce pollution-related health issues and contribute to a peaceful world by stopping conflicts among countries due to energy issues. Furthermore, the integration of renewable technologies in HEPs can facilitate and encourage the transition towards green energy production.

Figure 2.1a illustrates a tri-generation system, where the outputs are power, hot water and space heating. In addition, a heat storage is used in order to store solar energy in the form of thermal energy for overnight heating. The heat engine is a cogeneration system and it can be a steam power plant with steam extraction. This heat engine can be supplied with primary fuels (e.g., coal) other than solar radiation.
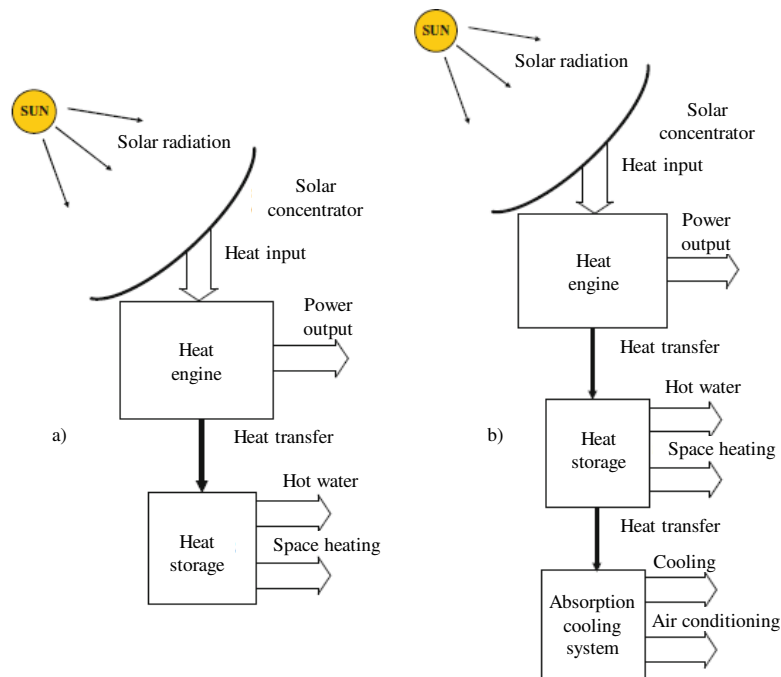
Fig.2.1. Examples of tri-generation and multi-generation energy systems (modified from [18]).

Other typical systems for cogeneration are gas-turbine cogeneration plant, diesel engine and geothermal cogeneration plant. Figure 1.1b shows an extension of the tri-generation system to multi-generation. In this case, power, heating and cooling are simultaneously produced from the system, where cooling is used for air conditioning and other purposes such as food preservation and heating is used for domestic hot water and space heating applications. The system in Fig.1b integrates several components such as the heat engine, heat exchangers, thermal storage unit and an absorption chiller. With such systems efficiencies of about 90 % can be reached.

The use of renewable energy systems alone may not ensure a stable, continuous and reliable energy production due to their stochastic and intermittent nature, they are dispersed and not easy to harvest. HEPs are one way to produce energy from intermittent renewable sources reliably. HEPs are combinations of two or more energy technologies, both renewable and non-renewable, or two or more primary energy sources for the same system, that when integrated, overcome limitations that may be inherent in either [19]. There are various types of HEPs, which use different combinations of thermal and electric devices such as cogeneration systems, electric chillers, absorption chillers, fuel cells, boilers, solar thermal collectors and photovoltaic panels [20].

Hybridization is a valuable method which can help transitioning away from fossil fuel based systems to cleaner and more sustainable technologies. Particularly in the short term, backing up renewable generation with conventional thermal electric production can actually help expand the use of renewable energy sources.

The use of HEPs can create market opportunities for the diffusion of energy systems that are not yet mature. For example, if a particular technology, such as a new type of fuel cell, is not yet efficient or reliable enough to produce energy as a stand-alone system, it may be suitable as an integrated component in a HEP in which other components can cover possible inefficient working during the production process.

2.3. Optimization of hybrid energy plants

The increase of energy demand and the urgent need for the reduction of environmental impacts calls for efficient and environmentally friendly energy systems. The use of renewable energy is widely considered as a promising alternative to conventional systems which are based on fossil fuels [21]. However, renewable energy is usually intermittent, unstable and is characterized by low energy density. To overcome the abovementioned drawbacks, the integration of various renewable energy sources and backup systems to form a HEP which is more reliable and environmentally friendly, has been proposed [22, 23].

In [24] the authors studied a hybrid solar-biomass system for space heating and hot water production. The studied system is composed of solar collectors, a hot water storage, an auxiliary biomass boiler and other space heating elements. The biomass boiler is used as backup system to fulfill energy demands at night or on cloudy days. It was found that, over a period of 6 months, solar collectors satisfy 52.9% of the total heating demand. Geothermal energy has been also identified as a reliable renewable energy resource for space heating and hot water production by means of ground source heat pumps. A hybrid solar-geothermal heating system is discussed in [25]. Prasartkaew et al. [26] investigate a solar-biomass hybrid cooling system which consists of a solar water heater, a biomass gasifier-boiler, an absorption chiller and a hot water storage. The boiler is used as an auxiliary system when the solar radiation is weak and the storage is used to store the energy collected by the solar heater. The absorption chiller is driven by the solar or biomass energy. A typical solar and biomass hybrid power generation system using a parabolic trough collector is presented in [27]. Soares et. al [28] presented a HEP based on solar and biomass energy. The heat provided by the parabolic trough collector or the biomass boiler is used to drive an Organic Rankine Cycle (ORC) used for power generation. In addition, a phase change material storage unit is integrated to stabilize the system and maximum the solar energy potential.

A key factor for saving as much primary energy as possible is the correct sizing of the various technologies of the HEP. Regarding this topic, several research papers have proposed optimization models. Barbieri et al. [29] developed a model to study the effect of different climatic scenarios on

multi-source energy plant sizing using a Genetic Algorithm (GA) with the goal of minimizing primary energy consumption.

The size of an HEP composed of a wind generator, a photovoltaic panel, a battery and an inverter is optimized in [30] by using an adaptive GA. An optimization model based on the use of a GA is adopted in [31] to optimize hybrid renewable energy system sizing. The system consists of photovoltaic panel, wind and cogeneration systems. Yousefi et al. [32] used a GA to optimize the size of a hybrid system consisting of a co-generator, photovoltaic panels, solar thermal collectors and an Internal Combustion Engine (ICE). In [33] a GA based system sizing method is developed, with the aim of minimizing initial total system costs. The system includes air conditioning equipment, PV panels, wind turbines, thermal energy storage and electrical energy storage. Sharafi et al. [34] proposed the particle swarm optimization approach for the optimal design of a hybrid renewable energy system and to minimize the total system cost, the unmet load and the fuel emissions. Wei et al [35] proposed a multi-objective optimization model to determine the size of small scale integrated energy systems. A multi-objective optimization approach using GA is employed in [36] to determine the optimal design variables of solar heating and cooling systems by minimizing the primary energy consumption and the annual cost of the system.

In residential applications, thermal and electrical demands vary significantly depending on the time of year and even on the time of day. Moreover, they are not synchronized. For these reasons, there is a need for a tool to manage and optimize the operation of HEPs. Regarding operating optimization applications, Dynamic Programming (DP) is widely used in dealings with multi-source energy systems. Marano et al. [37] applied a DP method to the optimal management of an HEP with wind turbines, PV panels and compressed air energy storage. Bianchi et al. [38] used DP for managing wind variability with pumped hydro storage and gas turbines and Facci et al. [39] optimized a tri-generation system operation strategy by means of a DP algorithm.

A linear programming algorithm is used in [4]0 in order to optimally plan the operation of a system composed of a co-generator system fed by biomass and an energy storage system. The optimization problem is solved with the objective of minimizing the overall net acquisition cost for energy. An optimal operating strategy was also considered for an integrated co-generator/solar utility [41]. Carpaneto et al. [42] developed a procedure for the optimization of unit commitment in a network with different power sources. In their work, they focus on minimizing the overall operational cost. In [43] an optimization model is built under the objective functions of energy rate, total operating cost and carbon dioxide emissions, in order to obtain the optimal operating strategy in a combined cooling,

heating and power system. Sakawa et al. [44] proposed GAs to approximate the solution of mixed 0-1 linear programming with the aim of optimizing the operational planning of a district heating and cooling plant.

Research articles have also been presented in literature to optimize the size and operation of HEPs. Evins [45] addressed the optimization of an energy plant's design and operating variables applying a multi-level optimization approach. The plant's design variables are optimized using a GA and its operational variables are optimized using Mixed Integer Linear Programming (MILP) techniques. A similar approach is used by the authors of [46]. They developed an optimization model with an evolutionary algorithm and MILP and split the model into two levels (i.e. master and slave). In [47], the design and operating optimization of distributed energy systems using MILP model is discussed. A tri-generation system consisting of a photovoltaic, a diesel co-generator engine, a reversible heat pump, a boiler, hot and cold reservoirs and a hybrid storage is investigated by the authors in [48]. The aim of their study is to find the optimal design and management strategy of the system by using a model based on the Particle Swarm Optimization (PSO). The optimization target is to minimize the overall costs, while the main constraint is the fulfillment of drinking water request and the heating, cooling and electric energy demands. The same authors of [48] have also performed in [49] the optimization of size and operation of a hybrid cogeneration system composed by a co-generative ICE, a photovoltaic panel, an auxiliary boiler, a pump as turbine and different energy storage units including a pack of batteries, a water reservoir and a hot thermal storage.

It can be deduced from the literature review presented above that a variety of methods has been developed to solve optimization problems [50]. The most prominent of these methods is linear programming, which has the disadvantage of its incapability to address nonlinearity whereas many problems are nonlinear [51]. Concerning the sizing and operating optimization problem of HEPs, most of these methods solve the problem by coupling two optimization methods such as evolutionary methods and linear programming techniques [52]. Despite the effectiveness of some of these methods, there are still some disadvantages such as long execution time, high memory usage and addressing the nonlinearity found in the objective function, constraints or characteristics of the HEP [53].

2.4. Life cycle assessment of energy systems

Environmental sustainability and energy conservation are some of the most challenging tasks faced by humanity. Different indicators can be used to evaluate the environmental performance of renewable and non-renewable energy systems. Such indicators can cover a part or the entire life cycle of the systems and can also be applied to compare them from an environmental perspective. They can

be used as a decision support to select the products which are more environmentally friendly and support decision makers for design and optimization purposes.

As can be noted from Section 2.3, for the optimization of HEPs, which can be composed of renewable and non-renewable energy systems, only the on-site energy demand is usually considered, whereas, in order to avoid burden shifting, the primary energy consumption associated with the upstream and downstream life cycles should be also accounted for, i.e. the benefits associated with the use phase should be compared with the impacts produced during the other phases of the life cycle of the plant. This, can be achieved by adopting a life cycle approach.

Different methodologies are suggested for the evaluation of the off-site environmental impacts of energy systems, i.e. the impacts produced during the manufacturing, transportation and disposal phases. One of the most effective methodologies for the quantification of the environmental performance of energy systems is LCA [54]. LCA is a tool for the evaluation of energy and environmental loads associated with the development of a product throughout its life cycle (cradle-to-grave) including extraction and processing of raw materials, manufacture, transport, use and finally disposal [55].

Many studies were focused on primary energy consumption as an indicator to analyze goods and services [56]. One of the indicators which are currently used to estimate the primary energy consumption for the entire life cycle of a product is the Cumulative Energy Demand (CED) [57, 58]. The CED accounts for the total primary energy (direct and indirect) which is used during the complete life cycle of a product or service [59, 60].

The CED indicator is a potentially convenient option when no enough information is available in the inventory analysis, i.e. its calculation does not require emission estimates and impact factors. In fact, the CED indicator can be transformed into the cumulative CO_2 which is an indicator widely used for environmental analysis [61]. Furthermore, different studies show a strong link between CED and some environmental impact categories like Global Warming Potential (GWP) and Abiotic Resource Depletion (ARD) [61, 62].

LCA studies of energy systems are usually performed by considering a specific size and by using data which are available in literature, e.g. from databases or measurements. The most relevant studies dealing with the LCA of energy technologies considered in this research are reviewed in the following.

For instance, Moore et al. [63] investigated the GWP and CED associated with the life cycle of electric storage hot water system, solar electric system, gas storage, gas instantaneous and solar gas

instantaneous system installed in Australia. They found that the electric storage hot water system has the highest environmental impact and primary energy consumption. Colclough et al. [64] used the cumulative energy and cumulative carbon consumption approaches to highlight the importance of adding a solar and a seasonal energy storage in achieving nearly zero energy heating in passive house buildings. The CED of renewable energy technologies such as wind, solar and PV systems was investigated in [65] with the aim of exploring the energy converter that tends to be environmentally preferable. Compared to solar and photovoltaic systems, the study [65] found out that wind turbines are preferable.

Various LCA studies were carried out on wind turbines for both onshore and offshore applications. Onshore wind power systems were investigated and analyzed in [66]. The aim of the study was to quantify the environmental loads for producing 1 kWh of electricity compared to other traditional power plants, i.e. fed with coal and natural gas. The results show that producing electricity in onshore wind power plants leads to a reduction in acidification, eutrophication, human toxicity and eco-toxicity and increases abiotic and ozone layer depletion. Huang et al. [67] evaluated the environmental impact and energy used within the life cycle of offshore wind turbines. Their analysis consisted of the evaluation of the CED, energy return on investment, energy payback time and environmental impact both with and without recycling. A lower impact and energy demand was found by recycling the waste materials at the end-of-life stage of the systems. Furthermore, the depletion of energy resources was estimated by Wagner et al. [68] for two wind turbines with 1.5 and 0.5 MW capacities by adopting the CED and energy yield ratio as the indicator of environmental impacts. It was found out that there is no big difference regarding the CED between the two types of wind power plants, while the variation in energy yield ratio does not exceed 10%. Another work about wind energy systems was presented in [69]. It deals with the analysis and reduction of the CED associated with the services provided to customers during the life time of wind turbines.

CHP systems are also popular and widespread because of their benefit of producing thermal and electric energy simultaneously. A number of studies was conducted in order to evaluate their environmental performance via LCA [70]. A micro-co-generator system based on alkaline fuel cell was investigated via LCA in [71]. They evaluated the environmental impacts produced from the manufacturing and disposal stages of an alkaline fuel cell and compared the results with other LCA studies of fuel cell technologies, concluding that an alkaline fuel cell has less environmental impacts than the oxide or phosphoric acid fuel cells. Moreover, Kelly et al. [72] exanimated the application of an industrial co-generator system via an energy and carbon LCA. They concluded that the

employment of industrial heat to generate electricity could lead to a significant reduction of carbon emissions and an improvement of energy efficiency.

Solar thermal collectors and photovoltaic systems are one of the most common renewable energy systems as they are always considered as a clean energy source considering that there are no environmental loads associated with the operation of these technology. However, some studies investigated the environmental impacts related to the manufacturing and disposal phase showing the importance of examining these life cycle phases. For instance, Ardente et al. [73] carried out an energy and environmental analysis on a passive solar collector unit finding that the primary energy consumption and the GWP throughout the life cycle of the system are 11.5 GJ and 721 kg CO2-eq, respectively. The system life cycle included the manufacturing, installation, maintenance and disposal phases. A more recent work [74] dealt with the investigation of a small size solar space heating and cooling system through an LCA methodology. Results were compared to a conventional system consisting in an electric heat pump finding that the solar heating and cooling system performs better than the conventional system by varying the useful life of the system from 10 to 20 years. The LCA of two types of solar systems, glazed and unglazed, were studied in [75], by highlighting that the energy and CO2 payback times of both systems are very low compared to their life service. In addition, they found that the impact of the disposal phase is lower than 2% in both cases.

The number of studies about photovoltaic systems is rising as a result of the increasing deployment of this technology in the energy sector. Problems about climate change and environmental impacts have led to the analysis of these systems as an efficient eco-friendly alternative compared to other existing non-renewable technologies. Several authors have conducted LCA studies about photovoltaic technologies. Most works attempt to evaluate parameters such as CED, energy payback time, GWP and eutrophication [76-78]. Moreover, a cradle-to-grave analysis of a PV plant was carried out by Desideri et al. [79] aiming at estimating the released environmental impacts. The studied plant has an energy payback time of about 4 years and a ratio of energy return on energy invested equal to 4.83. The main phase responsible for the environmental impacts was the installation phase, while the disposal and maintenance phases were environmentally less harmful.

Ground source heat pumps are another type of energy systems which have proven to be environmentally convenient. Koroneos and Nanaki [80] investigated a ground source heat pump and quantified the environmental impacts as the acidification effect, greenhouse effect and eutrophication over a life cycle of 25 years. Huang et al. [81] found that the principal impacts associated with the life cycle of a ground source heat pump are the global warming, acidification and eutrophication.

2.5. LCA scaling and integration in system's design and optimization

As reported in Section 2.3, the improvement of the efficiency of energy plants can be achieved by sizing properly the technologies employed for the fulfillment of building's energy demands. However, in order to achieve an optimal design of the energy plant, it is not sufficient to only minimize on-site primary energy consumption. In fact, off-site primary energy consumption has to be also accounted for, especially when considering renewable energy systems.

As mentioned in Section 2.4, an effective and widely used methodology, for the quantification of the off-site primary energy consumption, is LCA. Whereas, the on-site primary energy may be quantified by simulating the plant throughout its useful life. For the sizing optimization of HEPs which can be composed of renewable and non-renewable energy systems, the Life Cycle Inventory (LCI) of the considered technologies has to be available in a range of sizes, to calculate the off-site primary energy.

In spite of the achievements reported in Section 2.4 about LCA studies for some specific technologies and conditions, the lack of data remains a common problem which LCA analysts face in conducting their study about new or already existing energy technologies. In [82] a series of interviews with designers, product development managers and environmental managers was done to understand what is the main obstacle for conducting design optimization studies, and it was found that the scarcity of environmental information is a major barrier to design improvement. This problem is often overcome by applying linear scaling for the estimation of the LCI data or by using literature data that are not necessarily consistent since these are collected from different sources. With this approach, it is not possible to evaluate the effects of design changes, technology's size and future installation. Therefore, the integration of LCA in system's design to target the environmental impacts becomes an obstacle for decision makers.

Keoleian [83] addresses the problem of application of LCA to product design and development. In his study he presented practical issues to apply the LCA in a product design context, but without providing guidelines and indications on how to specifically use and integrate the LCA with optimization techniques. Gasafi et. al [84] presented an approach for the application of LCA in system design and decision making process. Their approach is based on a dominance analysis which can be performed to identify the subsystems in the process chains that contribute most to the overall environmental impacts of a system. The proposed procedure allows to obtain an environmental profile of the entire system. Then, the obtained profile is analyzed by designers which identify the critical processes of the supply chain and make a change of the product design that could reduce the environmental impacts. However, the method is hierarchical and is not possible to implement the

proposed approach in a computer-aided optimization tool. Lu et. al [85] developed an approach to life cycle design and evaluation with the aim of optimizing the functional, environmental and economic performance of a product. The proposed design process model was applied on a simple case study consisting of a "Z" section of a piping structure system. In order to evaluate the impacts of associated with the life cycle of the system, an evaluation table is constructed for each stage of the life cycle. however, the suggested model is based on qualitative analysis techniques, iterative and requires inventory data each time a change is made on the product design. In addition, the application of the proposed approach to design complex products such as energy systems is time consuming. Therefore, it could be not suitable for energy systems optimization. Stefanis et. al [86] presented a methodology to integrate LCA in the design of chemical process systems, considering a global environmental impact vector, and integrated these environmental criteria in the minimization of objective functions. However, for the implementation of their methodology, inventory data should be available for each process design option and operating conditions. The study [87] performed a multi-objective optimization of a nitric acid plant by linking economic models to environmental models. The aim of the study is to minimize environmental impact and maximize economic returns. Using the same multi-objective approach, authors in [88] combined LCA and economic studies on a biomass gasification energy production process. Azapagic and Clift [89] proposed an approach to apply LCA in a multi-objective optimization framework to calculate the trade-offs between economic and environmental objectives. In their study, they supposed that inventory data are sourced from a database supposing that inventory data are always available for any design option and size.

Regarding the optimization of HEPs in a life cycle perspective, several research papers were presented in literature. The sizing optimization problem of a HEP composed of a photovoltaic system, a wind turbine, a diesel generator and a battery used for residential building applications is presented in [6]. The optimization of the system is achieved by using a GA and considering only the operation phase of the system. The optimal design of a stand-alone photovoltaic-wind-diesel engine system with batteries storage is investigated by the authors of [90]. In their study, the optimization is conducted by using an evolutionary algorithm which minimizes the levelized cost of energy and life cycle emissions over the lifetime of the HEP. They found that considering the emissions associated with the manufacturing and decommissioning phases in the optimization process may affect the final configuration of the optimized HEP. Jing et al. [9] optimized the size of a building energy system with the purpose of maximizing its life cycle energy saving and pollutant emission reduction. The works mentioned above performed the optimization study of the energy plant by applying a linear scaling for the estimation of the impacts of each technology involved in the plant. However, it is well known that the relationship between the flows of the LCI and the size of a product follows a power

18

law [91], similarly to product cost scaling known as economies of scale [92]. Thus, there is a need for a more reliable approach.

Gerber et al. [93] made a comparison between the conventional LCA approach which use linear extrapolation to evaluate the impact at different sizes and the approach based on the analogy with cost scaling. They observed that the use of power law for the scaling and the use of cost exponents is more accurate than using linear scaling approach which assume a specific constant impact with system's size. Values of cost exponents for energy technologies, such as micro-gas turbine and Stirling based co-generator systems, absorption chillers and hot water tanks may be for example found in [94-96]. Authors in [97] investigated the whether the size of wind turbines affects the environmental profile of the generated electricity. In order to derive scaling factors and to evaluate the effect of the size on the environment, hey considered LCIs of 12 different onshore wind turbines and quantified the environmental impact of each system. The results showed that the bigger the turbine is, the greener the produced electricity is, concluding that scaling size affect the environmental profile. A similar work has been presented in [98] for the quantification of the scaling effect of energy systems such as biomass boilers and heat pumps on the environmental impact. They concluded that scaling exponents can be used for the quantification of the inventory data at different scales. Furthermore, they observed that scaling exponents vary between 0.5 and 0.8 and based on their analysis, they stated that the cost scaling exponent is a good indicator for the scaling exponent used in the LCA to quantify the inventory data of an equipment production. The same authors of [98] have explored the relationship between the size of energy conversion technologies such as boilers, engines and generators and variables such as mass and fuel consumption in [99]. The results showed that a non-linear behavior and scaling effect occur concluding power-law scaling relationships can be used to estimate key properties (i.e. the total mass of the equipment) relevant in early system design stage.

2.6. The novel contribution of this PhD thesis

Based on the literature review reported in this chapter, the main novel contribution of this work to the scientific literature is summarized in the following:

- A new DP based optimization method, called the DP-DP method, to solve both sizing and operating optimization problems of HEPs is proposed. As can be noted from the review reported in Section 2.4, the DP method is mainly used to solve energy management and systems scheduling problems. Unlike previous research, the proposed methodology extends the use of the DP method and attempts to apply it to solve both the sizing and operating optimization problems. The methodology is demonstrated by considering a case study and a comparison with a commonly

used optimization methodology based on GA techniques will be made. The optimization problem will be made on an energy-based criterion, i.e. with the aim of minimizing the on-site primary energy consumption over the simulation period, to demonstrate the effectiveness of the presented methodology. The proposed method does not require any supplementary evolutionary algorithms to solve the problem. Thus, the proposed method is fast, easy to implement and also addresses the nonlinearity associated with the characteristics of the plant. Compared to a GA based methodology, the DP-DP methodology allows better results in terms of primary energy saving and computation time saving.

- At present, technologies such as Solar Thermal Collector (STC), Photovoltaic Panel (PV), Combined Heat and Power (CHP), Absorption Chiller (ABS), Air Source Heat Pump (ASHP), Ground Source Heat Pump (GSHP), Pellet Boiler (PB) and hot water storage are widely used in residential applications. However, there is no comprehensive research dealing with the LCA scaling of all the mentioned systems. The LCA of renewable and non-renewable energy systems which can be employed for residential applications is investigated. Energy technologies, such as STC, PV, CHP, GSHP, ASHP, ABS, PB and hot water storage are considered. For each system a cradle-to-gate LCA is carried out. The considered impact parameter is the CED. Furthermore, the problem of LCA scaling is addressed and appropriate scaling factors and their relevance for calculating environmental impacts are presented. For each technology, the inputs and outputs flows of the LCI are extrapolated in a range of sizes relevant for residential buildings by using scaling power law relationships. The scaling procedure used in this work allows to obtain impact curves which can be used for optimization purposes. In addition, this work provides a dominance analysis and a detailed comparison of energy alternatives of different sizes from an environmental impact point of view.

- A general procedure for the integration of LCA into system's design and optimization. A case study consisting of a complex HEP, which is composed of STC, PV, CHP, ASHP, GSHP, ABS, Auxiliary Boiler (AB) and hot water storage, is considered to demonstrate the proposed approach. The optimization is carried out by taking into account of the non-linear LCI scaling of energy systems. The optimization is conducted with the aim of minimizing the primary energy consumed during the manufacturing, transportation and operation phases. The primary energy consumed during the manufacturing phase of the HEP is represented by the CED and is calculated by carrying out a cradle-to-gate LCA. The primary energy consumed during the operation phase is evaluated by simulating the system throughout one year. Two approaches are considered to assess the influence of the integration of LCA into the optimization process. The first approach consists

of solving the optimization problem by minimizing only on-site primary energy consumption, while in the second approach the on-site and off-site primary energy consumption considered by integrating the LCA into the optimization process.

3. Life cycle assessment methodology

Sustainability often leads authorities to include environmental considerations at the conceptual process design stage. The need to meet basic human requirements and aspirations, combined with the increasing population, is a main factor that drives toward successful implementation of sustainable design and development. In order to know which course of action, e.g. regulation or environmental adaption of industry, is more environmentally friendly, there is a need of assessment tools as well as structured procedure to think about the environment. LCA is a commonly method used to analyze the life cycle of a system, product or process from cradle to grave and is a key tool for identifying the best paths leading to sustainable development. The cradle to grave concept means that a system is tracked from the extraction of raw materials "cradle" from natural resources through production and use to the end of life or disposal "grave" [100].

The power of LCA is that it allows to avoid sub-optimal solutions that may be the result of the study of a partial life cycle of a system, because it considers the whole life of a product system. LCA is an engineering that studies technical systems and the potential changes in them and it enables:

- The quantification of environmental emissions to air, water and soil within each life cycle phase of a particular product;
- The evaluation of the environmental effects associated with a given product, process or activity;
- The assessment of the material and energy consumption to the local, regional or global community;
- The comparison between various technologies from an environmental point of view;
- The design of environmentally better energy products and systems.

A number of international standards has been issued by ISO for the application of LCA since 1997:

- ISO International Standard 14040, 1997: principles and framework;
- ISO International Standard 14041, 1998: goal and scope definition and inventory analysis;
- ISO International Standard 14042, 2000: life cycle impact assessment;
- ISO International Standard 14043, 2000: life cycle interpretation.

The standard ISO 14040 states that, "LCA is a technique for assessing the environmental aspects and potential impacts associated with a product by:

- compiling an inventory of relevant inputs and outputs of a product system;

- evaluating the potential environmental impacts associated with those inputs and outputs;

- interpreting the results of the inventory analysis and impact assessment phases in relation to the objectives of the study."

As mentioned before, LCA considers the whole life cycle of a product, starting from raw material extraction and acquisition, through production and manufacturing, to use and final disposal. Through such an orderly overview, it is possible to identify and avoid the shifting of a potential environmental burden between the stages of the life cycle or individual processes. Moreover, in LCA the analysis is structured around a functional unit which defines the studied reference flow. All other modelled flows, such as inputs and outputs in the LCI, are then related to the functional unit.
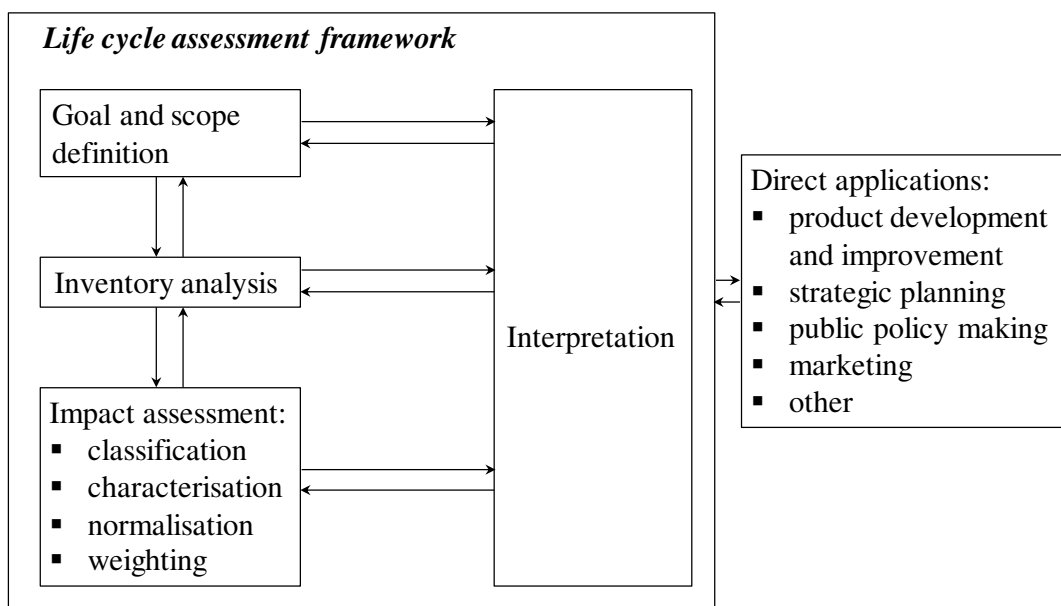
Fig. 3.1. LCA framework in the ISO 14040 [100].

Figure 3.1 shows the procedure of LCA defined by the international standard ISO. In particular, the framework of LCA includes four phases:

- the goal and scope definition;

- inventory analysis;

- impact assessment;

- interpretation.

The LCA methodology is characterized by an iterative approach. In other words, the single phases of an LCA are connected and the individual phases use the results of the other phases.

3.1. Goal and scope definition

The goal of a study, according to the ISO standard 14041, "shall unambiguously state the intended application, the reason for carrying out the study and the intended audience". All these things have to be defined within the context of the study, such as why to carry out the study and how and who is going to use the results.

Reasons for conducting an LCA study may for example be to support product development, to determine a strategic plan or for marketing purposes. The type of destined audience depends on the application and these may be product designers, authorities, managing directors, customers or the combination of these groups. Some examples on how to formulate the purpose of an LCA study are reported in the following:

- Discovering of the improvement possibilities in the life cycle of a particular product;
- Determination of the activities that contribute the most to the environmental impact associated with the life cycle of a particular product;
- Analysis of the environmental consequences associated with design modifications conducted to product;
- Assessment of the environmental consequences of using recycled raw material instead of virgin material for the manufacturing of a product;
- The choice between different products for a particular application from an environmental point of view.

While stating the goal of the study, it is important to define which specific products, product designs or process options are to be examined. For example, there is a difference between an LCA of an average product used in Europe and an LCA of a product produced by a specific vendor.

At the goal and scope definition stage, it is helpful to construct a first general flowchart of the system to be investigated. It is not necessary that the flowchart contains all the details of the product's life cycle, but it may be an advantage if it includes all investigated products in a comparative study.

Moreover, once the goal, the product and the flowchart have been decided, the functional unit must be defined. The functional unit represents the reference flow to which the all the modelled flows and the environmental impact of the system are related. The functional unit needs to be defined in quantitative term and the specific flow considered as reference flow should be indicated in the flow chart. When the system or product has more than one function (i.e., food provides nutritional benefits

but it also gives pleasure), one of the functions must be selected and represented by the functional unit.

In comparative studies, the functional unit must represent the function of the compared systems in a fair way. In some cases, the compared options may satisfy the function more or less well, or have functions in addition to the selected functional unit (e.g., the floor can be made of a parquet floor or wall-to-wall carpet, but the parquet floor is more aesthetically pleasant and the wall-to-wall carpet is less noisy). In such case, the functional unit must be defined so that a certain minimum level of quality must be fulfilled by the compared alternatives.

During goal and scope definition it is necessary to decide which environmental impacts to consider, because the choice of impact categories defines which inventory data to collect as not all emissions contribute to all types of impacts. Furthermore, the way of interpretation of results must also be decided.

The decision of which processes and activities are included in the LCA is determined by the definition of the system boundaries. In other words, the system boundaries define where the life cycle begin and end, i.e. where is the system's "cradle" and where is its "grave". Generally, the activities included in the flow model of the technical system, which represents the inventory model, are activities carried out by human being. Flows entering or leaving the technical system are also entering or leaving the human control. The boundary between the inventory analysis and impact assessment is defined by the boundary between technical system and the surrounding natural system. System's boundaries are usually defined during the goal and scope definition phase. However, the exact details of the system's boundaries can be decided during the inventory analysis, i.e. when enough information has been collected. Another important factor to decide within the system's boundaries is the inclusion or exclusion of the products disposal and waste treatment.

The system's boundaries must be specified in relation to surrounding natural system, geography and time. The limits of what is and is not included in technical system define the boundaries of the studied system. Figure 3.2 illustrates the different approaches that can be adopted to define the boundaries of a system.
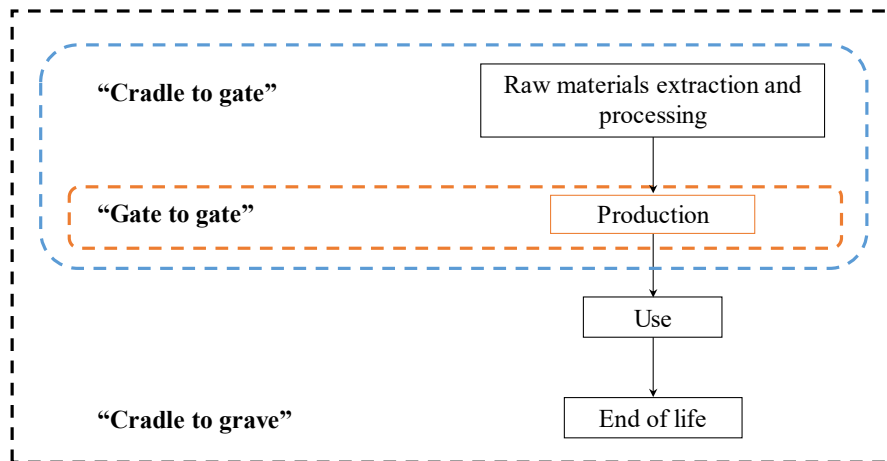
Fig. 3.2. Different approaches for the definition of system's boundaries.

The different approaches are defined as follows:

- Gate to gate: this option is the simplest approach where the analysis begins from the reception of the processed raw materials, ready to use, and ends at the production phase, when the product is ready to be consumed or received by the consumer. This kind of approaches are usually adopted when there is a need to study a specific unit process.

- Cradle to gate: in this case, in addition to the production process, the previous steps including raw material selection, extraction, processing and also the transportation steps that are needed between the different steps are considered. This approach includes more information compared to the gate to gate approach.

- Cradle to grave: in this approach, everything is included within the system's boundaries, starting from raw material extraction, through production, transportation and use, to the final disposal of the product.

According to the ISO standard, assumptions and should be described in the goal and scope definition phase. The assumptions described are the major ones and not on the individual data sets. Limitations such as the validity of the study for a certain geographical area or a certain time should also be stated.

Depending on the goal of the study, two different types of LCA can be used; accounting and change-oriented. The accounting type helps to assess and evaluate the environmental impact that can be associated with a product, service or activity, while the change-oriented type allows to compare the environmental impacts of a number of modelling changes. The choice of LCA type helps setting up systems boundaries and choosing the type of data to represent the system.

3.2. Inventory analysis

The inventory analysis consists of constructing a flow model for the technical system. the model only considers the flows which are environmentally relevant where mass and energy balance is set over the considered system. flows such as diffuse heat and emissions of water vapor are environmentally indifferent and therefore are not modelled. The model is usually modelled as a flowchart. A LCI analysis includes the following activities:

- Building of the flow model according to the system boundaries defined in the goal and scope phase;
- Collection and documentation of data for all the activities involved in the product system;
- Evaluation of the environmental impacts such as resource consumption and pollutant emissions, of the product system with reference to the functional unit decided in the goal and scope definition.

LCI is a cumulative and iterative process, because during the collection of data more is learned about the studied system and the decisions taken in the goal and scope phase muse be revised.

Flowchart construction: in the goal and scope definition, a first general flowchart is usually designed and principles for system boundaries and modelling requirements are decided. In the inventory analysis, the flowchart is extended and more details are added, pointing out all modelled processes and the flows among them.

Figure 3.3 shows an example of a first general flowchart defined in the goal and scope phase, related to a study on waste packaging options for a number of packaging materials. In particular, the goal is to evaluate and compare the environmental consequences of packaging waste by landfilling, incineration with heat recovery, material recycling and reuse.
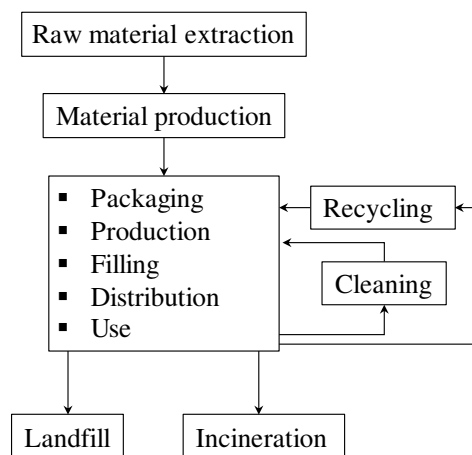
Fig. 3.3. General flowchart of packaging materials.

An example of a detailed flowchart developed during the LCI of aluminum is illustrated in Fig. 3.4. The detailed flow model shows the activities of all three options for packaging materials, i.e. landfill, incineration and recycling.

Multiple recycling loops (see Fig. 3.4) make the flowchart more complex. In practice, the complexity of flowchart may also depend on the industry structure, for example the petro-chemical industry is highly networked. Complex products which are composed of many different components also makes the flowchart like a tree with a large number of branches.

Fig. 3.4. Detailed flowchart of aluminum packaging material [100].

The collection of data: one of the most time consuming activities in LCA is the collection of data. In particular, the searching of data is more challenging than collecting them. Moreover, numerical data

representing the inputs to all modelled processes and the outputs need to be collected. Collected data must be descriptive, qualitative and consist of data on the amounts and types of:

- raw materials, energy consumption, ancillary inputs and other physical inputs such as land use;
- products and co-products;
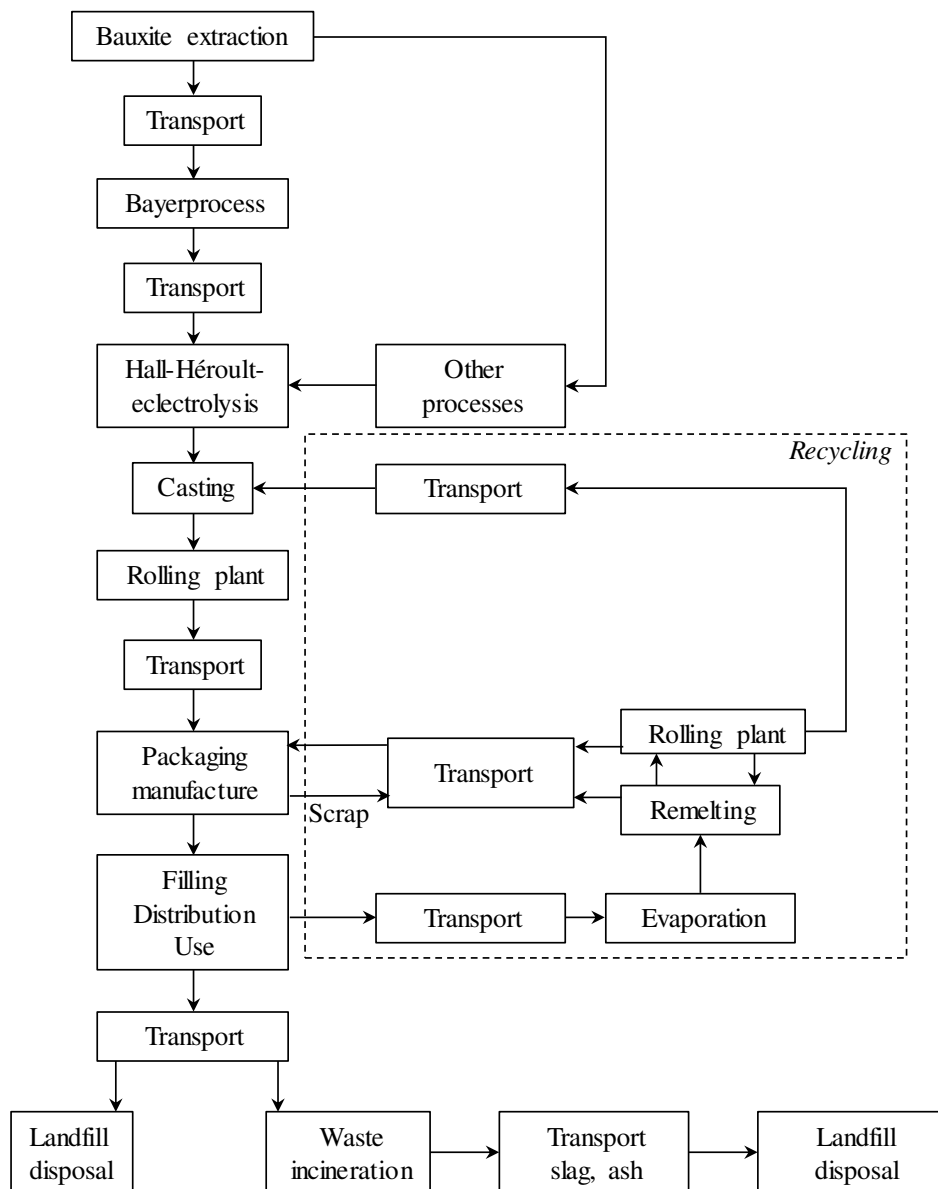- environmental loads such emissions to air, water and land.

Figure 3.5 illustrates an example of a process described by different categories of numerical data.
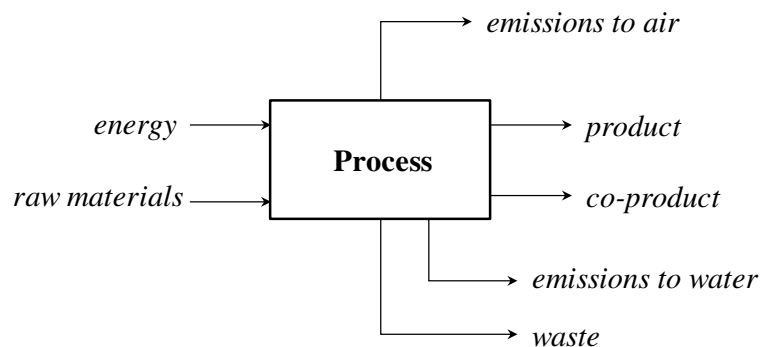

Fig. 3.5. Description of a process and typical collected data.

Regarding the collection of data for transports, information about distances between the different processes and routing data are typically needed. Each mode of transport is characterized by energy use and emissions. Furthermore, information about the technology used in the process, time and method of measurement of the emissions, the geographical location of the process, the origin of input flows and the destination of output flows.

One common problem that LCA analysts face is the lack of relevant data sources, because no LCA analyst can be a technical expert on all the different technologies modelled in a life cycle study. So, there is a need of asking other people who are expert in the field. In LCA studies that are performed on a company basis, the collection of data is usually made by asking the suppliers about the environmental data associated with the raw materials purchased. Commonly, the suppliers provide data only for the processes carried out by them, but sometimes cradle to gate inventories are also provided. When information about the process is only provided, data for processes which belong to the upstream life cycle have to be collected. upstream LCI data may be collected directly from producers of the raw materials or from other sources.

When a cradle to grave LCA is modelled, data referring to the downstream processes have to be also collected from customers and waste management companies. In these phases in the life cycle, often, average data are preferred.

Several types of data source are available including LCI data published by industrial organizations, reports from LCAs and similar projects, databases issued by organizations as parts of LCA software packages. Data gaps in LCIs may be filled with estimates and calculations by using the support of technical experts or model calculations.

Validation of data: according to the ISO 14041 standard, a check of the validity of collected data should be performed. Such controls can be made by comparing the collected data with other data sources and mass and energy balances. In addition, it is for example necessary to check if the data represent the required type of technology, if they represent the site which was intended to be modelled, if system boundaries of the collected data are in line with what was required, if the data are still valid or too old.

Calculation procedure: once the flowchart model is drawn and the data collection is end, the calculation procedure of the LCI phase can be done. It is best practice to illustrate the procedure by means of an example which is reported in Fig. 3.6. As reported, Mineral raw material, a, and plastic material, b, are used to manufacture the product c in process C which uses no energy and has no emissions. The distribution process described by activity D consumes energy in the form of oil and releases carbon dioxide (CO_2) because of the combustion of the oil used. In order to produce the mineral raw material a, the process A uses mineral A as a resource. In addition, the process consumes oil as energy and releases CO_2.
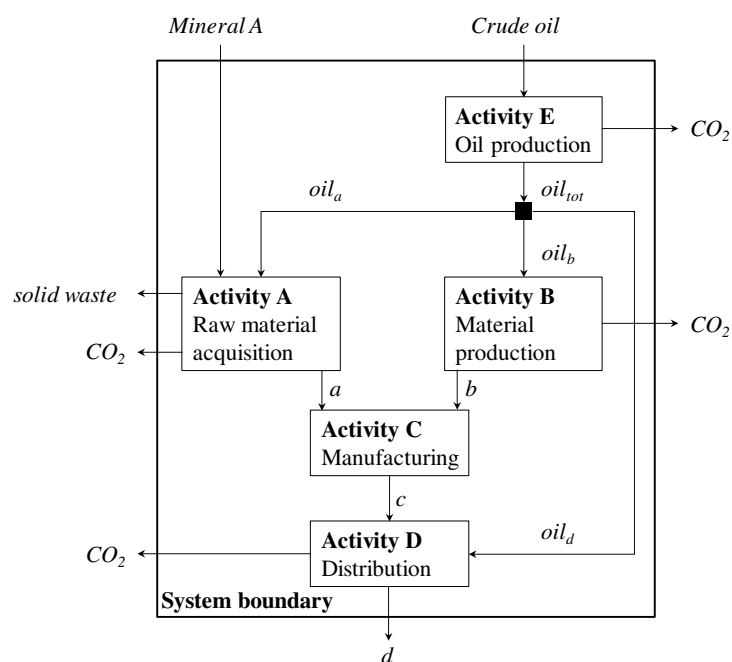

Fig. 3.6. Flowchart model of a product system [100].

Plastic raw material is produced by process B and the oil used in activities A, B and D is produced in process E which uses crude oil as a resource. The flowchart model represents a cradle to gate life cycle analysis.

For each activity of the flowchart model of the considered product system, data are collected and reported in Table 3.1 in the column named "Data as collected". The first step of the calculation procedure is normalization of the collected data which means to relate the data to one tonne, or one kg, or other unit of each process's production or input for waste treatment activities. For all activities the unit chosen for normalization of data is kg per kg of product. Normalized data are shown in the column named "Normalized per activity".

The next step consists of calculating the flows linking the activities. This can be made by using the input data to formulate a system of equations describing the relationships between the flows. The system of equations is reported in the following:

$$\begin{cases} oil_a = a \times 0.0625 \\ oil_b = b \times 2.4 \\ a + b = c \\ a/b = 0.25/0.75 \\ c = 1 \\ oil_d = d \times 7 \\ oil_{tot} = oil_a + oil_b + oil_d \end{cases} \tag{3.1}$$

As a functional unit, the reference flow 1 kg of product is considered. As can be seen from Eq. (3.1), the definition of the reference flow is always one of the equations. The column named "Linked flows, normalized to functional unit" is the result of solving the set of equations. At this point, the remaining flows passing system boundary can be calculated.

Finally, the inventory results of the whole system can be calculated by summing the flows passing the system boundary. The results are presented in the section named "Aggregated over system" of Table 3.1. It should be mentioned that not all flows passing system boundary are elementary flows, i.e. flows passing between the technical system and the natural system. For example, the product flow d goes to some other part of the technical system.

In practice, in order to conduct LCIs calculations, dedicated software tools are used because of the large amounts of data included in a LCI. These tools use methods such as matrix inversion methods, sequential calculation of the inputs and outputs or linear programming techniques.

Table 3.1. Collected data of the different activities [100].

		Data as collected [tonne/year]	Normalized per activity [kg/kg$_{product}$]	Linked flows, normalized to f.u. [kg/kg$_c$]	Flows passing system boundary, normalized to f.u. [kg/kg$_c$]
Activity A	*inflows*				
	mineral A	1000	1.25		0.31
	oil$_a$	50	0.0625	0.016	
	outflows				
	a	800	1	0.25	
	CO_2	150	0.1875		0.047
	solid waste	200	0.25		0.0625
Activity B	*inflows*				
	oil$_b$	120000	2.4	1.8	
	outflows				
	b	50000	1	0.75	
	CO_2	210000	4.2		3.15
Activity C	*inflows*				
	a	5000	0.25	0.25	
	b	15000	0.75	0.75	
	outflows				
	c	20000	1	1	
Activity D	*inflows*				
	c	1	1	1	
	oil$_d$	7	7	7	
	outflows				
	d	1	1		1
	CO_2	21	21		21
Activity E	*inflows*				
	crude oil	100000	1.05		9.28
	outflows				
	oil$_{tot}$	95000	1	8.82	
	CO_2	15000	0.16		1.39

Aggregated over system		Flows passing system boundary, normalized to f.u. [kg/kg c]
inflows		
mineral A		0.31
crude oil		9.28
outflows		
CO_2		25.59
solid waste		0.0625
d		1

3.3. Life cycle impact assessment

The aim of the Life Cycle Impact Assessment (LCIA) phase is to describe the environmental consequences of the environmental loads calculated in the inventory analysis. The impact assessment is performed by translating the environmental loads from the inventory results into environmental impacts, such as global warming potential, abiotic resource depletion, acidification.

The reason for this translation is to have impacts that are more environmentally relevant, comprehensible, readable, and easier to communicate. An inventory analysis may contain a very large number of parameters, which make the understanding of the inventory results difficult. However, the LCIA phase can reduce the number of parameters to about 15 or even to 1 by grouping and weighting the inventory environmental loads of the inventory analysis. The application of LCIA on the results of the inventory results also allows to have more comparable results. Environmental impacts may be classified into three general categories which include resource use, human health and ecological consequences. The three categories are also subdivided into more specific impact categories, such as GWP, acidification, ozone depletion, human toxicity, etc. Figure 3.7 shows the LCIA method as described by the ISO standard for LCIA (ISO 14042).

LCIA procedure

Mandatory activities

1. Impact category definition

2. Classification

3. Characterization

Optional activities

- Normalization
- Grouping
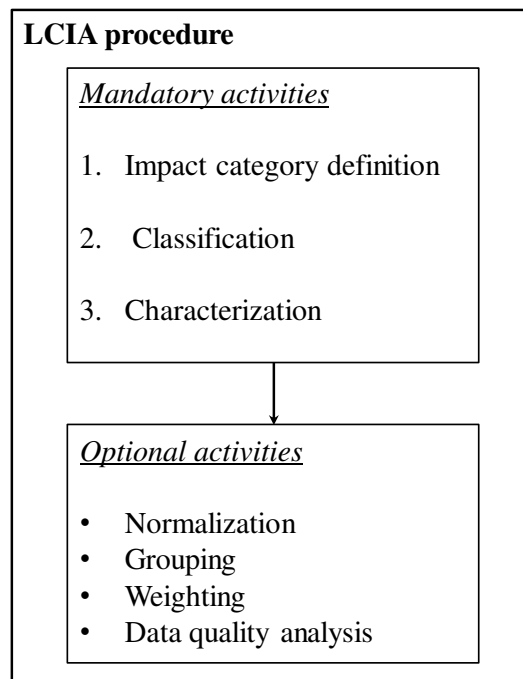- Weighting
- Data quality analysis

Fig. 3.7. LCIA method defined by the ISO standard [100].

As illustrated, the LCIA phase consists of the following elements:

- Impact category definition: in this step, impact categories are identified and selected;
- Classification: the LCI results are assigned to their respective impact categories;
- Characterization: quantitative evaluation of environmental impacts per category;
- Normalization: for each impact category, the results of the characterization step are related to a reference value;
- Grouping: the characterization results are sorted into one or more sets;
- Weighting: the relative importance of an environmental impact is weighted against all the other;
- Data quality analysis: uncertainty and sensitivity analysis of the LCIA results.

It should be mentioned that, the main phases of an LCIA are classification, characterization and weighting, while the other elements are optional for an LCA. In particular, an LCA analyst typically performs an LCA study by conducting the three main steps.

Impact category definition: in this sub-phase a specification is made for environmental impacts which were considered relevant in the goal and scope definition phase. This specification depends on the type of information collected during the inventory analysis. Impact categories must be decided taking into account the following properties:

- Completeness: the chosen impact categories should include all environmental impacts that are considered relevant for the particular LCA study;
- Independence: in order to avoid double-counting, impact categories must be reciprocally independent;
- Possibility to link the LCI result parameters in the LCA calculations, i.e. impact categories and characterization methods;

Table 3.2 reports a list of impact categories defined according to the SETAC working group on LCIA. Inventory results represented by flows to and/or from other technical systems are those flows which cannot be assigned to any of the impact categories.

Table 3.2. Impact categories decided by SETAC-Europe working group on LCIA [100].

Input-related categories:	9. Acidification
	10. Eutrophication
1. Abiotic resources	11. Odour
2. Biotic resources	12. Noise
3. Land	13. Radiation
	14. Casualities
Output-related categories:	**Flows to/from other technical systems:**
4. Global warming	
5. Depletion of stratospheric ozone	Input-related (energy, materials, plantation wood, etc.)
6. Human toxicological impacts	
7. Ecotoxicological impacts	Output-related (solid waste, etc.)
8. Photo-oxidant formation	

Classification: in this step, the LCI result parameters are sorted and assigned to their respective impact categories. Knowledge of what type of impacts pollutants and resource use the different results of the LCI lead to, is always required. Table 3.3 illustrates the list of pollutants for the different impact categories.

As can be seen, some environmental loads must be assigned to different impact categories, such as NO_x which can be assigned to both acidification and eutrophication impact categories. The multiple assignment of an environmental load to more than impact category should be made only if the effects are independent of each other. For example, the assignment of a certain load to global warming and global warming induced impacts on biodiversity leads to double-counting.

Characterization: this step consists of calculating the contribution of the different pollutants to the different impact categories by using suitable equivalency factors. For example, the extent of the acidification impact is determined by summing the all acidifying emissions (SO_2, NO_x, HCl, etc) based on their equivalency factors. The equivalency factors of the pollutants are usually defined by the common denominator of the different emissions. For instance, acidifying emissions all form H^+, which causes the acidification, then, adding the number of hydrogen ions liberated by the different pollutants provide an information about the potential impact of these pollutants.

Characterization methods and equivalency factors are defined by considering the physico-chemical mechanisms of how different emissions contribute to the different impact categories. Moreover, the potential impact represents the maximum impact that the different pollutants can lead to, because the adoption of physico-chemical mechanisms to define the equivalency factors makes the effects of deposition in geographical areas with different sensitivities to pollutants disregarded.

Table 3.3. List of various substances for each impact category [100].

Depletion of abiotic resources	Global warming	Ozone depletion potential	Acidification	Eutrophication
Aluminum	CO_2	(CFC-11), (CFC-12), (CFC-13), (CFC-113), (CFC-114)	SO_2	PO_4^{3-}
Iron	CH_4	(HCFC-22), (HCFC-123), (HCFC-124)	HCl	H_3PO_4
Silicon	1,1,1-trichloroethylene	(Halon 1201), (Halon 1202), (Halon 1301), (Halon 2401)	HF	P
Uranium	CCl_4	CCl_4	NO_x	NO_x
Crude oil	N_2O	1,1,1-trichloroethylene	NH_3	NO_2
Natural gas	SF_6	CH_3Br		NH_3
Hard coal	CF_4	CH_3Cl		NH_4^+
Soft coal	(CFC-11), (CFC-12), (CFC-13), (CFC-113), (CFC-114)			NO_3^-
Fossil energy	(HCFC-22), (HCFC-123), (HCFC-124)			HNO_3
				N
				COD

Tables 3.4 and 3.5 show the equivalency factors of the different elements which contribute to the GWP category (Table 3.4) and depletion of abiotic resources (Table 3.5). The common denominator of the different pollutants of GWP impact category is the carbon dioxide expressed in CO_{2eq}, while equivalency factors for the different substances of the depletion of abiotic resources are determined considering antimony (Sb_{eq}) as a reference.

Table 3.4. GWPs for different time horizons [100].

pollutants	GWP 20 years (kg CO$_{2eq}$/kg)	GWP 100 years (kg CO$_{2eq}$/kg)	GWP 500 years (kg CO$_{2eq}$/kg)
CO$_2$	1	1	1
CH$_4$	56	21	6.5
1,1,1-trichloroethylene	360	110	35
CCl$_4$	2000	1400	500
N$_2$O	280	310	170
SF$_6$	16300	23900	34900
CF$_4$	4400	6500	10000
CFC-11	5000	4000	1400
CFC-12	7900	8500	4200
CFC-13	8100	11700	13600
CFC-113	5000	5000	2300
CFC-114	6900	9300	8300
HCFC-22	4300	1700	520
HCFC-123	300	93	29
HCFC-124	1500	480	150

The common property of greenhouse gases is their capacity to absorb infrared radiation and thereby increase the temperature of the atmosphere. The characterization of greenhouse gases is based on this property. Gases such as carbon dioxide, methane, chlorofluorocarbons (CFCs) and nitrous oxide all absorbs infrared radiation and causes climate change. The GWP of a gas expresses the potential contribution of a gas to climate change. The GWP is defined as the ratio between the increases infrared absorption caused by a substance and the increased infrared absorption caused by 1 kg of CO$_2$. GWP is usually calculated for different time horizons because greenhouse gases have different life spans in the atmosphere.

Table 3.5. Equivalency factors for abiotic resources depletion based on ultimate reserves [100].

Substance	Static reserve life (years)
Aluminium (Al)	1×10^{-8} kg Sb$_{eq}$/kg
Iron (Fe)	8.43×10^{-8} kg Sb$_{eq}$/kg
Silicon (Si)	2.99×10^{-11} kg Sb$_{eq}$/kg
Uranium	0.00287 kg Sb$_{eq}$/kg
Crude oil	0.0201 kg Sb$_{eq}$/kg
Natural gas	0.0187 kg Sb$_{eq}$/m^3
Hard coal	\0.0134 kg Sb$_{eq}$/kg
Soft coal	0.00671 kg Sb$_{eq}$/kg
Fossil energy	4.81×10^{-4} kg Sb$_{eq}$/MJ

Resources can be divided into renewable and non-renewable resources or into abiotic and biotic resources. Abiotic resources include so called non-living resources such as iron ore, crude oil and wind energy, while biotic resources are those considered as living resources ad which are characterized by a biological character, such as forests, animals and plants. resources can be also categorized as deposits, funds and flows. Deposits are non-renewable resources, such as fossil fuels and minerals. Funds are resources that can be regenerated within human lifetimes, such as groundwater and topsoil. Flows are renewable resources, such as wind and solar energy. The equivalency factors for abiotic resources in Table 3.5 are defined by considering the size of reserves and extraction rates.

Normalization: in this step, for each impact category, the results of the characterization step are divided by the actual magnitude. In this way, the impacts caused by the system under investigation is better understood. Indeed, for example, normalization allows to observe if the acidification impacts of a certain product are enormous compared to the total acidification impacts in the country where the product is produced and used. It should be mentioned that, in order to have a meaningful comparison, the comparison must be made between the total impact of the total use of the considered product and the total impact in the region of country.

Grouping: this step consists of sorting the results of the characterization in a way that can be useful for the analysis and the presentation of the results. An example of grouping is to sort the characterization results in group headings, such as global/ regional/local impacts, and impacts with high/ medium/ low priority. LCI results can also be sorted and presented in the groups emissions to air, emissions to water and emissions to soil.

Data quality analysis: this step helps to better understand the significance, uncertainty and sensitivity of the LCIA results. In particular, the following techniques can be used:

- Gravity analysis: identification of the activities which contribute more to the environmental impact;
- Sensitivity analysis: identification of the LCI data for which small variations change the ranking between compared options;
- Sensitivity analysis: identification of impact assessment data for which small variations change the ranking between compared alternatives;
- Uncertainty analysis: integration of uncertainty to the calculation procedure.

3.4. Interpretation and presentation of results

In an LCA study, the number of LCI results may exceed a hundred. Then, it may be difficult to analyze all the obtained result parameters. In order to extract something significant, there is a need of way to refine the raw results. One way is to select and present the most important LCI results, another way is to present weighted results.

In order to have useful, presentable and final results, a process that includes screening of the raw results, identification of critical data and assessments of the importance of missing data, is required. In LCA terminology, "interpretation" is the process of assessing results to draw conclusions. In an LCA study, evaluations such as sensitivity analysis, uncertainty analysis and data quality analysis are usually used in the interpretation phase to check the robustness of the conclusions drawn. Figure 3.8 describes the interpretation phase according to the ISO standard.
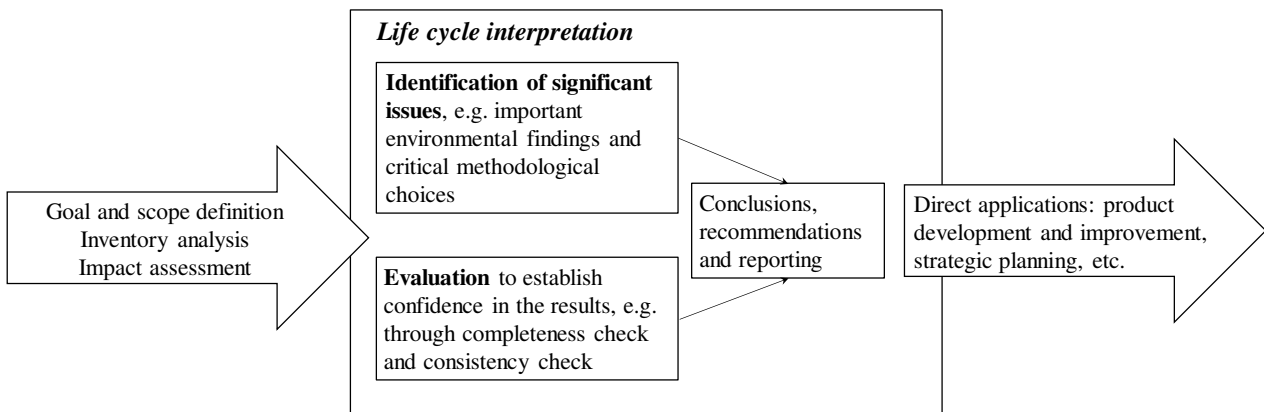

Fig. 3.8. The structure of the interpretation phase according to the ISO standard [100].

As said before, the LCI results can be more than one hundred. Characterization procedure reduces the number of parameters up to around 15, which is the number of environmental impact categories. Furthermore, it is possible to aggregate the results of the characterization phase and obtain a single number that represents the total environmental impact. Figure 3.9 shows how the results are reduced and the information is aggregated by going all the way from inventory results to weighted results.
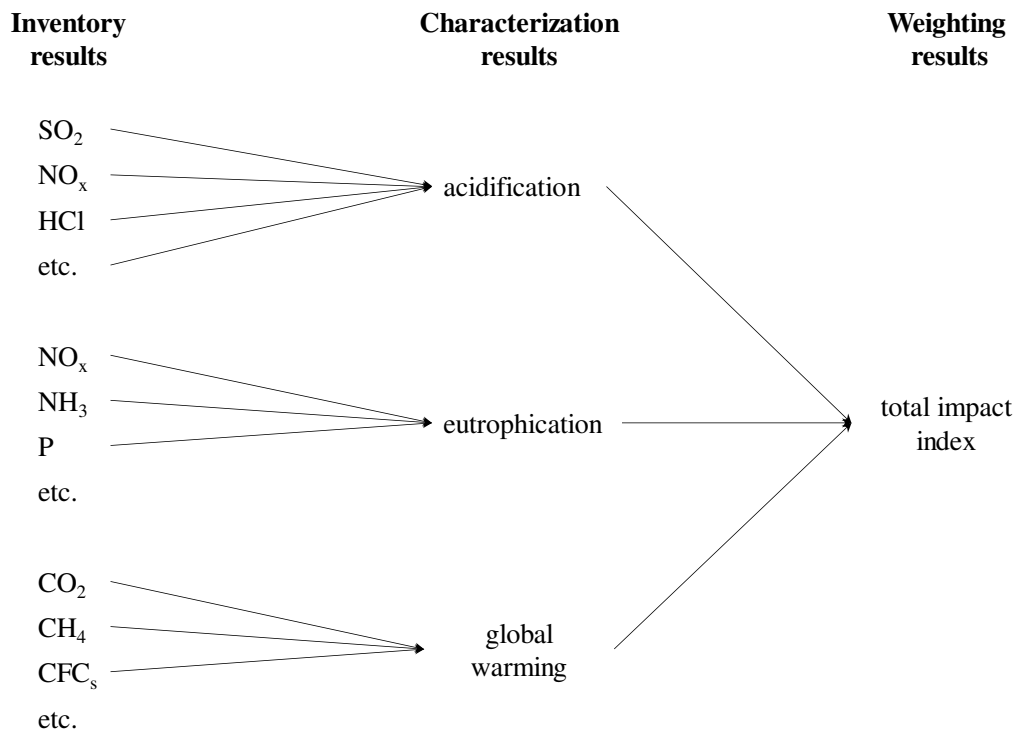
Inventory results	**Characterization results**	**Weighting results**

SO_2
NO_x
HCl
etc.

NO_x
NH_3
P
etc.

CO_2
CH_4
CFC_s
etc.

acidification

eutrophication

global warming

total impact index

Fig. 3.9. Aggregation steps of LCA results.

The presentation of LCA results at the characterization level for a more total result illustration. In addition, the aggregation process from the inventory to the characterization allows to condense the information and to highlight all impact parameters in a one diagram. In some cases, the results at the characterization stage are conclusive and sufficient to draw a conclusion, for example, in a comparative LCA study and the presentation of weighted results is not necessary. However, the choice of a presentation format of LCA results depends on the intended users or audience. Inventory results are usually presented for people whole understand chemical substance names and work in process industries that produce relatively simple products, while highly aggregated results are often used in manufacturing industries that produce products consisting of a large number of parts and materials. An additional reason is that engineers don't have much time and competences to understand complex and detailed environmental information.

4. Energy systems for residential building applications

This chapter deals with energy technologies which can be used for the fulfillment of building's heating, cooling and electric energy demands. Renewable energy systems, partially renewable energy systems and systems powered by fossil fuel are taken into account. For each system, the working principles, the main characteristics and the different types available in the market are presented.

4.1. Solar thermal collector

The use of solar energy to heat a fluid was one of the first means of taking advantage of solar radiation. Solar collectors can gather solar thermal energy in almost any climate to provide reliable, low-cost source of energy for many applications including domestic hot water application and residential space heating. Today more than 30 million square meters of solar collectors are installed across the world for domestic hot water application. Moreover, hot water produced by solar collectors and used for space heating has grown in Europe over the last 10 years. STCs and an AB or heat pump are usually combined for space heating application by using of a low temperature thermal distribution system operating in the building.

In recent years, utilities have begun to use solar thermal energy to generate electricity by using steam turbines. The steam is produced by concentrating the solar energy into a water boiler. Solar thermal electric power plants use various concentrating devices to focus sunlight and achieve high temperatures necessary to produce steam for power generation, while, small scale water heating systems use flat plate collectors to capture heat from the sun. In particular, solar heat without concentrating can be used for:

• Solar water heating;
• Solar space heating in buildings;
• Solar space cooling.

The solar collector absorbs solar radiation and generates usable thermal energy. The thermal energy or heat is then transferred to a fluid medium, such as water, another heat transfer fluid, or air, which flows through the collector. The thermal energy can also be stored for night time use or other times when solar radiation is not available.

Different types of solar collectors are present in the market, the choice of the type mainly depends on the application and the required operating temperature of the fluid.

4.1.1 Flat plate collectors

Flat-plate collectors are the most common types of solar collector. They are mainly used to provide low temperature heat for ambient heating, domestic hot water systems, and swimming pools by transferring the heat of the sun to water either directly or through the use of another fluid and a heat exchanger. These mostly consist of three components; transparent cover, collector housing and an absorber. a description of a typical flat-plate collector is reported in Fig. 4.1.
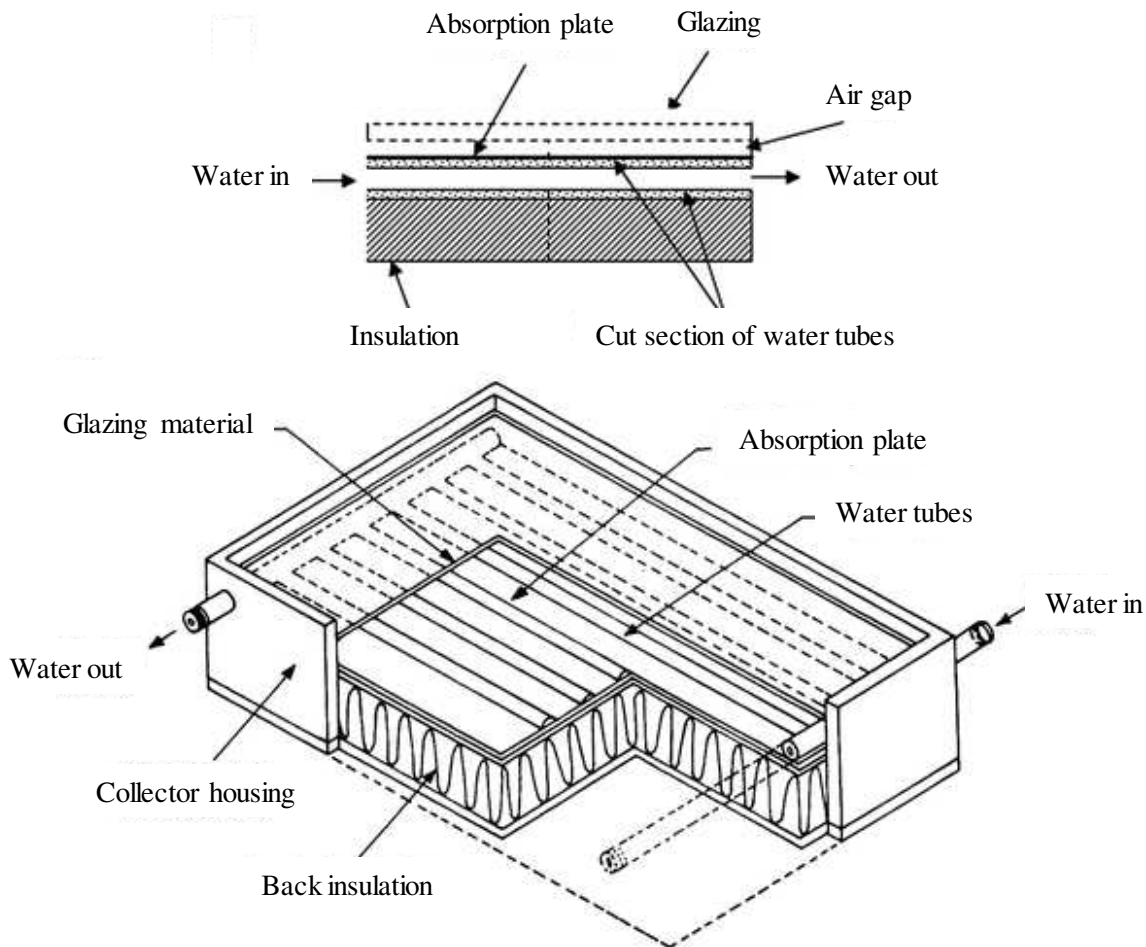

Fig. 4.1. A typical liquid flat-plate collector (modified from [101]).

The absorber is inside the flat-plate collector housing and it converts radiation to heat and transfers it to water in tubes inside the system. In order to keep heat losses to a minimum, the collector housing is highly insulated on the back and sides. However, if the temperature difference between the absorber and ambient air is high there may still some collector heat losses. These are mainly convection and radiation losses. The absorber is usually made of metal such as copper, steel or aluminum. Generally, black materials absorb sunlight very well and warm up to higher temperatures. However, metallic materials do not naturally have black surfaces and must therefore be coated.

The cover consists of a panel of glass which is used to avoid most of the convection losses. Moreover, it helps to reduce heat radiation from the absorber to the environment in the same way as a greenhouse. It should be mentioned that, the glass also reflects a small part of the sunlight that can no longer reach the absorber.

The collector housing can be made of plastic, metal or wood and it must seal the front glass cover so that no heat can escape and no dirt, animals or humidity can get into the collector.

Flat collectors can be found with glazing or without glazing. Collectors without glazing are low-cost collectors and lose significant heat to the environment, which limits their use to low temperature applications such as swimming pools, water temperature boosters in fish farming applications. In cold climates, they are exclusively used in the summer because of the high heat losses.

Flat collectors with glazing limit thermal losses and allow applications at moderate temperatures for the heating of domestic water, the heating of buildings and for industrial processes.

In order to ensure a hot water supply that is as comfortable as we expect from conventional systems, further components such as a hot water storage tank, pump and an intelligent control unit are usually needed.

4.1.2 Evacuated tube collectors

As shown from Fig. 4.2, this type of collectors consists of two concentric cylinders, the outer one of glass and the inner, a pipe through which the liquid flows. A vacuum is established between the two cylinders, reducing the convection heat losses. In fact, in this case the thermal losses are extremely small and these collectors are well adapted to applications requiring medium and high temperatures, such as the production of domestic hot water and the heating of buildings and a number of other commercial and industrial applications, particularly in cold climates.
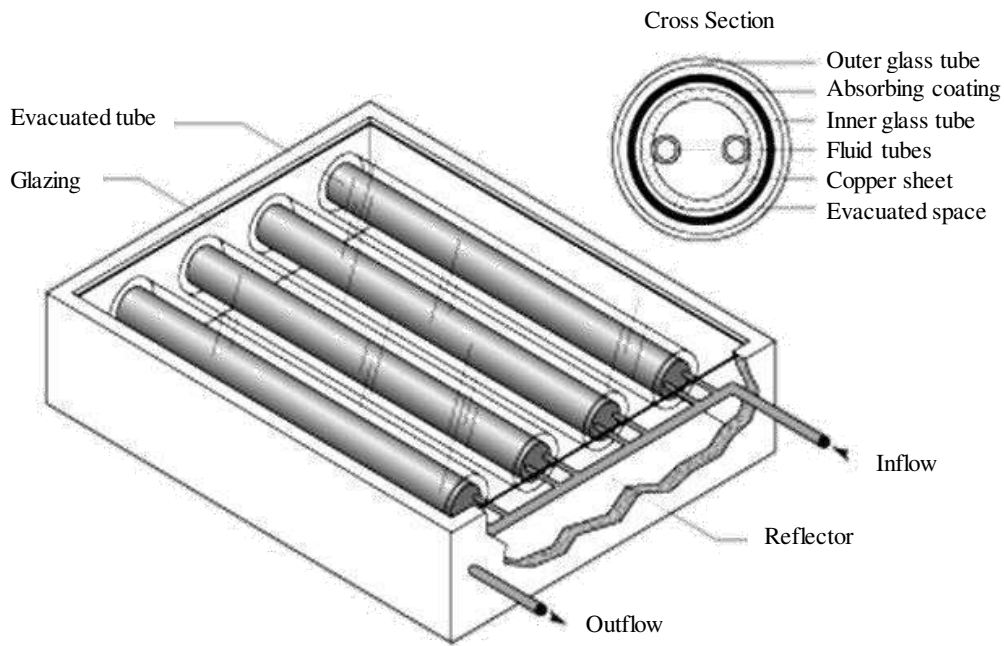
Fig. 4.2. A typical evacuated tube collector (modified from [102]).

Compared to flat plate collector, the specific price of evacuated tube collectors is higher. Glass tubes are placed in parallel rows below the glazing surface. The conductive and convective heat losses are minimized in this type of collectors by removing the air present between the two glass tubes.

Evacuated collectors are characterized by a significant higher energy gain especially in the cold months. Thus, compared to a flat plate collector, a solar system with evacuated tube collectors needs a smaller area. Moreover, evacuated tube collectors must always be installed on top of the roof because they can't be integrated directly into a roof.

Evacuated tube collectors can also have heat pipes which is embedded inside a closed glass tube with a diameter of a few centimeters. The heat pipe is a two phase equipment that contains low boiling heat transfer fluid. In the evaporator section of the heat pipe, the low boiling fluid gets vaporize and rises to condenser section of heat pipe. In order to allow the vapor to rise and the fluid to flow back, the tubes must have a minimum angle of inclination. Otherwise, the systems will not work properly.

Residential and commercial building applications that require temperatures below 94°C typically use flat plate collectors, whereas those requiring temperatures higher than 94°C use evacuated tube collectors.

4.1.3 Concentrating solar collectors

Concentrating solar devices constitute a separate class of solar collectors. This type of solar collectors is usually used when very high temperatures are required, but may in principle also be considered for heating purposes involving modest temperature rises over the ambient.

In order to concentrate the sun's heat energy, these devices use reflective materials, such as mirrors. The energy is concentrated into a boiler to generate steam which drives a steam turbine used to generate electricity. Three types of concentrating solar power systems can be found:

Trough systems: in these systems, the concentrated solar energy onto a receiver pipe by using trough-shaped reflectors (see Fig. 4.3). The receiver pipe is running along the inside of the reflectors surface. The heating fluid is generally oil flowing through the receiver pipe. The solar energy heats the oil which is used to generate electricity in a conventional steam generator.

In order to generate power on a large scale, a number of troughs are aligned in parallel rows on a north-south axis in a collector field. These systems generally incorporate thermal storage for electricity generation in the evening. Moreover, a backup system fed by fossil fuels is always used to supplement the solar system during low solar radiation periods.

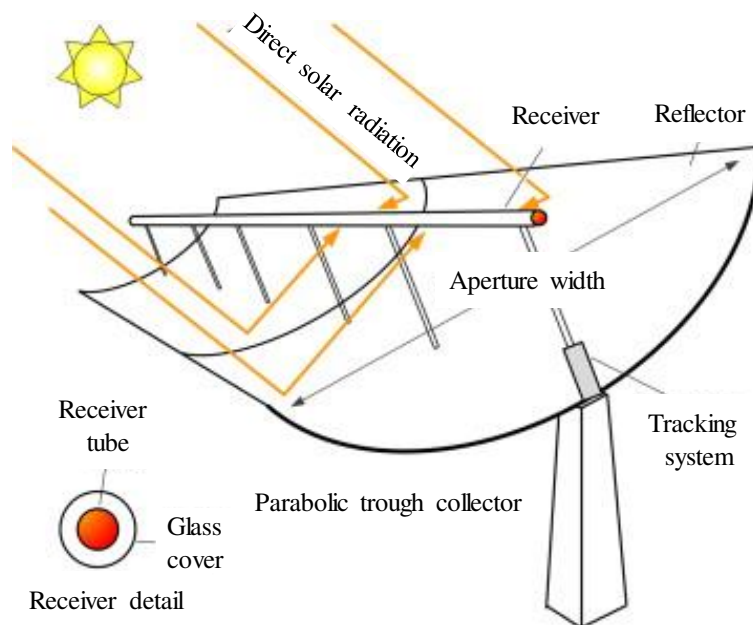**Fig. 4.3.** A parabolic trough solar collector (modified from [103]).

Power tower systems: these systems are characterized by sun-tracking mirrors (heliostats) that focus solar energy on a receiver at the top of a tower (see Fig. 4.4). The heating fluid is generally molten nitrate salt which is used to transfer energy to the receiver, which in turn is used to generate electricity by means of a conventional steam turbine.
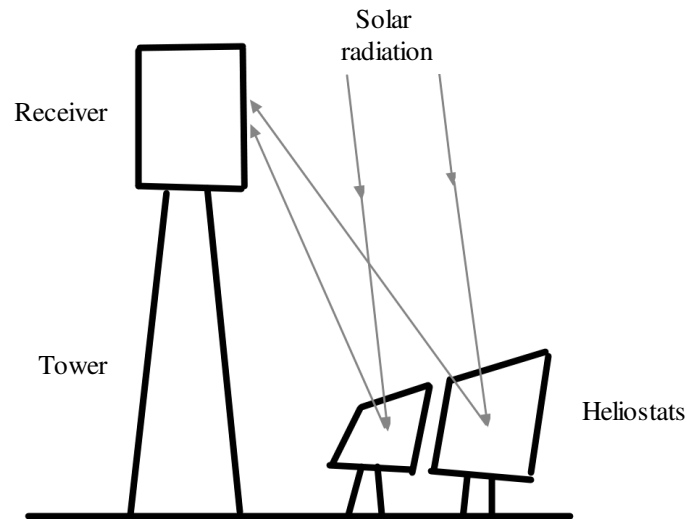
Fig. 4.4. Solar tower system (modified from [104]).

Dish systems: as highlighted in Fig. 4.5, in these systems, a dish shaped parabolic mirrors are used as reflectors to concentrate the sun's energy onto a receiver. The receiver is mounted on individual dish. In the dish system the sun's energy is concentrated in a small area so that it can be used more efficiently. A tracking system allows the dish device to track the sun continuously to reflect the beam onto the thermal receiver. The dish is usually equipped with an engine for direct generation of electricity. The working fluid can be hydrogen or helium which is contained in a thermal receiver composed of a bank of tubes. Stirling engine is the most common type of heat engine used in dish-engine systems.
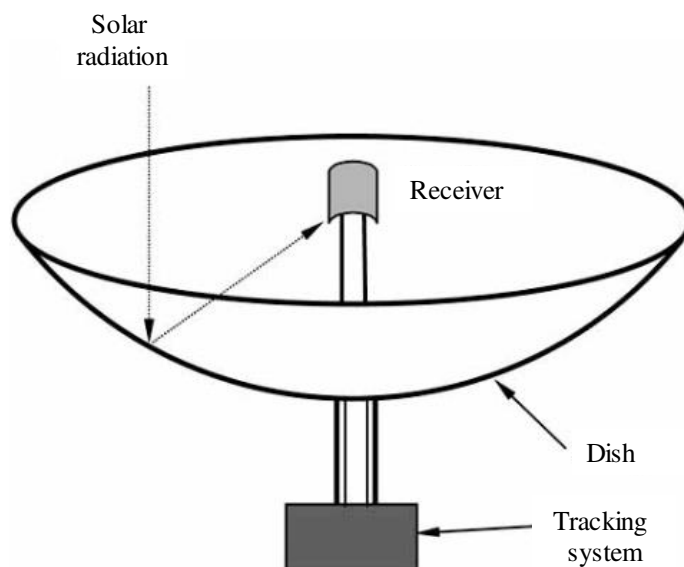

Fig. 4.5. A parabolic dish collector (modified from [105]).

4.2. Photovoltaic panel

Systems which are based on PV effect are commonly known as "solar cells", and are currently used in a number of devices including calculators, watches and emergency radios. PV cells convert the solar radiation directly into electricity and they represent the basic element from which the PV systems are made. Large scale PV systems can be used to produce electricity for pumping water, satellites and lighting homes.

PV systems are very reliable when they are subjected to harsh conditions such as space conditions. In fact, the Hubble space telescope and virtually all communications satellites are powered by PV technology. Furthermore, the most of the electronic devices in satellites are powered by PV systems.

In order to capture the sun's energy, which is composed of photons, PV cells use semiconducting materials. When photons hit a PV cell, depending on their wavelengths in the solar spectrum; they can pass straight through the cell if their energy is less than the band gap energy of the material, reflect off the surface depending on the surface characteristics of the material or are absorbed by the PV cell.

When photons with a certain level of energy are absorbed, they are able to free electrons from their atomic bonds. The electrons cause a hole to form, by leaving their positions and the other electrons from nearby atoms will move into this hole. This process continues until it reaches the external electrical circuit. Finally, depending on the band structure of the material, heat can be generated if the energy of the photons is higher than the band gap energy.

The semiconductor layers are the most important parts of solar cells. Various types of materials which can be used for the production of these semiconductor layers.

Crystalline silicon is most widely used in PV cells. A number of other semiconductors have been also used. However, the basic principles of all these materials are the same. Three different forms of silicon can be used to make PV cells.

Single Crystal: single crystal silicon is characterized by its uniformity which is ideal for efficiently transferring electrons through the material.

Amorphous silicon: this type of silicon is commonly used for devices that have low power requirements (e.g. watches and calculators). Compared to the single-crystal silicon, amorphous silicon absorbs radiation 40 times more efficiently. Moreover, the production of amorphous silicon requires lower temperature and can be deposited on low-cost substrates reducing the cost. Amorphous silicon is the leading thin-film PV material due to the mentioned characteristics.

Polycrystalline Thin Films: polycrystalline thin-film units can be manufactured cheaply because they require little amount of semiconductor material. The films can be deposited on low-cost substrates such as glass or plastic, even on flexible plastic sheets.

Compared to single crystal cells, thin-film devices can be made as a single unit by depositing sequentially several layers on a glass substrate. The layers are antireflection coating, a conducting oxide layer and a back electrical contact.

PV systems produce direct current. For off-grid systems, these systems can be directly used to run direct current devices. Generally, direct current devices are few and are also costly. Therefore, it would be better if the direct current is converted to alternating current because appliances and lights running on alternating current are much more common and generally cheaper. Some loss of power appears during the conversion of direct current into alternating current. This conversion is generally 80% efficient.

An individual PV cell typically produces between 1 and 2 W. Modules are formed by connecting together a number of individual cells. By connecting several cells in series, the voltage increases while the current is the same as expressed in the following:

$$\begin{cases} I = I_1 = I_2 = \cdots = I_N \\ \quad V = \sum_i^N V_i \end{cases} \tag{4.1}$$

Commercial modules are usually composed of a number of cells in the range of 36-72 cells. The corresponding voltage intervals are 15-20 V and 30-40 V, respectively, while the output power intervals are 80-90 W and 160-180 W.

The module efficiency can be determined by using the cell efficiency as shown in the following equations:

$$\eta_{module,ref} = \eta_{cell} \cdot c_1 \cdot c_2 \tag{4.2}$$

With:

$$c_1 = \frac{N_{cell} \cdot A_{cell}}{A_{module}} \tag{4.3}$$

Where N_{cell} is the number of cells composing the PV module, A_{cell} is the cell area and A_{module} is the area of the PV module. c_1 is a coefficient which takes into account of the cell shape. It is about 0.8 for circular cells and around 0.9 for rectangular chamfered cells. The coefficient c_2 takes account of dissipations along the connecting cables of the cells and it assumes values around 0.95. Therefore, the

module efficiency is lower than the cell efficiency with a range of about 12-14 % for modules made of single-crystalline cells and a range of 5-6 % for modules made of amorphous crystalline cells.

Arrays are formed by connecting a number of modules and large scale units are produced by joining together several arrays. Therefore, a PV system is composed from several strings that are connected together in parallel. This type of connection provides an increase of current and keeps unchanged the voltage, as expressed in the following:

$$\begin{cases} V = V_1 = V_2 = \cdots = V_N \\ \quad I = \sum_{i=1}^{N} I_i \end{cases} \tag{4.4}$$

4.3. Combined heat and power systems

A CHP plant is a system where the waste heat of power generation provides beneficial use. The waste heat from a CHP can be used to provide high pressure steam, low pressure hot water, hot gas, heated air, chilled water or sub-zero brine water for low temperature refrigeration applications through the use of ABS.

An important aspect is the heat-to-power ratio to be served by the CHP system. Commonly, when the heat demand is very large, the power from the system to the grid is exported to ensure a thermal match. Due to transmission difficulties of heat, the export of heat by using district heating or cooling schemes is less common. The choice of the appropriate CHP technology is usually determined by the heat-to-power ratio. For example, when the application requires the production of steam, this will certainly will be best served by a gas turbine. In fact, the heat energy in a gas turbine has a high temperature exhaust which is ideal for steam generation. Instead, for building air conditioning, a tri-generation system composed of a gas ICE and a lithium bromide ABS is most likely the best option. Therefore, the type of the thermal energy demand and the heat-to-power ratio are the key factors that determine the best CHP solution.

CHP systems are usually used to fulfill seasonal demands such as hot water and space heating of buildings during the colder months of the year. However, buildings air conditioning allows the integration of other technologies with CHP systems where a part of the thermal energy produced from the CHP is used (e.g. by an ABS) to produce cooling energy.

By recycling the waste heat of CHP system, overall efficiencies of 50-80% can be achieved. Which is a dramatic improvement compared to the average 33% efficiency of conventional fossil fueled power plants. The higher efficiencies of cogeneration allow to reduce fuel consumption and greenhouse gas emissions since CHP systems produce two forms of energy in one process.

Possibly the widest range of technologies and applications for CHP fall into the category of small-scale systems. Generally, small-scale CHP refers to systems with electric power less than 100 kW, while CHP units with an electric capacity smaller than 15 kW are usually denoted micro-scale systems.

The small-scale and micro-scale CHP systems are suitable residential and commercial building applications, such as hospitals, schools, and domestic buildings of single or multifamily dwelling houses.

Most CHP units operate in grid-parallel mode, so that some of the building electric demand can be fulfilled by the electrical network, but the excess of electric energy may also be exported to the grid. A safe connection to the electric grid is always required to ensure that under a fault condition, the grid is fully protected whether the fault is with the installation or on the grid itself.

Conversely to conventional power plants which are centrally located, CHP is a form of distributed generation located at or near the consumer. Therefore, CHP has the advantage of reducing the energy cost, the risk of electric grid disruptions and enhancing energy reliability for the user.

In CHP applications, the electric efficiency is defined as the ratio of the net electric output (P_{el}) to the fuel input (P_{fuel}):

$$\eta_{el} = \frac{P_{el}}{P_{fuel}} \tag{4.5}$$

The overall efficiency which takes into account the useful heat output is represented by the ratio of the electric and thermal outputs to fuel input:

$$\eta_{total} = \frac{P_{el}+P_{th}}{P_{fuel}} \tag{4.6}$$

Where, the power associated to the fuel input can be calculated as follows:

$$P_{fuel} = m_{fuel} \cdot LHV \tag{4.7}$$

With m_{fuel} representing the mass flow of the fuel and LHV the lower heating value for the fuel. Table 4.1 lists the overall categories of CHP technologies, their power range and their electrical and total efficiency range.

Table 4.1. Characteristics of CHP technologies [106].

CHP technology	Power range	Power efficiency range (%)	Nominal efficiency (%)
Combined cycle gas and steam turbine	20 MW to 600 MW	30-55	85
Gas turbine	2 MW to 500 MW	20-45	80
Steam turbine	500 kW to 100 MW	15-40	75
Reciprocating engine	5 kW to 10 MW	25-40	95
Micro turbine	30 kW to 250 kW	25-30	75
Fuel cell	5 kW to 1 MW	30-40	75
Stirling engine	1 kW to 50 kW	10-25	80

A CHP unit consists of the following basic components:

- a prime mover to transform the fuel energy into mechanical and/or thermal energy;
- a generator to convert the mechanical energy into electric energy;
- a heat recovery to recycle the waste heat.

The CHP technologies suitable for buildings applications (mainly with an electric capacity lower than 100 kW_e) are those based on the following options:

- Internal combustion engine (ICE);
- Micro gas turbine (MGT);
- Micro Rankine cycle (MRC);
- Stirling engine (SE);
- Fuel cell (FC).

4.3.1 Internal combustion engine

After continuous development, ICEs are widely accepted technologies and well established engines. ICEs provide electric efficiencies in the range between 20% and 26%, high power-to-weight ratios, leading to their widespread use in different applications, such as transport and CHP systems. They are also characterized by a prominent dynamic properties during operation and can be scaled down to small sizes.

The main advantages of this type of engines include low capital cost for micro CHP applications, easy maintenance and they also can run with natural gas. On the other hand, with reference to the residential sector, the main challenges of this technology are noise, vibration and exhaust gas emissions.

Generally, ICEs are divided into Otto engines and Diesel engines. For both types of engines, the most common operating cycle is the four stroke cycle since it provides superior performance in most

applications. The Diesel engine is based on a direct injection compression mechanism, while in Otto engines, a spark plug is used to ignite a pre-mixed charge after compression in the cylinder.

Figure 4.6 highlights the influence of the compression ratio on the cycle efficiency. As can be seen, in order to have higher efficiencies it is better to have a high compression ratio. However, the increase of efficiency is limited by the fuel knock phenomenon which is a limit in spark ignition engines. In fact, the fuel knock leads to high gas pressures, heat losses and high gas temperatures. Compared to the ideal cycle, it can be noted that a significant potential for efficiency improvement in current engines is possible. However, a number of factors limits the increase of engines' efficiency such as mechanical friction, heat losses to the combustion chamber surface, etc…
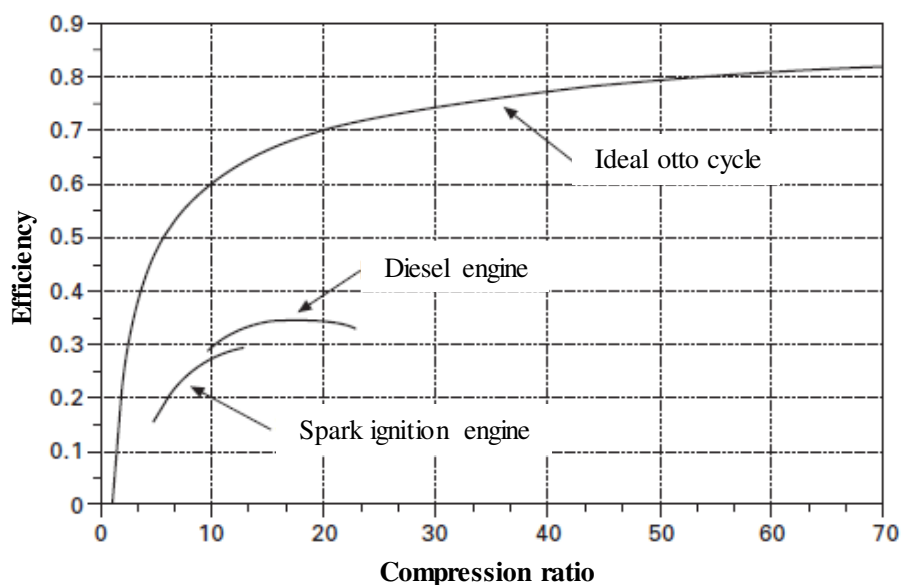

Fig. 4.6. Fuel efficiency for small-scale ICEs for micro-CHP systems (modified from [106]).

Micro CHP systems based on spark ignition engines most often use natural gas as fuel for many reasons, such as the low cost and high availability of this primary source. In this case, the flame propagates in the compressed chamber by using spark plug that ignites the charge near the center of the combustion chamber. In this type of engines, the maximum compression ratio is limited by the self-ignition of the fuel-air mixture which may leads to peak pressure, and thereby high mechanical loads on the piston rings. To avoid such phenomenon, compression ratios of about 10 are commonly used.

Nitrogen oxides (NO_x), carbon monoxide (CO), and unburnt hydrocarbons (HC) are the main emissions from spark ignition engines. Non-homogeneous fuel-air mixture throughout the combustion chamber may lead to incomplete combustion and increases emissions, as well as efficiency reductions since part of the fuel energy is not utilized.

54

The three-way catalyst is widely used for reducing spark ignition engine exhaust gas emissions, in particular, NO_x, CO and HC. To ensure efficient working condition of the catalyst, the engine fuel-air ratio must be controlled to obtain stoichiometric conditions. An efficient operation of a catalyst in an ICE based CHP system, can achieve a reduction of about 90% of all three species.

Conversely to spark ignited engines, in Diesel engines or compression engines the fuel is injected after compression and self-ignites because of the high gas temperature formed in the combustion chamber. This type of engines doesn't have the fuel knock problem (only pure is present in the chamber during compression) allowing higher compression ratios to be reached. However, the compression ratio is limited by structure problems such as pressure and temperature loads on the cylinder and the increase of emissions at high combustion temperatures.

A range of fuels can be used to run compression ignition engines including diesel fuel, heavy fuel oils, biodiesel and vegetable oils. The engine performance depends heavily on the quality of the fuel, such as good ignition, combustion properties and a viscosity suitable for efficient supply through the engine injection system.

Diesel engine emissions are usually reduced by using external means such as catalysts for NO_x and particulate filters. Catalysts are normally used in large-scale systems, while filters are used in automotive and other small-scale systems.

Generally, a part of the energy supplied to an ICE turns into mechanical work, another part is lost by the cooling water circuit and lubrication oil cooler and as friction losses and the remaining part is lost as heat in the exhaust gases. In CHP systems, the part of heat which is lost is the exhaust gases is also utilized leading to an increase of the efficiency of the ICE based CHP compared to the engine performance defined as the ratio of mechanical output to the fuel input energy. The efficiency that can be achieved in ICEs depends heavily on the engine size, design, fuel type and operational conditions.
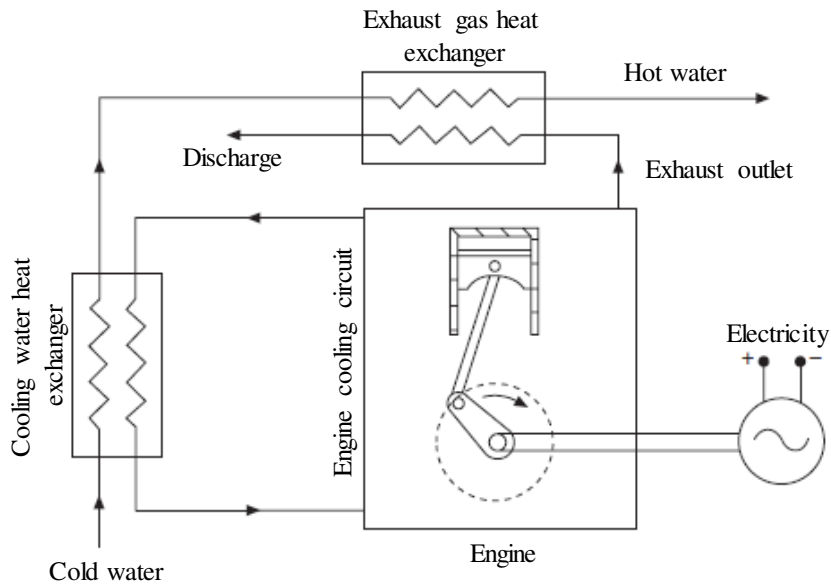
Fig. 4.7. Configuration of an ICE based CHP system (modified from [106]).

As illustrated in Fig. 4.7., the heat in the exhaust gas is recovered by using an exhaust gas heat exchanger. This heat can be recovered as hot water or low-pressure steam at 100-120 °C. The exhaust gas temperature depends on the load, ranging from around 600 °C at full load to about 300 °C at idle. As can be seen, a part of the heat is also recovered from the engine cooling system. The cooling water has a temperature of 85–95 °C, and this is maintained nearly constant over the load range by control of the cooling water flow rate. If the engine has a separate lubrication oil cooler, the heat can also be recovered in series.

4.3.2 Micro gas turbine

Gas turbines are small-size gas turbines (i.e. produced electricity is below 100 kW) and well-stablished technology for micro CHP applications. As shown from Fig. 4.8a, the simplest cycle of a micro gas turbine is composed of a compressor (C), combustion chamber, turbine (T) and generator (G). The compressor increases the air pressure to a higher pressure level (3-5 bars) and a part of the compressed air is used to burn the fuel in the combustion chamber. Then, the combustion gases enter the turbine at a temperature between 900 and 950 °C. The combustion gases expend in the turbine producing power. A part of the produced power is consumed by the compressor, while the remaining part is converted to shaft power to drive the generator.
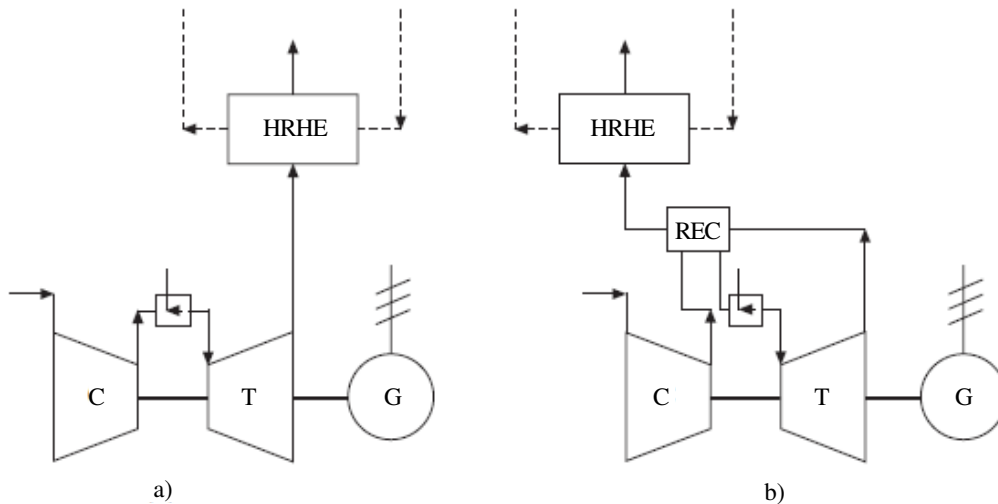
Fig. 4.8. Simple cycle a) and recuperative cycle b) of a micro gas turbine (modified from [106]).

The exhaust gases leaving the turbine can be at high temperature. So, as illustrated in Fig. 4.8b, it would be better if the thermal energy is transferred from the combustion gases to the air by using a recuperator (REC) before entering the combustion chamber. This allows to increase the fuel-to-power conversion efficiency. In a CHP operation, the remaining thermal energy is then recovered by an external heat recovery heat exchanger (HRHE) before discharging the gases.

With reference to the recuperated configuration (Fig. 4.8b) which is currently used by micro gas turbines, an electric efficiency of about 30% is possible, but with the simple configuration (without the recuperator) the efficiency is only around 15%. Considering a CHP application, the overall efficiency is typically between 75% and 85% depending on the considered application.

Two arrangements of micro gas turbines are present in the market. The first arrangement which is the one dominating the market, have the compressor, turbine and generator on a single shaft. In the second arrangement, named the two-shaft arrangement, the first turbine drives the compressor on one shaft, while the generator is powered by the second turbine on another shaft.

Due to the high rotational speed, micro gas turbines produce high frequency alternating current with about 1500 Hz which is 25-30 times higher than the normal electric grid frequency. So, the high frequency of the gas turbine is first transformed to DC current then to 50 or 60 Hz.

Generally, emissions from micro turbines are lesser than those of larger turbines. The main pollutants are NOx, CO and unburnt hydrocarbons, where the last two are indicative of incomplete combustion. In order to lower the emission of NOx, in micro turbines that operate on gaseous fuels, a lean premixed combustion is usually used. However, the use of lean premixed technology tends to increase CO emissions.

Micro gas turbines are a promising technology and suitable to produce electricity and heat for residential applications, hospitals, office and factory buildings. They can also be integrated in a tri-generation system for summer absorption chilling and winter heating.

Due to their flexibility, micro turbines are also suited for distributed generation applications where a reliable operation is always required. However, the availability of commercial micro-turbines is scarce as the manufacturing capacity has not reached the economical requirements.

4.3.3 Micro Rankine cycle

The ORC is a Rankine process, where the working fluid is an organic fluid instead of water, which is used in conventional steam power plants. ORC power plants can operate in two modes. The first is a cogenerating mode, where the thermal power rejected from the condenser in a CHP plant is used for space heating or in an industrial process. The other possibility is to only produce electricity by condensing the working fluid at a lower temperature. In this case, the heat is discharged to the external ambient.

ORC plants become a great option when the heat source is at low or medium temperature or if the plant is characterized by a low capacity. In such situations, selecting an organic fluid instead of water as the working fluid gives several benefits. Otherwise, if the heat source is at high temperature and the design power is sufficiently high, conventional steam power plant are an excellent choice.

Most of the ORC plants present in the market are based on conventional turbine technology including an air cooled generator, a lubricating oil system, a reduction gear and shaft seals.

Most ORC plants produce electric power from a relatively low temperature heat source such as geothermal heat and the waste heat from combustion engines and gas turbines or by burning limited amounts of fuel difficult to use in other processes, for e.g. by burning of biomass, landfill gas, or biogas and heat generated by concentrating solar collectors. The highest number of sold ORC plants is in the power range 300-200 kW, but plants in the range 200-22000 kW are also available. Micro ORC units in the power range 0.5-5 kW are also present, but they are characterized by a low efficiency.

Compared to a conventional steam Rankine power plants, ORC plants have the advantage of employing an organic fluid as a working fluid that remains in the superheated vapour region throughout the entire expansion in the turbine, thus avoiding the problem of condensation in the low-pressure stages typical of all steam turbines.
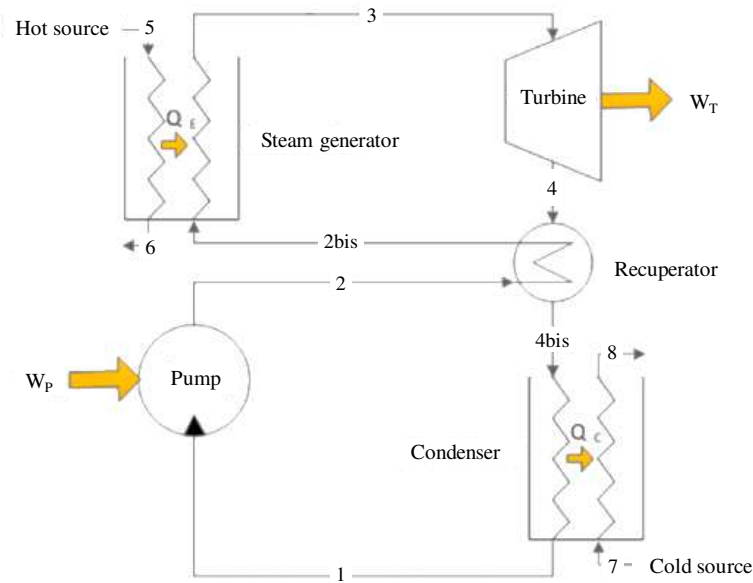
Fig. 4.9. The technology of typical ORC plants (modified from [107]).

Figure 4.9 illustrates the working principle of a conventional ORC process. As can be seen, the organic liquid process is pumped from the condenser to the recuperator where a preheating process is carried out. The preheated fluid is then sent to the steam generator where it is converted to vapor by using hot heat source gases. After exiting the vaporizer, the working organic vapor characterized by high pressure and temperature expands in the turbine and produces electricity by means of a generator. The expanded vapor goes to the condenser through the recuperator. In the regenerator the working fluid is de-superheated, then it is converted back to a liquid state in the condenser.

ORC plants may be realized in small power sizes that would make it suitable as a household CHP power plant, where local fuels could be used as heat source to produce electricity and heat for single-family dwellings.

The cycle consists in the following steps:

- from 1 to 2, the pressure of the organic liquid is increased by using a pump;
- from 2 to 2bis, the liquid is preheated in the recuperator;
- from 2bis to 3, the working fluid is vaporized and superheated by the steam generator;
- from 3 to 4, the organic vapor expands in the turbine;
- from 4 to 4bis, the vapor is de-superheated in the recuperator;
- from 4bis to 1, the vapor is transformed to the liquid state in the condenser.

For power plants in the range 4000-5000 kW or bigger, the specific is higher for the ORC plants than the conventional steam power plants. In addition, in such cases, water vapor plants are more efficient than ORC plants. Therefore, for big sizes, the water vapor processes are a favorable option.

In order to not affect the plant efficiency, the working fluid must be characterized by a thermal stability. In other words, the decomposition of the process fluid at the working temperatures should be avoided because this decomposition produces non-condensing gases which fill the condenser and affect the efficiency. For most organic fluids, decomposition appears at temperatures higher than 400 °C or in presence of metals that act as catalysts.

In most cases ORC plant efficiency is in the order of 18-22%.

4.3.4   Stirling engine

The Stirling engine is an external combustion engine which is characterized by a high combustion efficiency and very low pollutant emissions. It does not need valves or an ignition system to operate, thus allowing long life service and low operating costs. These characteristics make the Stirling engine well suited to micro CHP applications. Indeed, the majority of micro CHP plants are currently based on external combustion systems which allow stationary operation.

In external combustion engines, the combustion process is separated from the working gas which does useful work, and this characteristic makes these systems more efficient, cleaner and quieter than ICEs.

Figure 4.10 shows the simplest schematic of a Stirling engine. As can be seen, the engine is composed of a cylinder, regenerator, piston and displacer.
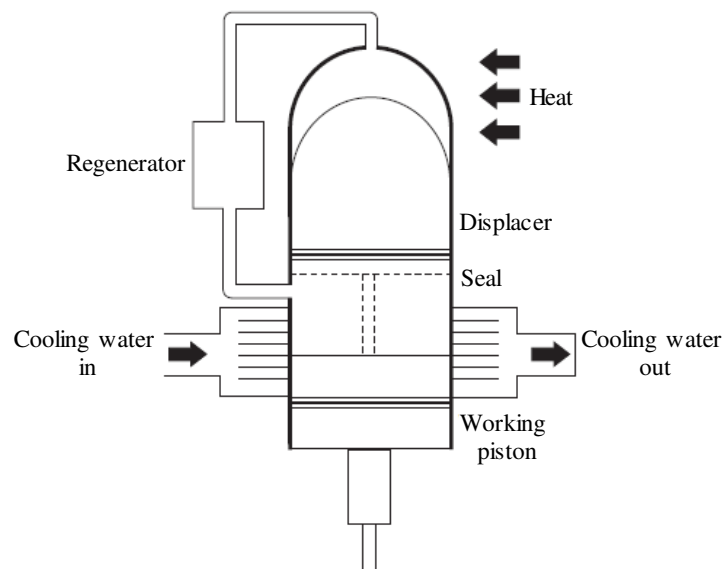

Fig. 4.10. A basic Stirling engine (modified from [106]).

In order to maintain the upper end of the cylinder at high temperature, the heat is continuously applied by, for example, a gas burner outside the system, while cooling water is used to maintain the opposite end of the cylinder at low temperature. The hot end can be as high as 800 °C and the cold end around

80 °C. The displacer moves the working gas between the hot end and cold end of the piston. The pressure fluctuations acting on the piston produce power by driving a generator, since the fixed volume of working gas is alternately heated and cooled within the engine. The displacer is 90° in advance of the working piston and is needed to move the working gas between the cold and hot zone. This configuration allows a sinusoidal power output which results in low vibration and noise levels.

Differently from ICEs, the instantaneous power variation is not possible in Stirling engines. This makes Stirling engines not ideal for applications where rapid variations are required, such as automotive applications. This is because Stirling engines have a significant time delay between the fuel supply and power production.

Since the Stirling engine is based on external combustion process, so the gas within the cylinder is completely sealed from the atmosphere and the combustion process. The heat produced from the burner can only be transferred to the working gas by conduction through the walls of the cylinder.

The theoretical thermal cycle of a Stirling engine is highlighted in Fig. 4.11. As shown, the cycle consists in the following steps:

- the working gas is in the cold end of the cylinder (at point 1) and a displacer moves the contained gas to the hot end without any increase of temperature;
- pressure and temperature increase towards point 3 by heating the gas;
- expansion of the gas from point 3 to point 4 and production of useful power;
- from point 4 to point 1 the gas is shuttled back to the cold end and it is ready to start the next cycle.
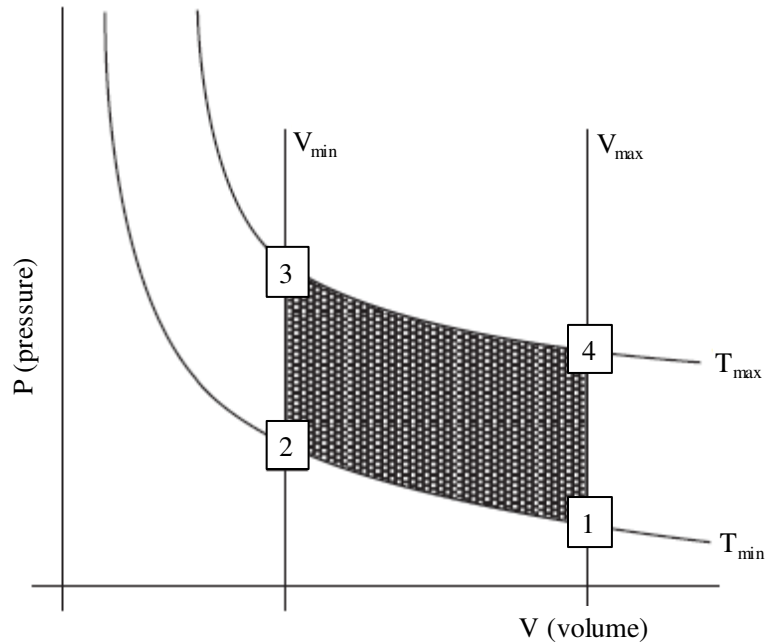
Fig. 4.11. Pressure/volume diagram of a Stirling cycle (modified from [106]).

Given the relatively small areas available for heat transfer, the working gas should have a low specific heat such that the exchanged heat increases the pressure of the gas to the maximum possible levels. Moreover, in order to transfer the heat effectively to the working gas through the limited area, combustion temperatures of around 800 ° are needed. Hydrogen and helium have this requirement, but the highest efficiency Stirling engines usually use helium as a working fluid.

In order to have electricity as final power, a generator is needed to transform the mechanical power to electric power. Both induction generators and synchronous generator can be used.

Stirling engines ca be classified into two basic categories. The first one comprises Kinematic Stirling engines in which the reciprocal piston motion is converted to a rotational movement that drives a generator, while the second category includes Free-piston Stirling engines which have no rotating parts.

Stirling engines can be further classified into three categories based on the configuration of the displacer and working pistons, as reported in Fig. 4.12.
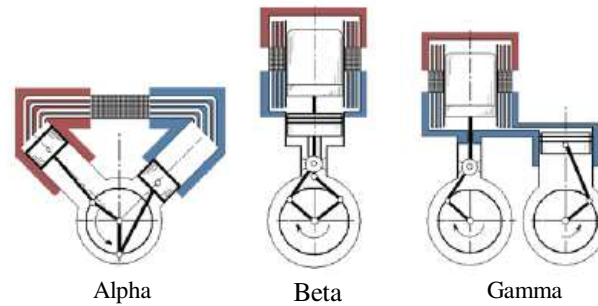
Fig. 4.12. Configurations of Stirling engines (modified from [108]).

Three typical configurations, known as alpha, beta and gamma are present in Fig. 4.12. In the alpha type, one piston compresses the fluid in the cold space and the other expands in the hot space. In the beta type, the working gas moves between hot and cold zones by using a displacer, and both compression and expansion are done by the working piston. Finally, in the gamma type, the working piston is placed in a separate cylinder.

Stirling engines have been distinguished as the leading technology for CHP applications (particularly the micro scale) for single dwellings. However, it is hard for the Stirling engines to compete available low cost, reliable and efficient systems, such as internal combustion based systems which are also suitable for small scale applications.

4.3.5 Fuel cell

Fuel cells are electrochemical systems in which the chemical energy of a fuel is directly converted into electricity and heat without including the process of combustion. Generally, fuel cells are characterized by a high efficiency, no moving parts, quiet operation, and low or zero emissions at the point of use. Fuel cells are present in the market with different designs, each suited to different applications.

Moreover, the modular stack design allows to overcome the obstacle of the minimum capacity limit, which is a problem for mechanical heat engines. Fuel cells can be used in many applications, such as prime movers or auxiliary systems in automobiles, large scale electrical power, micro scale CHP systems (1-5 kW_e) suitable to domestic application and small scale CHP systems (tens of kW_e) suitable for commercial and municipal applications.

As can be seen from Fig. 4.13, a fuel cell is composed of an anode, electrolyte and cathode.
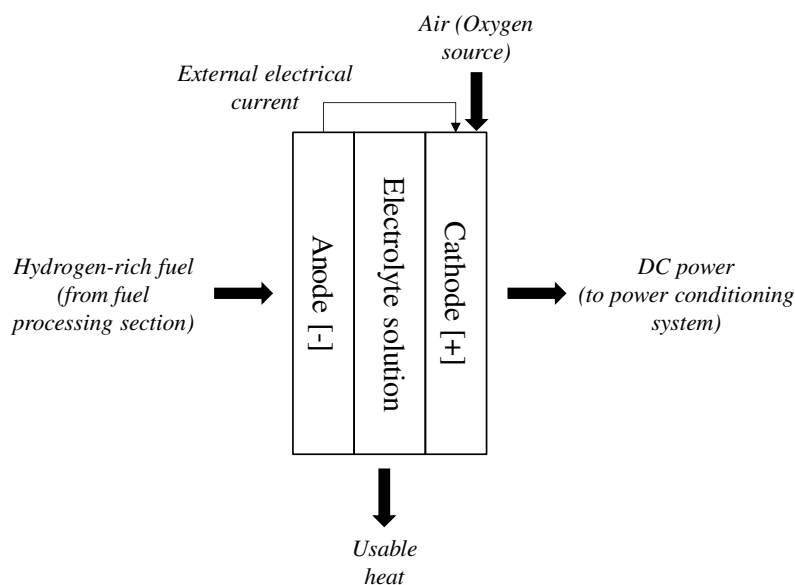
Fig. 4.13. PEFC operation (modified from [109]).

The basic operation of a polymer electrolyte fuel cell (PEFC) is highlighted in Fig. 4.13. The fuel processing section converts the input fuel into hydrogen-rich gas required to support an electrochemical reaction which takes place in the power section. The conversion of fuel into hydrogen is performed by using a steam reformer and shift converter. Gaseous and liquid fuels can be used depending on the design of fuel processing section.

In the power section or stack, the combination between hydrogen and oxygen generates dc power, thermal energy and steam. stacks are formed from several hundreds of identical electrochemical cells, and each cell consists of a porous cathode, a porous anode and electrolyte. The oxygen-rich gas passes over the surface of the anode, while air flows over the cathode. In some designs, the excess heat is removed by means of cooling coils.

The incoming hydrogen, entering the cell anode, discharges electrons and the formed ions pass through a conductive electrolyte to combine with oxygen at the cathode. The stripped electrons pass through the external circuit producing an electric current. Considering that several technologies exist, the exact reactions that occur depend on the fuel cell technology. Generally, for hydrogen fueled cells, the overall reaction is: $H_2 + \frac{1}{2} O_2 \rightarrow H_2O$.

The ideal fuel for most fuel cell types is hydrogen because its use allows a high performance and durability. However, it is not possible to use the hydrogen directly at the point of use as there is no hydrogen generation or distribution infrastructure. Alternatively, micro CHP systems based on fuel cells use hydrocarbons that can be reformed into hydrogen at the point of use. Generally, commercial

64

fuel cell micro CHP systems are fueled by natural gas, LPG or kerosene. In order to obtain the desired voltage and current flow, the stacks are constructed with a specific number of cells and cell area.

In the power conditioning section, direct current (DC) power is converted into alternating current (AC) power by using solid-state inverters. The alternating current power is produced at a given voltage and frequency (see Fig. 4.14).
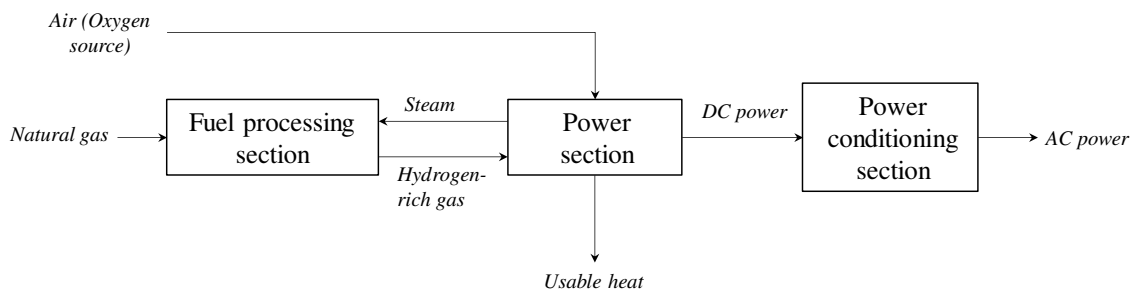
Fig. 4.14. Functional diagram of fuel cell (modified from [109]).

For domestic CHP applications, fuel cell stack must have low cost manufacture and long operating lifetime in suboptimal conditions, safety, practicality and high operating efficiency. Four fuel cell systems are suitable for CHP applications:

- PEFC: polymer electrolyte fuel cells;
- SOFC: solid oxide fuel cells;
- PAFC: phosphoric acid fuel cells;
- AFC: alkaline fuel cells.

The abovementioned technologies share the same operating principles, while they differ in the way they achieve their electrochemical reactions. In particular, the diverse materials of construction, the range of operating temperatures and fuels toleration are the main differences between the different technologies.

An intense research and commercial development interest domestic CHP systems based on PEFC and SOFC stacks, while PAFC and AFC stacks did not succeed to be commercialized due to high manufacturing cost and low life time.

The residential sector is the largest market for fuel cell micro CHP systems, where fuel cell systems are used to fulfill the thermal and electric energy demands needed by a typical home. The sizes of such systems are of the order of a few kW_e with nearly the same kW_{th} produced. An auxiliary condensing boiler is to satisfy the thermal demand possibly not fulfilled by the fuel cell.

Compared to CHP systems based on engines, fuel cells are characterized by a higher electrical efficiency. They can also compete modern combined cycle gas turbine. However, their overall efficiency, including heat and power, is lower than engines, due to difficulties in capturing low-grade waste heat.

4.4. Absorption chiller

The cycle of ABSs is similar to vapor compression cycle systems, but the compression process is replaced by the application of heat to drive the cycle. As highlighted in Fig. 4.15, a basic ABS cycle is composed of four components: absorber, generator, condenser and evaporator.
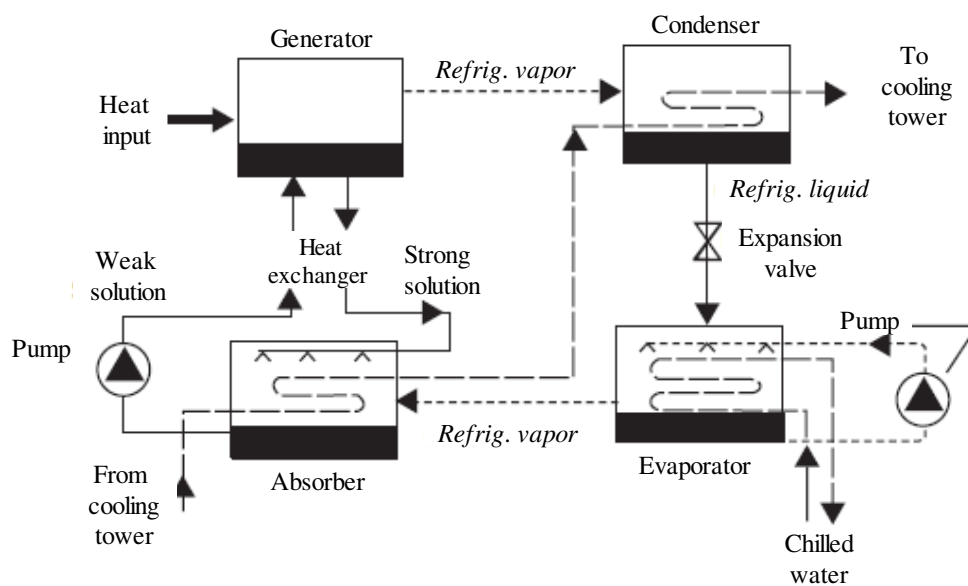
Fig. 4.15. Basic cycle of an ABS (modified from [109]).

As can be seen, the low pressure refrigerant vapor entering the absorber is condensed and absorber by the concentrated absorbent solution. Cooling water is used to remove the heat of condensation and heat of absorption. After, the weak solution which is a combination of the refrigerant vapor and the strong solution is pumped into the generator. The generator produces heat and a boiling process separates the refrigerant and absorbent. Hot concentrate solution is cooled by a heat exchanger using incoming weak solution as it leaves the generator and is throttled back to the absorber. Then, the refrigerant vapor characterized by a high pressure and high temperature flows to the condenser, rejects the heat and turns into liquid. Next, the warm liquid refrigerant expands through an expansion valve and enters the evaporator. The liquid evaporates at low pressure and temperature by absorbing heat from a low temperature source. In many ABSs, the refrigerant is pure water and the evaporation occurs under vacuum condition.

Compared to the vapor compression cycle, condenser, evaporator and expansion valve are the same in an absorption cycle, while the compressor is replaced by the absorber and generator.

Absorption cycles based on the lithium bromide (LiBr) cycle and ammonia-water ($NH3H2O$) are the two widely used absorption cycles. In the LiBr cycle, water is the refrigerant and LiBr is the absorbent, while in the ammonia-water cycle, the solution ammonia-water is the refrigerant and water is the absorbent. The LiBr cycle is mostly used in large capacity units, while the ammonia-water cycle is commonly used in small capacity direct fuel-fired single-effect systems or larger capacity custom-designed units for low temperature industrial applications.

For LiBr cycles, two variations are present: single-effect or double-effect cycles. In single-effect cycles, low pressure steam or hot water can be used as energy source. Typical temperature requirements are between 93 and 132°C. Systems which are powered by steam generally operates at pressures between 1.6 and 2.0 bar. Although single-effect absorption systems are considered relatively thermally inefficient by the actual standards, these systems are beneficial when steam costs are low or when recovered heat can be used. Double-effect cycles are more thermally efficient than single-effect cycles. In this type of cycles, the heat recovered from the first stage condensing process is used to boil additional refrigerant at a lower temperature in the second stage. Indeed, a second generator, condenser and heat exchanger (that operate at high temperature) are used in these systems, where refrigerant vapor is recovered from the first stage generator in the high temperature condenser and the heat from this condensing process is used to boil additional water from the low-temperature, second stage generator. Moreover, a heat exchanger is used to recover heat from solution leaving the low-temperature generator. The double-effect cycle allows a thermal efficiency improvement of about 70% to be achieved compared to the single-effect cycle. The double-effect cycle is highlighted in Fig. 4.16.
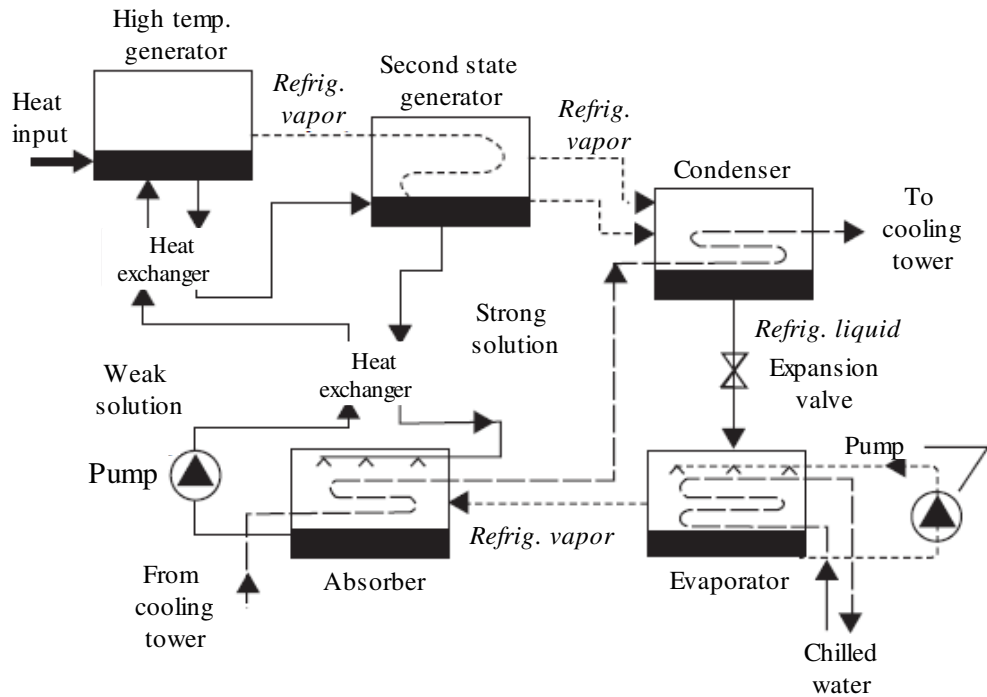
Fig. 4.16. LiBr double-effect absorption cycle (modified from [109]).

Double-effect cycles operate at a temperature of about 188°C which corresponds to a saturated steam pressure of about 8.9 bar.

Triple-effect LiBr ABSs have been also prototyped and developed. These systems follow the direct fired designs and are expected to provide about 50% thermal efficiency improvement over existing double-effect technologies. Moreover, they are expected to have full load COPs in excess of 1.4. Indeed, they increase the use of internally recovered heat to achieve high thermal efficiencies.

Double-effect LiBr ABSs are characterized by a higher COPs than the ammonia-water technologies. The LiBr units are not able to achieve temperatures below about 4.4°C. In contrast, ammonia water cycles may achieve extremely low evaporator temperatures and for some applications, they compete vapor compression technologies on a cost and efficiency basis. Ammonia water systems have been used for various process refrigeration, such as ice storage. In addition, the ammonia based refrigerant allows to operate at condenser pressures of up to 20.1 bar and at evaporator pressures of about 4.8 bar.

ABSs based on ammonia water cycle have been mostly used in residential refrigerators and air conditioners. Currently, they are used in custom designed systems for low temperature industrial applications and in small-capacity, direct-fired air-cooled units.

The performance of a refrigeration cycle is represented by the Coefficient of Performance (COP), which considers the amount of work required to remove a given amount of heat from the low-temperature source. in other words, the COP is defined as follows:

$$COP = \frac{Refrigeration\ effect}{Heat\ input} \tag{4.8}$$

Where; the refrigeration effect is represented by the net amount of heat the system removes from the conditioned space or process load, and the heat input is the net amount of energy transferred to the generator to accomplish the refrigeration effect. Single effect ABS systems may have COP values in the range 0.6-0.75, double effect ABS systems can have COP values in the range 1.1-1.3 and triple effect machines can assume COP values around 1.5.

4.5. Vapor compression chillers

In actual vapor compression cycle systems, the heat rejected from the cycle is equal to the refrigeration effect plus the driving energy to the compressor. As can be seen from Fig. 4.17, the four basic components used in the vapor compression cycle are: a compressor, a condenser, an expansion valve and an evaporator.
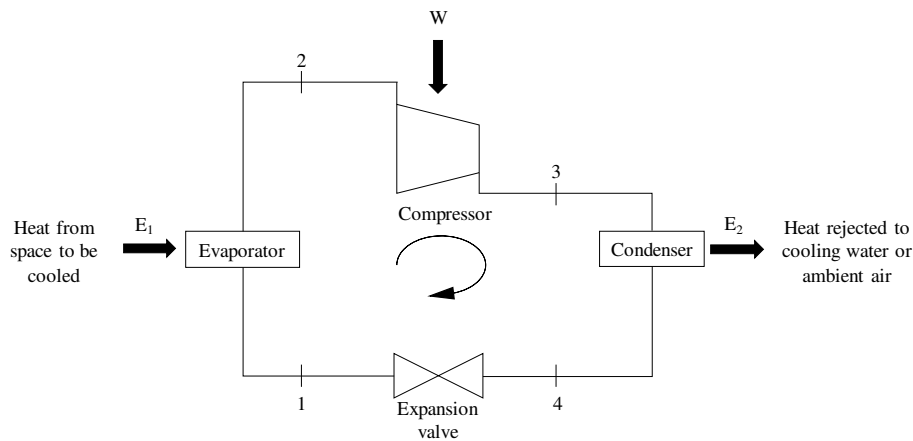
Fig. 4.17. Diagram of a basic vapor compression refrigeration cycle.

The vapor compression cycle system operates in the following manner:

- Evaporator (1-2): the refrigerant enters the evaporator as a two phase liquid-vapor mixture. The heat transferred from the conditioned space to the refrigerant allows a phase change of the refrigerant from liquid to vapor. The transformation occurs at a constant temperature and constant pressure.

- Compressor (2-3): the refrigerant is compressed causing an increase of both pressure and temperature. The compressor delivers the refrigerant to the condenser at a pressure and temperature at which the condensing process can be readily accomplished.
- Condenser (3-4): the refrigerant passes through the condenser where it changes from a superheated vapor to a subcooled liquid as heat is rejected to the warm air region. The transformation occurs at a constant high temperature and pressure.
- Expansion valve (4-1): the expansion valve reduces the pressure and temperature of the refrigerant.

Vapor compression technologies can be categorized by compressor type which can be hermetic or open-drive design. The five basic refrigeration compressors are: rotary compressors, scroll compressors, reciprocating compressors, screw compressors and centrifugal compressors. Rotary compressors are commonly used in appliances such as refrigerators of less than 18 kW and the scroll compressor is used in applications of about 18 to 35 kW. The reciprocating, screw and centrifugal compressor types are the three major types and are used for almost all larger-capacity applications [109].

Chillers which use refrigerant-to-liquid evaporators are almost used for large central air conditioning systems. They are also sometimes used in smaller units. Systems which use refrigerant-to-air type evaporators provide direct cooling as the refrigerant absorbs heat directly from the air being cooled. These systems are used in applications up to 100 kW.

The energy rejected to the higher temperature region (E_2) equals the work performed by the compressor (W) plus the thermal energy removed from the space to be cooled (E_1). The performance of a vapor compression cycle is defined by the Energy Efficiency Ratio (EER):

$$EER = \frac{E_1}{Work} \tag{4.9}$$

4.6. Heat pumps

Heat pumps are systems designed to absorb heat and transfer it to serve a heat requirement. They can provide thermal heating energy only or both heating and cooling energy. Numerous types of heat pump system designs are present in the market and various heat sources are used. Some systems are used to provide only heating, while others reverse their cycles to deliver both heating and cooling. However, all systems are based on the same operating principle, i.e. absorb heat from one medium and transfer to another [110].
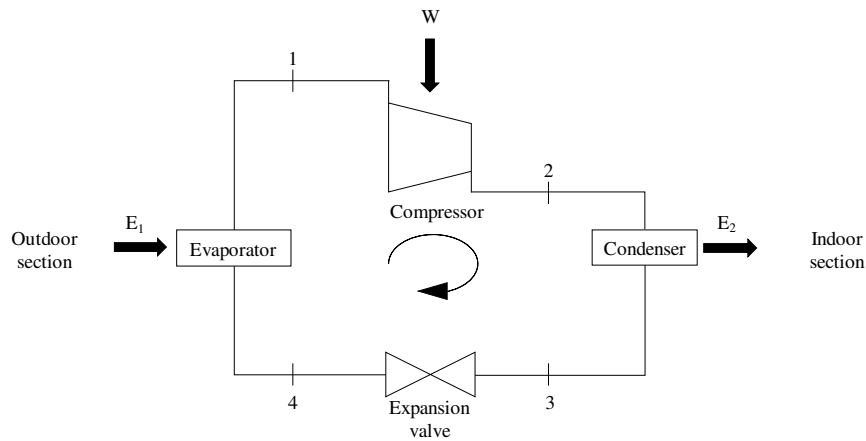
Fig. 4.18. Heating cycle of a heat pump.

Figure 4.18 shows a heat pump operating in heating mode. The heat is absorbed by the low-pressure liquid refrigerant which becomes a low-pressure vapor in the evaporator. The vapor then flows to the compressor and is transferred to the condenser as a high-temperature vapor. The heat absorbed from the evaporator and the compression is discharged from the refrigerant in the condenser, directly or indirectly, to the conditioned space.

The performance of a heat pump in heating mode is defined by the COP, represented by the ratio of heat output to energy input:

$$COP = \frac{E_2}{W}$$
(4.10)

In practice, most heat pumps operate as efficient heaters moderate temperatures, i.e. above 4.4°C. The capacity and efficiency decrease dramatically when the ambient temperature approaches freezing and eventually an auxiliary heating system is needed to maintain heating capacity.

When the unit is working in cooling mode, a reversing valve changes position to reverse the refrigerant flow. In this case, the heat is absorbed from the space to be cooled in the evaporator and the heat absorbed from the evaporator and the compression is discharged from the refrigerant in the condenser, directly or indirectly, to cooling water or ambient air.

In cooling mode, the performance of a heat pump is defined by the EER and is represented by the ratio of heat absorber by the evaporator to the energy provided to the compressor:

$$EER = \frac{E_1}{W}$$
(4.11)

Air source heat pump: Outdoor air is unlimited heat source for heat pumps and is widely used in small capacity systems. When air source is used, a large surface area is required for the heat exchanger because air is relatively inefficient heat transfer medium. The set point design of an ASHP is a critical task, because the outside air temperature fluctuates so widely. The heating capacity and efficiency of

an ASHP decreases if the outdoor temperature decreases. Thus, an auxiliary heating systems is usually necessary in colder climate zones. When the heat pump is working in cooling mode, the cooling capacity and efficiency decreases if the outdoor temperature increases.

During heating period, the heat pump removes heat from the outside air which evaporates the refrigerant in the outdoor coil. The absorbed heat is then transferred to the indoor space. ASHPs are usually the cheapest type of heat pumps and this is because heat transfer with air systems is not as efficient as with water systems [110].

Water source heat pump: Various types of water sources, such as surface water from lakes, oceans and rivers, can be used as heat source for heat pumps. Other sources including municipal water supply, cooling tower water and various types of waste water can be also used.

The temperature of the water source is a function of climate and source depth. When surface water sources are used, the temperature drop across the evaporator in winter may cause freeze-up. Therefore, the temperature-drop needs to be limited and water quality should be analyzed for the potential of scale formation and corrosion. The water source may directly enter to the evaporator or pass through a heat exchanger to avoid the potential for contamination [110].

There are two types of water source heat pumps: water-water heat pumps and water-air heat pumps. The last first type of system uses water in the outdoor coil as the heat source and water in the indoor coil, while the second option uses water in the outdoor coil as the heat source and air to transmit heat in the indoor coil. The water-water heat pumps are very efficient compared to other types, but are characterized by high capital cost and require a substantial amount of maintenance. Instead, the water-air system has a lower capacity than a water-water heat pump and the indoor coil requires less maintenance.

Ground source heat pump: In this type of systems, the coil is buried five or more feet underground. These systems are commonly designed to operate through a secondary loop in which heat is transferred between a circulating brine and the ground. The heat is extracted from the ground which is characterized by a fairly constant temperature all year. GSHP are usually not highly efficient and the cost of repairing damage occurring in the buried coil. However, costs of maintenance and repair may be reduced if coil degradation associated with corrosive air or water conditions is avoided [110].

4.7. Energy storage

Energy storage is highly important for any intermittent source of energy, such as the solar energy. Energy storage systems play a key role in matching the energy supply and demand because the profile

of the energy production system does not generally match the energy demand profile. Thermal energy storage has attracted increasing interest for many applications such as space heating, hot water, cooling and air conditioning.

Many benefits can be achieved by using thermal energy storage system, such as reduced energy costs, reduced energy consumption, improved indoor air quality, increased flexibility of operation, reduced initial and maintenance costs, reduced equipment size, more efficient and effective utilization of equipment and reduced pollutants and greenhouse gas emissions. The systems achieve also benefits by increasing the generation capacity, enabling better operation of cogeneration plants, shifting energy purchases to low-cost periods. Thermal energy storage systems can be classified as sensible heat storage and latent heat storage [111].

Sensible heat storage: In sensible heat storage, the temperature of the storage material varies with the amount of energy stored. Thus it is better to have a storage medium which have a high specific heat capacity, long term stability cycling under thermal cycling and most importantly, low cost. Water is one of the best storage media. It is characterized by a higher specific heat than other materials, and it is cheap and widely available. Water can be used in a range of temperatures between 25°C and 90°C. Hot water is required for washing, bathing etc., and it is commonly used for space heating. Indeed, it is the most widely used storage medium for space heating applications. Water storage tanks are made from materials like steel, aluminum, reinforced concrete and fiber glass. As insulation materials, glass wool, mineral wool or polyurethane can be used. The sizes of water tanks vary from a few hundred liters to a few thousand cubic meters. For large scale storage applications, underground natural aquifers may be used. These aquifers consist of geological formations containing ground water and offering a potential way of storing heat for long periods of time. The sizes of these aquifers range from hundreds of thousands to millions of cubic meters.

The most commonly proposed substitutes for water are petroleum based oils and molten salts. Compared to water, the substitutes fluids are characterized by lower heat capacities, e.g. 25-40% of that of water on weight basis. Nevertheless, the vapor pressure of these substitutes is lower than water and, consequently, they are capable of working at temperature levels exceeding 300°C. for stability and safety reasons, the operating temperature of oils is limited to less than 350°C. Terminol and Caloria-HT are some of the oil candidates that have been considered for thermal storage applications. As molten mixtures, sodium hydroxide could be used for temperatures up to 800°C [111].

Latent heat storage: Latent heat storage is an attractive technique because it provides a high energy storage density and is able to store heat as latent heat at the phase transition temperature of the

materials. Solid-liquid phase change materials are the most suitable for thermal storage applications because of their capability to store a relatively large quantity of heat over a close range of temperature, without a corresponding large volume change which occurs in liquid-gas phase change materials. The latent heat storage units utilize the sensible heat in the solid and liquid phases and additionally the latent heat corresponding to the phase change of the storage medium. The basic components of a latent heat thermal energy storage are: a heat storage medium that undergoes a solid-liquid phase change in the required operating temperature, a tank for holding the storage medium and a heat exchanger for the transfer of heat from the heat source to the storing medium and from the latter to the heat user.

A large number of latent heat storage mediums have been suggested for thermal storage applications in temperature ranges suitable for heating and cooling applications. These can be classified into: inorganic compounds, organic compounds and eutectics of inorganic and/or organic compounds. Inorganic compounds include salt hydrates, salts, metals and alloys, organic compounds are comprised of paraffins, non-paraffins and polyalcohols and eutectics consist in mixtures of two or more salts which have definite melting/freezing points. The abovementioned phase change materials have good potential for low temperature thermal energy storage applications [111].

5. Optimization of hybrid energy plants by accounting for on-site primary energy consumption

This chapter is dedicated to the application of a new methodology for sizing and operating optimization of HEPs by only minimizing on-site primary energy consumption. The methodology developed in this chapter, is based on Dynamic Programming (DP) techniques. After the introduction, the original DP-DP optimization method, the mathematical models of the HEP components considered in this study (solar thermal collector, photovoltaic panel, combined heat and power, ground and air source heat pumps, auxiliary boiler and hot water storage) are presented. Then, a methodology based on Genetic Algorithm (GA) used as a benchmark is described. After, the application of the two methods on a case study is illustrated and finally the results are discussed.

5.1. Introduction

DP is an optimization method which has recently attracted lots of research in the area of energy systems. Generally, DP is a method which can efficiently deal with linear and nonlinear functions and constraints and obtain global optimal solutions in the discrete state space [112]. This method is based on the principle of optimality, i.e., an optimal policy, whatever the previous state and decision, the remaining decisions must constitute an optimal policy with regard to the state resulting from the previous decision [112]. The basic idea of DP is a multistage optimization problem in the sense that at each of the finite set of times, a decision is made from a finite number of decisions based on the adopted optimization criterion. It is a general approach to making a sequence of interrelated decisions in an optimum way and is suitable for dynamic systems.

The DP method is mainly used to solve optimal control problems where the behavior of a physical system is described by a state variable and can be controlled by a control variable [113]. It is widely used to solve energy management problems and to make decisions on HEP operation [114]. However, it is only adopted for energy management and systems scheduling applications. Therefore, it would be interesting to find some new ways to extend the application of the DP method to deal with other optimization problems, particularly for solving sizing and operating optimization of HEPs.

This work proposes a new DP based optimization method, called the DP-DP method, to solve both sizing and operating optimization problems of HEPs. The optimization problem is made on an energy-based criterion, i.e. with the aim of minimizing the on-site primary energy consumption over the simulation period, to demonstrate the effectiveness of the presented methodology. However, any other objective function, such as pollutant emissions or total energy cost, could be implemented in the

framework defined here. Unlike previous research, the work in this part extends the use of the DP method and attempts to apply it to solve both the sizing and operating optimization problems. The proposed method does not require any supplementary evolutionary algorithms to solve the problem. Thus, the proposed method is fast, easy to implement and also addresses the nonlinearity associated with the characteristics of the plant.

5.2. Methods and materials

A new method based on the DP algorithm is presented in this study for sizing and operating optimization of HEPs. The optimization of the HEP is conducted by minimizing the primary energy consumed throughout the simulation period. However, a different objective function, such as pollutant emissions or total cost, may be also implemented. A model for the simulation of the HEP is implemented in Matlab®. The model takes into account the variability in terms of the performance of the considered systems according to both external air temperature and load. The analysis is carried out on an hourly basis.

5.2.1 The hybrid energy plant

Figure 5.1 shows a scheme of the HEP used to fulfill the building's energy demands. The HEP is composed of a Solar Thermal Collector (STH), Photovoltaic Panel (PV), Combined Heat and Power (CHP), Ground Source Heat Pump (GSHP), Air Source Heat Pump (ASHP), Auxiliary Boiler (AB) and hot water storage (STORAGE).
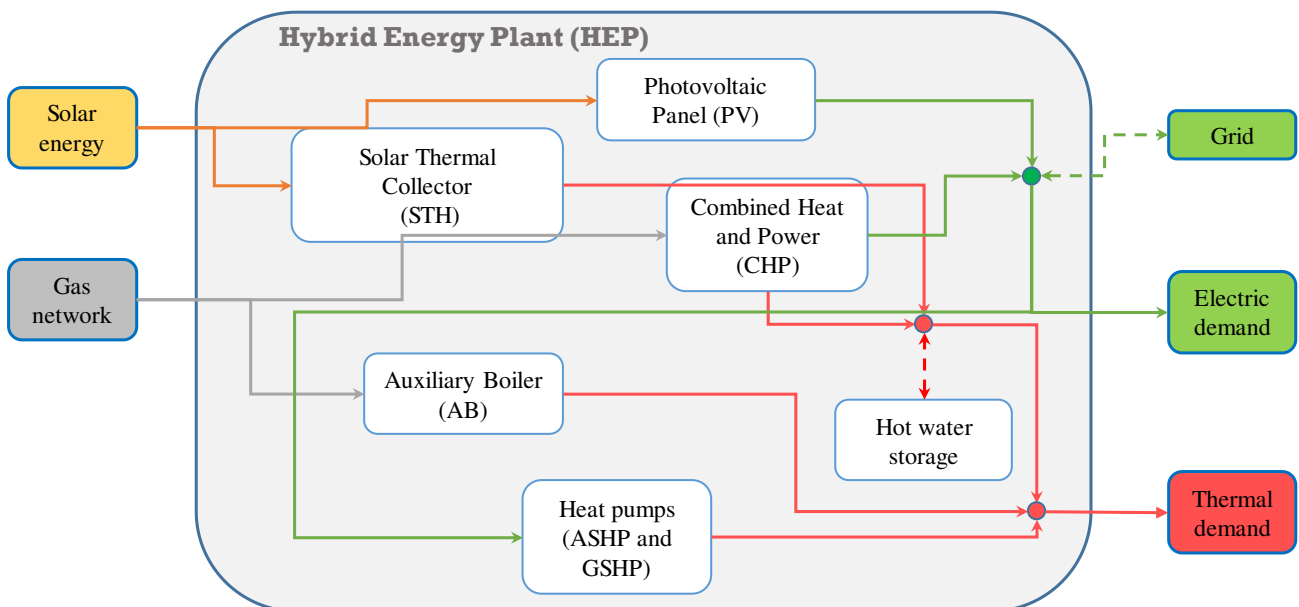

Fig. 5.1. Layout of the HEP

Thermal energy and electrical energy balance are expressed as following:

$$\mathcal{E}_{\text{th, k}} = \mathcal{E}_{\text{STH, th, k}} + \mathcal{E}_{\text{CHP, th, k}} + \mathcal{E}_{\text{GSHP, th, k}} + \mathcal{E}_{\text{ASHP, th, k}} + \mathcal{E}_{\text{AB, th, k}} + \mathcal{E}_{\text{STORAGE, th, k}} \tag{5.1}$$

$$\mathcal{E}_{\text{el, k}} = \mathcal{E}_{\text{PV, k}} + \mathcal{E}_{\text{CHP, el, k}} + \mathcal{E}_{\text{grid, el, k}} - \mathcal{E}_{\text{GSHP, el, k}} - \mathcal{E}_{\text{ASHP, el, k}} \tag{5.2}$$

These energy balances ensure the fulfillment of thermal and electrical energy demands at each time step k (equal to one hour). As can be seen from Eq. (5.1), building thermal energy demand ($\mathcal{E}_{\text{th,k}}$) is fulfilled by the thermal energy produced by the STH ($\mathcal{E}_{\text{STH,th,k}}$), CHP unit ($\mathcal{E}_{\text{CHP,th,k}}$), GSHP ($\mathcal{E}_{\text{GSHP,th,k}}$), ASHP ($\mathcal{E}_{\text{ASHP,th,k}}$) and STORAGE ($\mathcal{E}_{\text{STORAGE,th,k}}$). If the thermal demand is not fulfilled by the previous systems, the remaining part will be fulfilled by the AB ($\mathcal{E}_{\text{AB,th,k}}$). Moreover, the thermal energy produced by the CHP and STH is used to fulfill the thermal demand and to fill up the STORAGE. From Eq. (5.2), the electricity produced by the PV ($\mathcal{E}_{\text{PV,el,k}}$) and CHP ($\mathcal{E}_{\text{CHP,el,k}}$) systems is used to meet the building electricity demand ($\mathcal{E}_{\text{el,k}}$) and the electricity required by the GSHP ($\mathcal{E}_{\text{GSHP,el,k}}$) and ASHP ($\mathcal{E}_{\text{ASHP,el,k}}$) systems. If the PV and CHP systems are not able to fulfill the required electricity, the remaining part is imported from the grid ($\mathcal{E}_{\text{grid,el,k}}$). Otherwise the excess of the produced electric energy from these systems is sent to the grid.

The primary energy consumed throughout the simulation period to be minimized is defined as follows:

$$PE = \sum_{k=0}^{N-1} PE_{\text{fuel, CHP,k}} + PE_{\text{fuel, AB,k}} + \Delta PE_{\mathcal{E}_{\text{el,k}}} \tag{5.3}$$

where;

$$\Delta PE_{\mathcal{E}_{\text{el,k}}} = PE_{\mathcal{E}_{\text{el, taken,k}}} - PE_{\mathcal{E}_{\text{el, sent,k}}} \tag{5.4}$$

As can be seen from Eq. (5.3) and (5.4), the primary energy consumption (PE) is defined as the sum of the consumption of the CHP ($PE_{\text{fuel,CHP,k}}$), AB ($PE_{\text{fuel,AB,k}}$) and the primary energy associated with the electrical energy exchanged with the grid ($\Delta PE_{\mathcal{E}_{\text{el,k}}}$).

5.2.1.1 Plant components models

The energy systems composing the HEP are defined by power and efficiency as grey-box models. For each technology, the basic correlations are summarized below.

Photovoltaic panel

The total efficiency of the photovoltaic panel takes into account the efficiency of the photovoltaic panel ($\eta_{PV,ref}$) and the efficiency of the inverter and electrical connections (η_{BoS}) considering design condition values of 0.12 and 0.9, respectively [115]. The efficiency of the PV system is calculated by Eq. (5.5):

$$\eta_{PV} = \eta_{PV,ref} \cdot \eta_{BoS} \cdot \left[1 - \beta \cdot \left(T_c - T_{ref} \right) \right] \tag{5.5}$$

where β is a temperature penalty coefficient and T_c and $T_{c,ref}$ are the operating and reference temperature of the cell, respectively. The output power of the photovoltaic panel is not controlled by any device and it only depends on radiant power and electrical efficiency, both correlated with external air temperature.

Solar thermal collector

The efficiency of the solar thermal collector is calculated as follows [105]:

$$\eta_{STC} = \eta_o - a_1 \cdot \left(\frac{T_{av} - T}{R} \right) - a_2 \cdot \left(\frac{T_{av} - T}{R} \right)^2 \tag{5.6}$$

where η_O is the optical efficiency, a_1 and a_2 correction factors, T_{av} the average temperature assumed equal to 50 °C, T_k the temperature at the kth time step and φ the incident radiant power. Like the PV system, the output power of the STC is not controlled by any device and only depends on external conditions.

Combined heat and power system

The combined heat and power technology considered is based on an internal combustion engine. The nominal electrical efficiency and thermal power are calculated using Eq. (5.7) and (5.8) obtained by carrying out a market survey on CHP technologies with nominal electrical capacities in the range $0 \div 100$ kW$_e$ [29]:

$$\eta_{CHP,el,nom} = 0.232 \cdot \left(P_{CHP,el,nom} \right)^{0.084} \tag{5.7}$$

$$P_{CHP,th,nom} = 2.5 \cdot \left(P_{CHP,el,nom} \right)^{0.91} \tag{5.8}$$

A linear variation of the performance of the CHP with external air temperature and thermal load variation is assumed [29]. The minimum thermal load is supposed to be equal to 10% of the nominal load [116]. In order to reflect the physical behavior of the CHP, a penalty corresponding to the fuel consumed in five minutes at nominal conditions is added to model the CHP start-up.

Heat pumps

GSHP and ASHP systems are considered and modelled. It was supposed that the nominal performance of both systems is affected by the temperature of the external and internal heat exchangers and the thermal load. For both heat pumps, the minimum load is assumed equal to 10% of the nominal thermal load [29, 117].

Hot water storage

The hot water storage tank is linked with both the STH and CHP systems and can be filled up by the excess energy produced by these systems. The heat dissipation is also included in the storage model and assumed proportional to the stored energy. In particular, a dissipation coefficient of 0.5% is considered according to [118].

Auxiliary boiler

An auxiliary condensing boiler is considered and used to fulfill the thermal energy possibly not fulfilled by the other systems. The variation of the performance of the AB is also taken into account and it is assumed that the performance varies linearly with load variation. The nominal efficiency of the AB (on a LHV basis) is assumed equal to 1.06 [29].

5.2.2   The DP-DP method

In this context, the optimal size and control of the HEP are found by performing two runs of the DP algorithm. The main difference between the two runs lies in the way in which the technologies are modelled. The first run of the DP algorithm allows the combination of sizes considered as an optimal solution to be calculated, while the second run defines the optimal operating strategy of the different technologies.

5.2.2.1   Dynamic Programming

The DP method is a recursive method, like a computer routine that calls itself and adds information to a stack each time, until certain stopping criteria are met. Once the stopping condition is reached, the solution is get by removing information from the stack in the proper sequence [119]. The method consists of the following steps:

1. Define a small part of the entire problem and find an optimum solution to this small part.
2. Extend the small part slightly and find an optimum solution for it by using the optimum solution which was found previously.
3. Continue with Step 2 until the current problem turns into the original problem.

4. Track back the optimum solutions which were found for the small problems and obtain the solution of the whole problem.

A simple example of DP problem that helps to understand the working principle of the DP method is to find the shortest route to reach a certain destination. In this case, at each stage, the small part of the problem is described by the definition of the next closest node to the origin. Then, at each stage, the problem is slightly enlarged by adding all the unsolved nodes and arcs (lengths between two consecutive nodes) that are directly attached to a solved node. The problem is solved when the next closest node is the destination node. finally, the solution of the original problem is obtained by tracking back along the arcs, determined by solving the small sub-problems from destination back to the origin.

The main characteristics of DP method are reported in the following:

- *Stages:* the problem can be divided into stages. For example, in the shortest route problem, in order to find the next closest node to the origin, each stage constitutes a new problem to be solved. In DP control applications, the stages are related to time. In this type of applications, the stages are solved backwards in time, i.e. from a point in the future to back towards the present. The problem is solved backwards because it is more efficient to work in this way. In other words, the paths that lead from the present state to the future goal state are always just a subset of all the paths leading forward from the current state.

- *States:* in order to solve the small problem at a stage, an information about the states of the small problem to be solved, is needed. For example, the state in the shortest route problem is represented by the set of solved nodes, the arcs in the arc set and the arcs and nodes which are unsolved and directly connected to the solved nodes.

- *Decision:* the state at a stage is updated into the state for the next stage by making a decision. For example, in the shortest route problem, the decision determines which arc to add to the arc set and the corresponding unsolved node.

- *Principle of optimality:* given the current state, the optimal decision for the remaining stages is independent of decisions made in previous states. In other words, the original problem can be solved by breaking it into smaller pieces and solve them independently. In the shortest route problem, decisions are made by using only the information about the distance from the origin to a solved node and not the actual route (i.e. previous decisions) from the origin to that solved node.

- *Recursive:* a recursive relationship exists between the optimum decision at a stage and the optimum decisions at previous stages. In other words, the optimum decision at a stage is made by

using the optimum decisions at previous stages. In the shortest route problem, the recursive relationship between the actual decision and the previous decisions is as follows:

"length of shortest route from origin to node i= $\min_{i,j}$(length of shortest route from origin to solved node j + length of arc from solved node j to unsolved node i)"

The relationship is recursive because the "length of shortest route" appears on both sides of the relationship. As can be noted, the new optimum is always derived from the old optimum.

5.2.2.2 State-space model representation

In this research, the optimization problem is implemented using a Matlab® solver developed by [120] that deals with discrete-time optimal-control problems using Bellman's DP algorithm. The formulation of the optimization problem requires a state-space representation of the model as follows:

$$\chi_{z,k+1} = F\left(\chi_{z,k}, U_{z,k}, k\right) \tag{5.9}$$

$$\varepsilon_{z,k} = G\left(\chi_{z,k}, U_{z,k}, k\right) \tag{5.10}$$

where; χ represents the state variables, U the input variables and ε the output variables of the technology z at time step k. In this study, the state-space model is discretized with a discretization interval k of one hour. Two states are identified, χ_{CHP} and $\chi_{STORAGE}$, corresponding to the CHP operating condition and the storage state of charge, respectively. The CHP state (χ_{CHP}) is represented by the binary numbers 1 and 0 which represent the on-off condition of the CHP at the beginning of the kth time step. The state of the CHP is updated as follows:

$$\chi_{CHP,k+1} = \begin{cases} 1 & if & U_{CHP,k} \neq 0 \\ 0 & if & U_{CHP,k} = 0 \end{cases} \tag{5.11}$$

The storage state of charge is updated as follows:

$$\chi_{STORAGE,k+1} = \left(1 - c_{diss}\right) \cdot \left(\chi_{STORAGE,k} + \varepsilon_{STORAGE, th, in, k} - \varepsilon_{STORAGE, th, out, k}\right) \tag{5.12}$$

Input variables U are used to control the HEP and they represent the load share (i.e. the fraction of thermal energy demand) of the controllable technologies involved in the plant. For each technology the power output can be represented by the following equation:

$$\varepsilon_{z,k} = U_{z,k} \cdot \varepsilon_{z,k,\max} \tag{5.13}$$

$\varepsilon_{z,k,\max}$ is the maximum energy which can be produced by the technology z at the kth time step. For the definition of the problem, constraints and discretization of states and inputs should be defined as follows:

$$\chi_{z,k} \in \left[\chi_{z,\min}, \chi_{z,\max}\right] \tag{5.14}$$

$$U_{z,k} \in \left[U_{z,\min}, U_{z,\max}\right] \tag{5.15}$$

$\chi_{z,\min}$ and $\chi_{z,\max}$ are the minimum and maximum states that technology z can assume. While, $U_{z,\min}$ and $U_{z,\max}$ represent the minimum and maximum load.

Four input variables U_{CHP}, U_{GSHP}, U_{ASHP} and $U_{STORAGE}$ are used to control the HEP plant and they represent the load shares of the CHP, GSHP, ASHP and STORAGE systems. In particular, for the CHP system, the output thermal energy and electrical energy at the kth time step are described by the following equations:

$$\varepsilon_{CHP,th,k} = U_{CHP,k} \cdot P_{CHP,th,\max,k} \cdot \Delta k \tag{5.16}$$

$$\varepsilon_{CHP,el,k} = \eta_{CHP,el}(U_{CHP}, k) \cdot \frac{\varepsilon_{CHP,th}(U_{CHP}, k)}{\eta_{CHP,th}(U_{CHP}, k)} \tag{5.17}$$

For the GSHP and ASHP systems, the output thermal energy is represented by Eq. (5.18), while the consumed electric energy is expressed by Eq. (5.19):

$$\varepsilon_{XSHP,th,k} = U_{XSHP,k} \cdot P_{XSHP,th,\max,k} \cdot \Delta k \tag{5.18}$$

$$\varepsilon_{XSHP,el,k} = \frac{\varepsilon_{XSHP,th}(U_{XSHP}, k)}{COP_{XSHP,th}(U_{XSHP}, k)} \tag{5.19}$$

where XSHP stands for GSHP and ASHP.

The thermal energy taken from the storage and used to fulfill the thermal energy demand is calculated as follows:

$$\varepsilon_{STORAGE,th,out,k} = U_{STORAGE,k} \cdot \chi_{STORAGE,k} \tag{5.20}$$
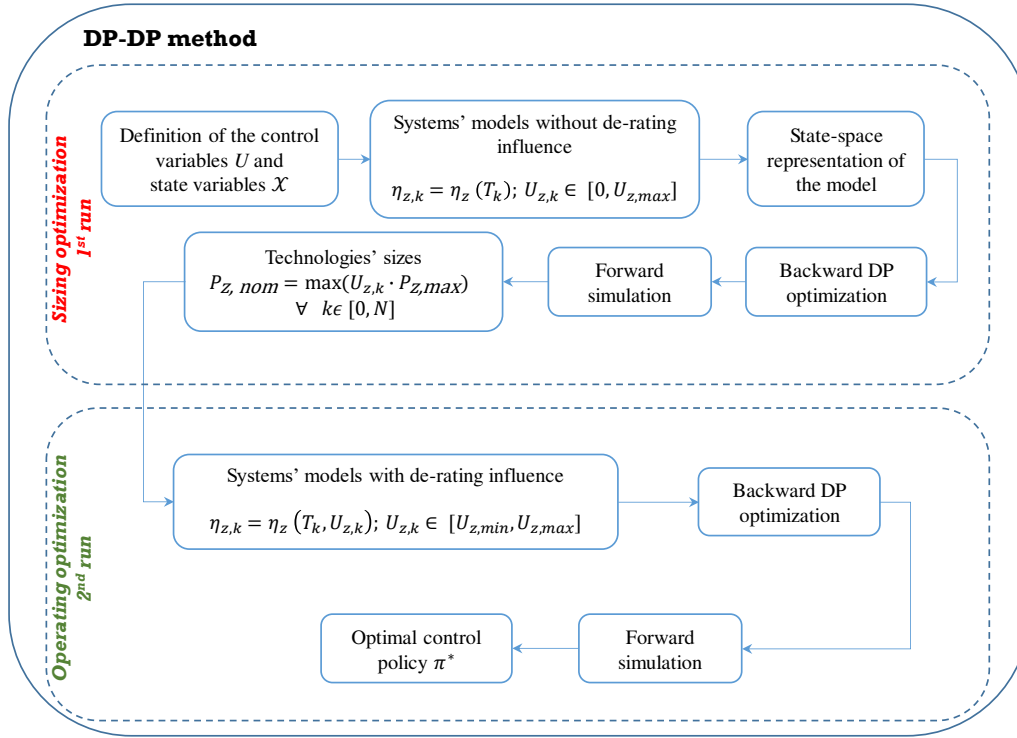
Fig. 5.2. Optimization flowchart of the new DP-DP method

Figure 5.2 outlines the methodology for sizing and operating optimization of HEPs.

5.2.2.3 Sizing optimization

As highlighted in Fig. 5.2, the first run of the DP is conducted considering only the variability of the efficiency (η_z) of the technology with external air temperature, i.e. supposing that load variation has no effect on the performance of the various technologies.

$$\eta_{\text{CHP,el},k} = \eta_{\text{CHP,el},k}(T_k) \tag{5.21}$$

$$COP_{\text{XSHP},k} = COP_{\text{XSHP}}(T_k) \tag{5.22}$$

Moreover, the technological limit of the technologies is ignored assuming that the systems are able to operate at a load $\mathcal{U}$ lower than their minimum load as reported in the following equations:

$$U_{\text{CHP},k} \in \left[0, U_{\text{CHP,max}}\right] \tag{5.23}$$

$$U_{\text{XSHP},k} \in \left[0, U_{\text{XSHP,max}}\right] \tag{5.24}$$

The sizing optimization range, for the considered technologies, is defined by calculating the maximum power that can be produced by the CHP, GSHP and ASHP systems:

$$\varepsilon_{\text{CHP,el,max}} = \max(\varepsilon_{\text{el},k}) \qquad \forall k \in \left[0, N\right] \tag{5.25}$$

83

$$\varepsilon_{\text{XSHP,th,max}} = \max(\varepsilon_{\text{th},k}) \qquad \forall k \in [0, N] \tag{5.26}$$

$\varepsilon_{\text{CHP,el,max}}$ and $\varepsilon_{\text{XSHP,th,max}}$ represent the upper limit of the sizing optimization range for the CHP, GSHP and ASHP systems. Thus, during the first run of DP algorithm, the abovementioned technologies are free to modulate between 0 and $\varepsilon_{\text{CHP,el,max}}/\varepsilon_{\text{XSHP,th,max}}$. From Eq. (5.25) and (5.26), depending on the type of technology, the term ε on the right side, could be a thermal, cooling or electric energy demand. If the system is a co-generator or a reversible heat pump, ε represents the energy demand that the system is most required to meet, i.e. the energy demand which governs the system operation (i.e. heat led, electricity led, etc…). It should be mentioned that, during the first run, the performance of the CHP, GSHP and ASHP systems is defined considering their maximum load.

Once the first run is performed, the optimal size of each technology *z*, is defined by calculating the maximum power allocated to each technology as follows:

$$P_{z,\text{nom}} = \max\left(\frac{U_{z,k} \cdot \varepsilon_{z,\text{max}}}{\Delta k} \right) \qquad \forall k \in [0, N] \tag{5.27}$$

5.2.2.4 Operating optimization

The second step of the DP-DP optimization method consists of optimizing the operation of the HEP once the optimal combination of sizes is found by the previous step. In this step, the optimal control policy is defined taking into account the variability of systems efficiency according to both external air temperature and load. Therefore, the operating optimization step is performed by modifying Eq. (5.21) and (5.22) to the form expressed in Eq. (5.28) and (5.29), respectively:

$$\eta_{\text{CHP,el},k} = \eta_{\text{CHP,el},k}(T_k, U_{\text{CHP},k}) \tag{5.28}$$

$$COP_{\text{XSHP},k} = COP_{\text{XSHP}}(T_k, U_{\text{XSHP},k}) \tag{5.29}$$

Therefore, the performance of the CHP, GSHP and ASHP systems turn into a function of both external air temperature and load. Moreover, the control variables U are set again so that they can assume values in the actual interval of loads in which each technology can modulate:

$$U_{\text{CHP},k} \in [U_{\text{CHP,min}}, U_{\text{CHP,max}}] \tag{5.30}$$

$$U_{\text{XSHP},k} \in [U_{\text{XSHP,min}}, U_{\text{XSHP,max}}] \tag{5.31}$$

5.2.2.5 Optimal policy evaluation

The sizing and operating optimization steps are conducted with the aim of finding the optimal policy which minimizes the primary energy consumption expressed by Eq. (5.3).

Let π^* be the optimal policy, which corresponds to:

$$\pi^* = \arg \min_{\pi \in \Pi} PE_\pi(\chi_0) \tag{5.32}$$

where;

$$PE_\pi(\chi_0) = \sum_{k=0}^{N-1} PE_{\text{fuel, CHP}}(\chi,U,k) + PE_{\text{fuel, AB}}(\chi,U,k) + \frac{\varepsilon_{\text{el,taken}}(\chi,U,k)}{\eta_{\text{el,taken}\to PE}} - \frac{\varepsilon_{\text{el,sent}}(\chi,U,k)}{\eta_{\text{el,sent}\to PE}} \tag{5.33}$$

$\eta_{el,taken \to PE}$ and $\eta_{el,sent \to PE}$ are the conversion efficiencies considering values of 0.40 [121] and 0.43 [122], respectively. The optimization problem is solved by constructing a sequence of interrelated decisions called backward DP optimization. In other words, the DP algorithm begins by defining a small part of the whole problem and determining an optimal solution to it. Then, the algorithm extends the small part slightly and finds an optimum solution for it using the optimum solution which was found before. This procedure is then repeated by the algorithm until the current problem turns into the entire problem. Finally, when the entire problem is solved, the optimal control policy π^* can be found by a forward simulation, i.e. by tracking back the optimum solutions which were found for the small problems.

The optimal control policy representing the optimal energy scheduling over the simulation corresponds to:

$$\pi^* = \left\{ U_0, U_1, ..., U_{N-1} \right\} \tag{5.34}$$

where;

$$U_k = \left[U_{\text{CHP},k}, U_{\text{GSHP},k}, U_{\text{ASHP},k}, U_{\text{STORAGE},k} \right] \tag{5.35}$$

5.2.3 The GA-SOP method

This section describes the GA-SOP method used as a benchmark against which the results of the DP-DP method are compared. The GA-SOP method is a traditional optimization method which was developed by the authors in [29, 123]. In this context, the sizing optimization is conducted using GA, whereas the operating optimization is done by means of a Switch-On Priority (SOP) mapping.

5.2.3.1   Genetic Algorithm

GA is a computational algorithm which is based on the principles of evolution described in Darwin's theory and it was first presented by Holland in 1975 [124]. GAs are the most popular evolutionary algorithms used in the design optimization community. GAs are also known as population-based metaheuristic optimization algorithms. The GA uses a population of solutions, whose individuals are represented in the form of chromosomes [50].

The set of solutions or individuals are repeatedly modified by the GA in the course of its entire run. At each iteration, a number of individuals are selected by the GA from the current population and used as parents based on certain criteria. The parents are used to create the next generation of individuals, called children. Over successive generations, the population evolves toward an optimal solution.
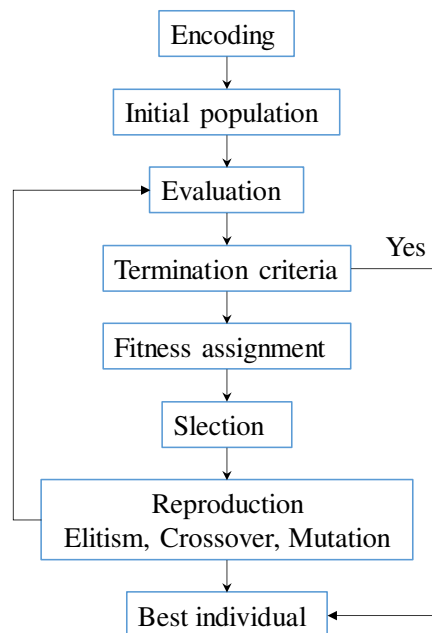
Fig. 5.3. Procedure for a GA (modified from [50]).

The procedure of a GA is as follows:

- Encoding: this step is used to represent the individual solutions. The individual solutions are coded as a finite fixed length string by using binary numbers (i.e. a string of 0's and 1's). The string is also known as chromosome.
- Initial population: in this step, the algorithm starts generating a population of individuals in the design space. The number of individuals must be decided by the designer. If the population is too large, the computational expense may increase too much, while too small population may lead to premature convergence to a local optimum. So, the choice of the number of individuals govern the performance of the GA.

- Evaluation: this step consists of calculating the value of the objective function for each of the individual solutions.

- Stopping criteria: the stopping criteria can be the maximum number of generations, the limit of computation time and the function tolerance.

- Fitness assignment: fitness assignment allows to rank and sort the individuals according to their objective values.

- Selection: this step filters out the individual solutions with poor fitness and preserves the candidate solutions with the acceptable fitness. The selected individuals are then used in the reproduction process.

- Reproduction: the previous generation is used to create a new generation through reproduction. Three mechanisms (elitist, crossover and mutation) are primarily used to create a new generation. The function values of the new generation are evaluated.

- Best individual: the global optimum that satisfies the termination criteria is selected.
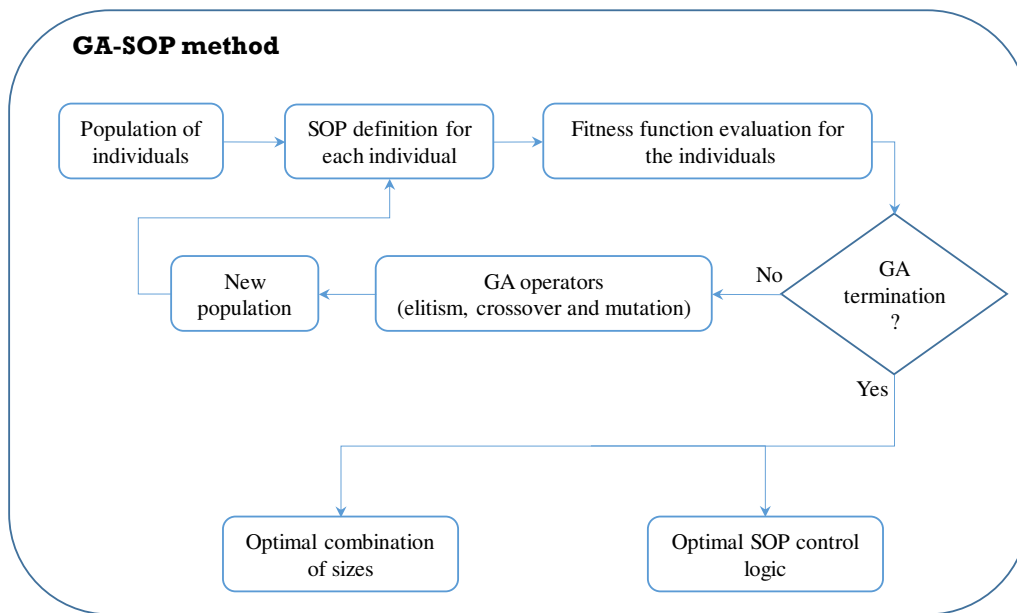
Fig. 5.4. Optimization flowchart of the GA-SOP method

5.2.3.2   Sizing optimization

The flowchart of the GA-DP method is shown in Fig. 5.4. As can be seen, at the first step GA begins by generating a population of individuals in the design space and each individual represents a combination of sizes of the different technologies involved in the optimization problem. For each individual, depending on the values of the combination of sizes, an SOP of the different technologies is defined and used by the GA.

Subsequently, the GA evaluates the fitness function, i.e. the primary energy consumption, of each individual in the current population. Then it creates a new population by selecting a group of individuals in the current population based on their fitness function values. In the reproduction phase, the GA uses three mechanisms, i.e. elitism, crossover and mutation, to create a new population of individuals. Individuals selected from the current population are called parents, while the individuals of the next generation are called children.

The GA repeats the mechanism multiple times until the population evolves toward an optimal value and a certain criterion is met.

Finally, once the convergence is reached, the best individual (Ind_best) representing the best combination of sizes is selected by the GA:

$$Ind_{best} = \left[P_{CHP,el,nom}, P_{GSHP,th,nom}, P_{ASHP,th,nom} \right] \tag{5.36}$$

5.2.3.3 Operating optimization

In a HEP, the control logic of the different technologies defines the basis on which the systems are switched on/off or regulated. Generally, control logic approaches such as time-led, heat-led, cold-led or electricity-led are implemented for the definition of the starting order of the systems involved [125]. Most centralized heating boilers consider the time-led control logic in which the systems start and stop following the heat demand during specified periods programmed and set up by the users. When the heat led control logic is adopted, systems' start and stop decisions are determined by the demand for space heating and hot water. On the contrary, when the cold led is considered, systems' start and stop decisions are governed by the space cooling energy demand. Finally, the systems' operation will be governed by the electric energy demand if the electric led is chosen. Furthermore, in order to enhance the performance of the supply/demand matching, some hybrid function may be implemented.

In this work, the control logic of the different technologies is defined by a Switch-On Priority (SOP) mapping which defines the starting order and allows the minimization of the on-site primary energy consumption during the considered simulation period.

5.3. Case study

The case study considered in this work is a tower intended for commercial and office use in the north of Italy. The building is composed of thirteen floors: i) the basement is designated for storage and a garage, ii) the ground and first floor are designated as a commercial area, iii) the 2nd to 12th floors

are designated for office use.

The sizing and operating optimization problem is carried out for a HEP composed of technologies that can be used for the production of electricity, space heating and hot water. Therefore, the sizing and operating optimization is carried out with the aim of minimizing the on-site primary energy consumption during winter and mid-season. In fact, the thermal energy demand required during summer is low compared to winter and mid-season.

5.3.1 Energy demands

The heating period for the climatic zone E where the building is located runs from October 15th to April 15th. The thermal energy demand for heating and hot water is obtained using the software EdilClimaEC700® on a monthly basis. Then the monthly thermal energy demand is transformed to calculate the hourly demand using non-dimensional profiles taking into consideration the type of user.

The electrical energy demand is for lighting, appliances and elevator operation. The thermal and electric energy demands distributed on an hourly basis in a typical winter day are shown in Fig. 5.5.

a)   b)
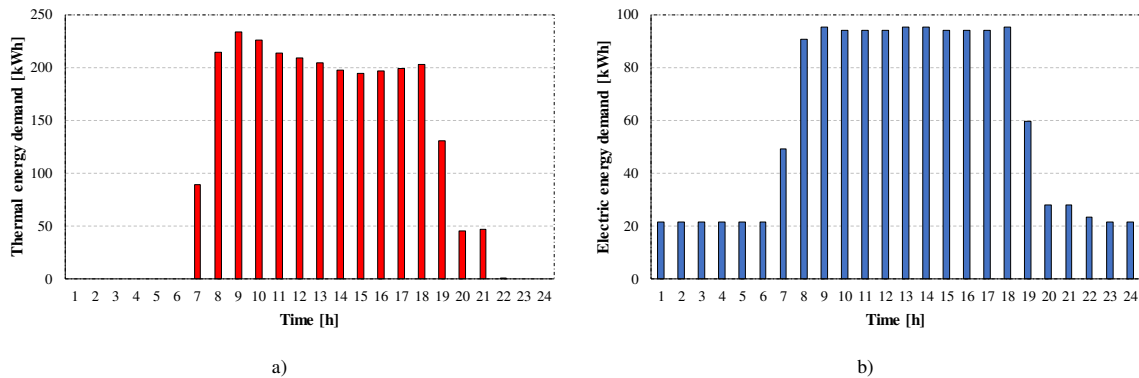
Fig. 5.5. Thermal a) and electric b) energy demands.

5.3.2 Application of the DP-DP method

Since the purpose of this study is to optimize both the size and operation of HEPs, only controllable technologies are involved in the optimization problem. Renewable energy technologies (i.e. STH and PV) are not controllable, so their optimization is not considered. In particular, PV and STH can exploit a total area of 328 m^2. STH covers an area of 2.5 m^2, while the remaining part is occupied by the PV system. Moreover, the capacity of the AB is set equal to the peak of the thermal energy demand (i.e. 234 kW), because a back-up system must always meet the thermal energy demand when the other systems are not working or turned off. The volume of the STORAGE ($V_{STORAGE}$) depends on the size of the CHP and STH technologies. It is calculated according to [126] considering a coefficient of 0.04

89

m^3/m^2 for the volume allocated to the STH and a coefficient of 2 kWh/kW$_{th}$ for the volume assigned to the CHP.

In this case, the size of CHP is represented by the nominal electric power $P_{CHP,el,nom}$, while the GSHP and ASHP are both represented by the nominal thermal power, $P_{GSHP,th,nom}$ and $P_{ASHP,th,nom}$, respectively. The upper limit of the optimization range, calculated using Eq. (5.25) and (5.26), is 95.97 kW$_e$ for the CHP and 233.73 kW$_{th}$ for the GSHP and ASHP systems. Finally, the upper limit for the CHP nominal power was fixed equal to 100 kW$_e$, whereas the upper limits for GSHP and ASHP were both fixed equal to 250 kW$_{th}$. The upper STORAGE volume limit ($V_{STORAGE,max}$) was calculated considering the maximum electric power of the CHP, i.e. 100 kW$_e$.

As previously mentioned, the CHP state ($\mathcal{X}_{CHP}$) is represented by the binary numbers 1 and 0 which represent the on-off condition of the CHP at the beginning of the kth time step. The stored energy ($\mathcal{X}_{STORAGE}$) is limited in the range [0, $\mathcal{E}_{th,STORAGE,max}$] and is discretized in 10 equally spaced values.

For the sizing optimization step, input variables U, for the CHP, GSHP, ASHP and STORAGE systems are discretized in 10 equally spaced values in the range [0, U_{max}]. Instead, for the operating optimization step, input variables are discretized in 9 equally spaced values in the range [U_{min}, U_{max}] and a tenth value ($U_z = 0$) is also added to the inputs representing the no action condition. Moreover, for the CHP, GSHP and ASHP systems, the maximum load U_{max} corresponds to the nominal load, while the minimum load $U_{z,min}$ is assumed equal to 10% of the nominal load (See Section 5.2.1.1).

Finally, the state-space model is discretized with a discretization interval k of one hour and the time horizon N for winter and mid-season period is equal to 4391 hours. Moreover, for the sizing and operating optimization steps, the states at the beginning are set so that the co-generator is off and the STORAGE is empty, while the final states are free. The optimization was conducted on a cluster with 24 Gb of RAM and 4 computing cores.

5.3.3 Application of the GA-SOP method

Table 5.1 reports the sizing variable of each technology and the range in which it is optimized. As shown, the CHP is represented by the nominal electric power $P_{CHP,el,nom}$, while the GSHP and ASHP are both represented by the nominal thermal power, $P_{GSHP,th,nom}$ and $P_{ASHP,th,nom}$, respectively.

Table 5.1. Optimization ranges of the different technologies.

	$P_{CHP,el,nom}$ [kWe]	$P_{GSHP,th,nom}$ [kW]	$P_{ASHP,th,nom}$ [kW]
Optimization range	[0, 100]	[0, 250]	[0, 250]

Regarding the GA options, 100 generations are evaluated and for each generation a population of 300 individuals is considered. Random mutations are set considering a crossover fraction of 0.8 and an elite count of 6.

The output of the GA is the vector $[P_{CHP,el,nom}, P_{GSHP,th,nom}, P_{ASHP,th,nom}]$ representing the optimal combination of sizes. The storage volume ($V_{storage}$) depends on the nominal power of the CHP and the area of the STC.

The mapping is developed by considering the demands for winter and mid-season, and the SOP control logic is defined by maximizing system's efficiencies depending on the nominal capacity and the types of systems utilized. Renewable energy systems, such as STC and PV are not considered in the mapping, since are not controllable and need to be activated first. Furthermore, the AB is not considered in the mapping because it is considered as auxiliary system and its size is set equal to the thermal energy demand. The CHP size ranges between 20÷200 kW, with a step of 20 kW and the ASHP and GSHP capacities range between 25÷250 kW with a step of 25 kW. The size of the storage varies as a function of the CHP and STC sizes. For each combination of systems' sizes, the model calculates the on-site primary energy consumption and evaluates the best SOP control logic. For the simulation of the HEP a model is developed in the Matlab® environment. At each iteration of the optimization process, the developed SOP mapping is used by the optimization model to define the proper SOP which minimizes the on-site primary energy consumption.

5.4. Results and discussion

The results of the DP-DP method are compared to those obtained from a traditional optimization method called GA-SOP method which is developed by the same authors in other works [29, 123]. In the GA-SOP optimization framework, the sizing optimization is conducted using GA, whereas the starting order of the different technologies composing the energy plant is defined by a Switch-On Priority (SOP) mapping which minimizes the primary energy consumed over the simulation period. For more details, the development procedure of SOP mapping is described in a previous work [123]. The SOP for the different technologies is set as follows:

1. Renewable energy technologies (i.e. solar thermal collector and photovoltaic panel);
2. Hot water storage;
3. Combined heat and power;
4. Ground source heat pump;
5. Air source heat pump;
6. Auxiliary boiler.

Table 5.2 lists the optimal sizes obtained using the GA-SOP and DP-DP methods. As can be seen, the optimal CHP capacity defined by the DP-DP method is greater (100 kWe) compared to the GA-SOP method (90 kWe), while the size of the GSHP (44 kWth) is smaller compared to the result found using the GA-SOP method (60 kWth). As can be noted, the results obtained by the two methods are different, which is expected because the GA-SOP and DP-DP methods use different algorithms to solve the sizing optimization problem. Furthermore, the two sizing optimization problems were implemented differently, i.e. the GA method is applied on a continuous optimization problem, while the DP-DP method solves a discrete optimization problem. Moreover, in the sizing optimization step, the GA-SOP method defines the control logic of the different technologies using the SOP mapping, while in the other case, the control logic is defined by the DP itself.

Table 5.1. Optimal sizes for the GA-SOP and DP-DP methods.

	$P_{CHP,el,nom}$ [kW$_e$]	$P_{GSHP,th,nom}$ [kW$_{th}$]	$P_{ASHP,th,nom}$ [kW$_{th}$]
GA-SOP method	90	60	0
DP-DP method	100	44	0

Table 5.3 lists the primary energy consumption and time execution for the GA-SOP method, DP-DP method and the case of a Traditional Plant (TP). In the TP case, the thermal energy demand is fulfilled by a boiler with a nominal power equal to the peak (234 kW), while the electrical energy demand is taken from the grid. It can be seen that the primary energy consumed during winter and mid-season in a TP is equal to 735.9 MWh. Due to the higher complexity of the plant and the introduction of renewable energy systems, the consumption in the GA-SOP and DP-DP methods is reduced to 585.9 and 554.3 MWh, respectively. As can be noted, the DP-DP method gives more advantage in terms of primary energy consumption compared to the GA-SOP method. In particular, compared to the GA-SOP method, the DP-DP method allows a primary energy saving of 5.4% to be achieved. Moreover, compared to the TP case, a primary energy saving of about 24.7% may be achieved.

Table 5.3. Primary energy consumption for the GA-SOP and DP-DP methods.

	TP	GA-SOP method	DP-DP method
Primary energy consumption [MWh]	735.9	585.9	554.3
Computation time [h]	-	31	18

It would be interesting to compare the computation time between the GA-SOP and DP-DP methods. As can be noted from Table 5.3, there is a huge difference in the computation time (the computation time is represented by the wall-clock time) between the two methods which can be explained by the fact that the GA takes more time than DP to solve the sizing optimization problem. Indeed, for the

presented case study, the use of the DP-DP method allows a computation time saving of around 41.4% compared to the GA-DP method.

Figures 5.6a and 5.6b show the fraction of thermal energy demand allocated to each technology of the HEP plant and the fraction of thermal energy which is lost to the atmosphere during the simulation period for both GA-SOP and DP-DP methods. The fraction of thermal energy demand fulfilled by the CHP is the highest for all cases with 91.5% for the GA-SOP method and 95.6% for the DP-DP method. The production of the GSHP varies from 2.6% to 5.3% and in all cases is used to meet the peak thermal energy demand. The minimum fraction is found in the DP-DP method because the HEP is characterized by larger CHP and smaller GSHP units. The amount of thermal energy produced by the STH is the same for all cases (0.3%), while the AB is only used in the DP-DP method (0.2%).

a) Thermal energy production for the GA-SOP method.   b) Thermal energy production for the DP-DP method.
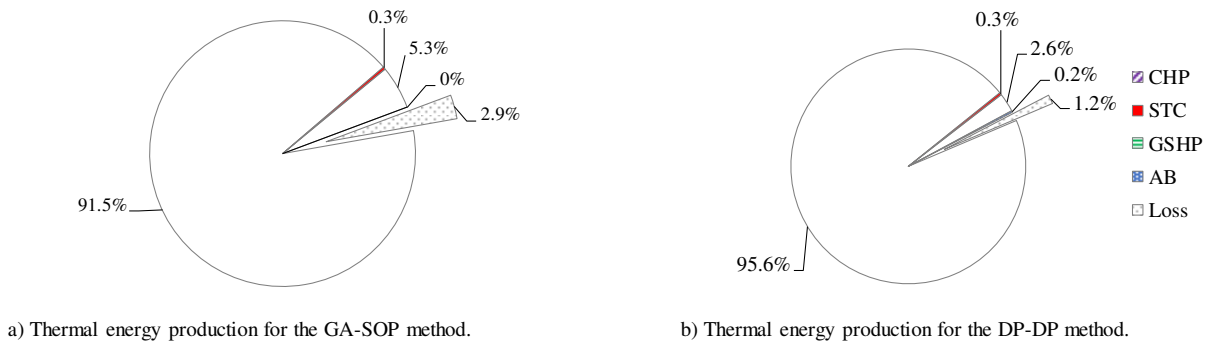
Fig. 5.6. Fraction of thermal energy demand met by the different HEP components.

The operating time of the CHP and GSHP systems for the GA-SOP and DP-DP methods is illustrated in Fig. 5.7. As shown, the CHP is the system employed the most for all cases. Furthermore, the operating time of the technologies is lower when using the DP-DP method compared to the GA-SOP method. The CHP is able to meet a larger fraction of thermal demand even when working fewer hours and this may reduce the maintenance costs of the CHP.

The average performance of the CHP and the GSHP is another interesting point to highlight. The average efficiency of the CHP ($\eta_{el,CHP,av}$) and the average coefficient of performance of the GSHP ($COP_{GSHP,av}$) were calculated over winter and mid-season period. It can be noted that, when using the DP-DP method, CHP and GSHP work at a higher average performance compared to the other case with values of 0.354 and 3.564, respectively. In other words, the DP-DP method tries to keep the CHP and GSHP working at full load and higher efficiency compared to the GA-SOP method and this allows the primary energy consumption to be minimized.

Fig. 5.7 The operating time of the CHP and GSHP during the simulation period.

The operational results of the GA-SOP and DP-DP methods are reported in Fig. 5.8 and Fig. 5.9 for a typical winter and mid-season day. They show the optimal operating strategy of the technologies defined in both methods.

It can be seen that the thermal energy produced by the STH and directly used for demand fulfilment is negligible. As can be noted from Fig. 5.8 and 5.9, there is a big difference between the operational results obtained from the two methods. Indeed, for the GA-SOP me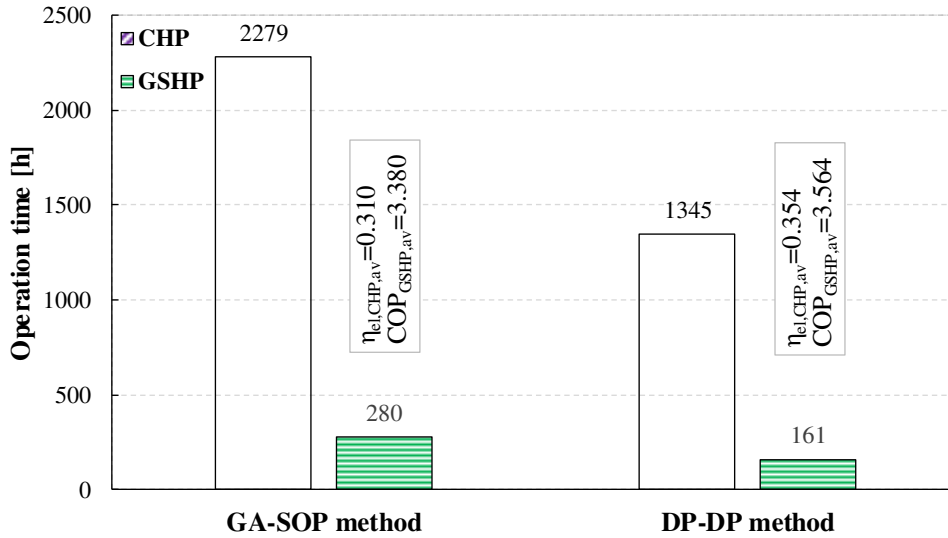thod, the operation is defined by a SOP mapping, while the DP-DP method defines the optimal control policy by means of a DP algorithm which leads to a reduction of 5.4% of primary energy consumption. From Fig. 5.8, with reference to the DP-DP method, a higher fraction of the thermal energy demand is fulfilled by the CHP which has a higher size compared to the GA-SOP method. Moreover, Figs. 5.8 and 5.9 show that, the control policy defined by the DP tries to directly meet the thermal energy demand by the CHP system storing any excess which allows to avoid the operation of the system at part loads and to minimize the number of start-ups. The stored energy is then used twice or three times a day, when this is enough to meet the thermal energy demand. For both methods, Fig. 5.8 shows that the GSHP is employed during peak days when the CHP and the stored energy are not sufficient to fulfill the whole energy demand.

It is interesting to note that, following the DP optimal policy, the amount of energy in the storage is always lower compared to the GA-SOP case (see Fig 5.8 and 5.9). Indeed, as the thermal energy lost to the atmosphere through storage is proportional to the amount of stored energy, the DP-DP algorithm tries to limit the thermal dissipation by reducing the amount of energy kept in the storage. In fact, it can be seen from Fig. 5.6 that the lost energy is reduced from 2.9% for the GA-SOP method to 1.2% for the DP-DP method.
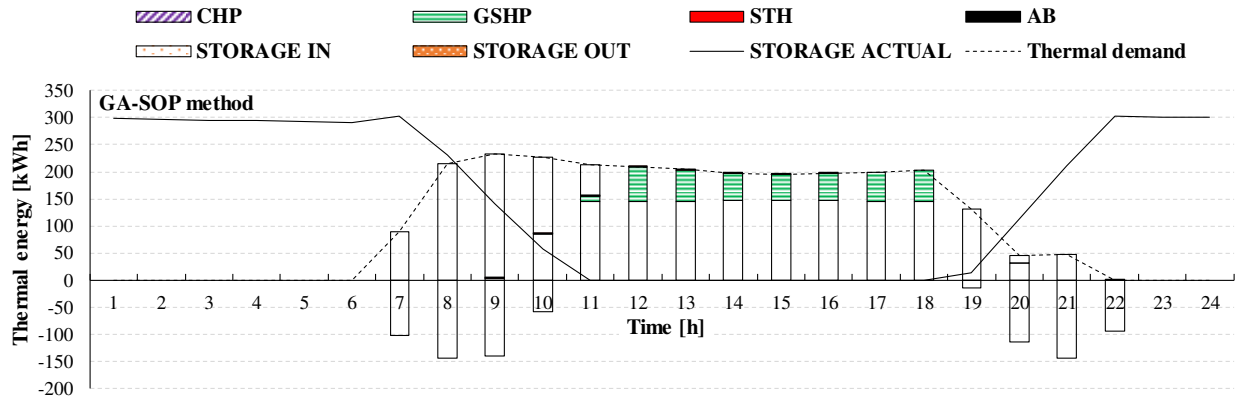
a) Thermal energy produced for the GA-SOP method.
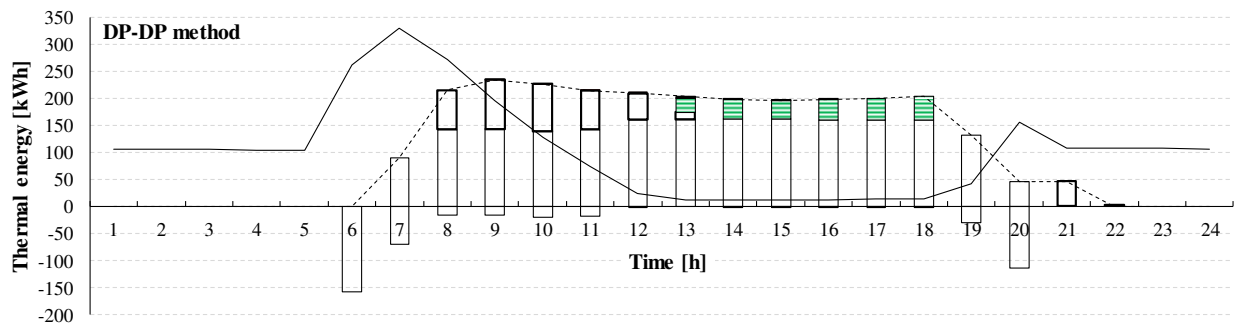
b) Thermal energy produced for the DP-DP method.

Fig. 5.8. Contribution to thermal energy demand of the CHP, GSHP, STH, AB and STORAGE during a winter day.

a) Thermal energy produced for the GA-SOP method.

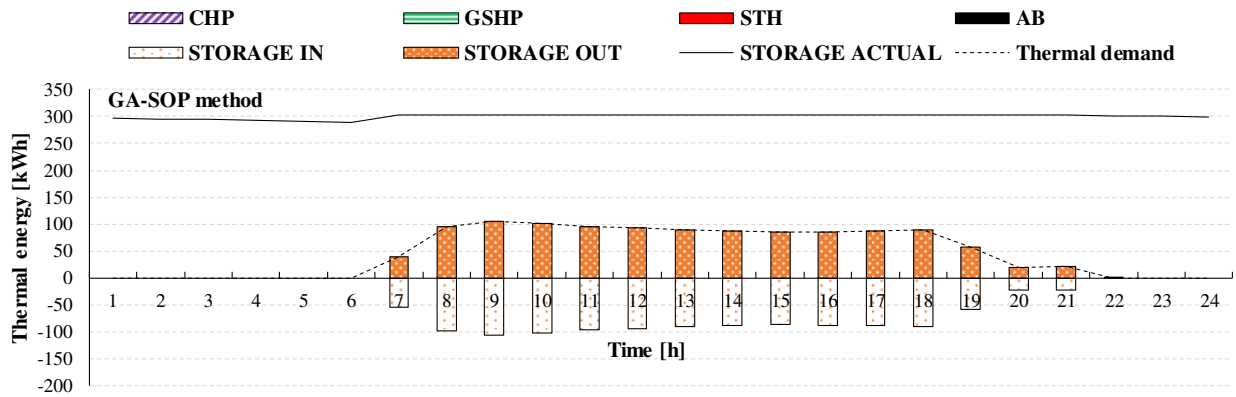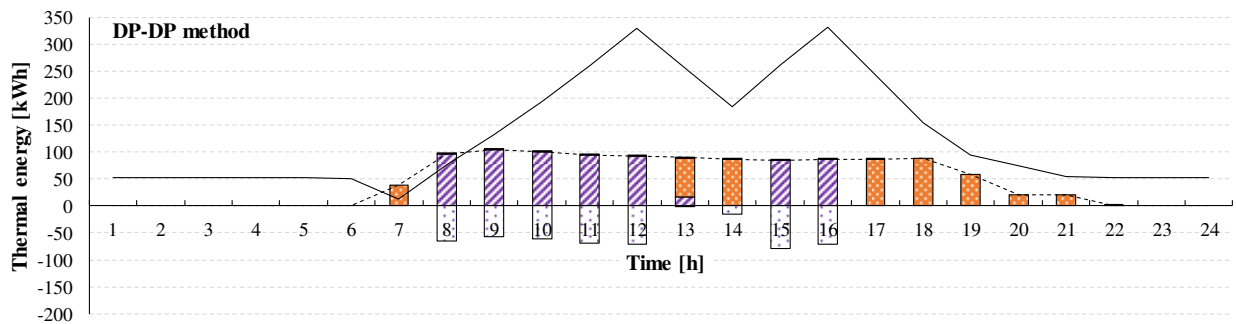b) Thermal energy produced for the DP-DP method.

Fig. 5.9. Contribution to thermal energy demand of the CHP, GSHP, STH, AB and STORAGE during a mid-season day.

6. Life cycle assessment of energy systems for residential applications by accounting for scaling effects

In this chapter, the LCA of energy systems which can be employed for residential applications is investigated. The aim of the analysis is to assess the off-site primary energy consumption and environmental impacts. The following sections introduce the problem, elaborate the goal and scope of the study in more depth, present the energy systems assessed in this study and describe the assumptions made for quantifying the resources and energy use. The challenge of LCA scaling for the considered energy systems is also addressed. Finally, the proposed scaling procedure is validated and LCA study is compared with other works.

6.1.   Introduction

In the last decades, environmental sustainability and energy conservation have become an important concern. To assess the off-site primary energy consumption and environmental impacts, i.e. associated with the upstream life cycle of energy technologies, LCA is a widely used and well-established method. Recently, the integration of LCA in design and feasibility studies has become an active research area. The main obstacle of integrating LCA in early system's design is the availability of only limited amount of data. Generally, this problem is overcome by assuming a linear relationship between inventory data and size. However, this could lead to an over- or under estimation of the emissions, if available data are scaled up or down.

This work investigates the LCA of renewable and non-renewable energy systems which can be employed for residential applications and provides impact curves which can be used for optimization purposes. In the following STC, PV panel, CHP system, ABS, ASHP, and GSHP and hot water storage are considered. In addition, water storage for thermal energy accumulation is also modeled. The considered technologies are widely used in the residential sector as single systems and also as an aggregate in a HEP. For each system, a cradle-to-gate LCA is carried out and a model is developed in openLCA® environment. Regarding the LCI of the considered technologies, data were obtained from the Ecoinvent® database. The scaling procedure developed in this chapter allows the estimation of the environmental impacts represented by the CED, GWP and ARD indicators of various technologies in a range of sizes, overcoming the obstacles of integrating the LCA in energy systems design and optimization, handling the problems arising from data gaps and comparing energy alternatives of different sizes from an environmental impact point of view.

6.2. Life cycle assessment of energy systems

The LCA methodology allows the quantification of environmental impacts caused by products, processes or services. This procedure is used to evaluate and compare the environmental effects of different products or systems and helps to identify the "hot spots" throughout their life cycle and improve products from the environmental perspective. The maturity of the methodology is demonstrated by the International Organization for Standardization (ISO) which published related technical standards, i.e. ISO 14040 [55] and ISO 14044 [127].

6.2.1 Goal and scope

The goal of this study is the evaluation of the environmental impacts and scaling effects by applying a cradle-to-gate life cycle assessment to renewable and non-renewable energy systems, widely used in the residential sector. In particular, the following energy systems are considered:

- Solar thermal collector (STC);
- Photovoltaic panel (PV);
- Combined heat and power (CHP);
- Ground source heat pump (GSHP);
- Air source heat pump (ASHP);
- Absorption chiller (ABS);
- Pellet boiler (PB);
- Hot water storage.

For a complete cradle-to-grave analysis, data on the product life cycle steps such as manufacturing, transportation, use, and disposal should be available. Since no consolidated information about the disposal phase of the energy systems considered in this work is available, this phase is not addressed in this research. The impacts associated with the use phase are highly influenced by the operating conditions of the energy system, which in turn depend on installation site; a model for the quantification of the on-site impacts is described in another work by the same authors [128].

Thus, the cradle-to-gate analysis carried out in this research only considers a part of systems life cycle, i.e. in our study from raw materials extraction to the transportation to the market. Figure 6.1 shows the approach adopted for the development of the cradle-to-gate analysis. For each of the abovementioned energy systems, the boundaries of the cradle-to-gate analysis include:

- Raw material extraction (cradle);

- Raw materials processing;

- Transportation of processed materials to manufacturing site;

- Manufacturing of the final product;

- Transportation to market (gate).

As hinted before, the aim of this research is the development of a general approach for LCA scaling. Therefore, for specific stages (e.g. transportation), general assumptions are implemented in the calculations. These assumptions have to be substituted in case of site-specific analyses. For the transportation of raw materials to the manufacturing site, 200 km in freight train and 100 km in a lorry are considered, while a 100 km of distance in a lorry is assumed for the transportation of the manufactured system from the factory site to the market [129].

The LCI documents the material, water and energy balances for all stages listed above, to quantify the resources in mass units and energy units (electric energy in kWh and thermal energy in MJ). Regarding the LCI of the investigated energy systems, data were obtained from the Ecoinvent® [129] database which contains a large number of production processes with a focus on the European market. Thus, the European energy mix is the reference for the calculation of the demanded energy carriers. The calculation was conducted by using the open source software openLCA® 1.6.3 [130]. For each technology, an LCI was constructed and the environmental impacts are analyzed accordingly.
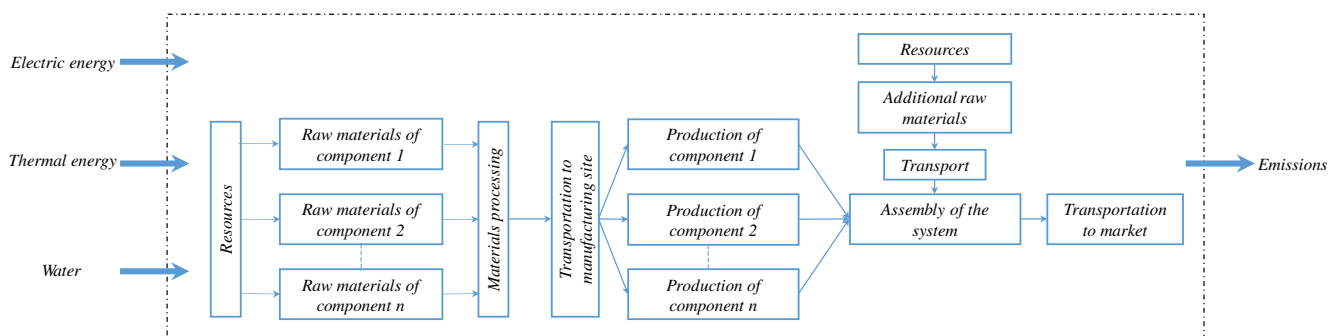
Fig. 6.1. Energy system boundary.

6.2.2 Scaling procedure

In literature, the impacts of a scaled system or process are usually calculated by assuming a linear relationship between the LCI flows/impacts and the equipment size. However, it is well known that this relationship is non-linear and tends to assume a similar behavior of the conventional cost scaling [93]. The cost scaling method is known as economy of scale and relates the capital cost of an equipment to its capacity as follows:

$$C = C_{ref} \cdot \left(\frac{S}{S_{ref}} \right)^{k} \tag{6.1}$$

where C represents the scaled capital cost, C_{ref} the reference capital cost, S the size parameter, S_{ref} the reference size and k the cost exponent. In this study, in order to calculate the impacts of an energy system in a predefined range of sizes, it is assumed that the LCI scaling is also made by assuming the economy of scale [63], i.e. it is described by a power law relationship as reported in Eq. (6.2):

$$G = G_{ref} \cdot \left(\frac{S}{S_{ref}} \right)^{L} \tag{6.2}$$

with G representing a key property of the scaled LCI dataset such as mass, energy or emissions associated with the production of the considered equipment, G_{ref} the LCI used as reference, L the scaling exponent and S and S_{ref} the size parameter and the reference size, respectively.

Figure 6.2 shows the procedure for the scaling of the LCI flows in a range of sizes. The first step of the methodology consists of defining the parameter S which represents the size of the assessed energy technology. If the LCI data are available for, at least, two different sizes the scaling exponent L can be directly estimated by assuming the scaling behavior described by Eq. (6.2). For instance, the scaling exponent can be estimated from the relationships between the total weight of the equipment and its size or from the final impact and its capacity.

However, if only one LCI dataset is available at one particular size, LCI data for different sizes may be estimated by using the scaling law described by Eq. (6.2). As reported by the third step of the procedure, the scaling exponent L can be derived from relationships between the total weight of the equipment and its size considering that the mass follows a similar law to cost scaling [93]; such exponents can be found in the literature for some applications [91, 97, 98]. Otherwise, the scaling exponent can be derived from economy of scale as an approximation by assuming a similarity between cost and LCI scaling. A scaling factor L of 0.6, which is known as the "six-tenths rule" [92], is also recommended when there is no information about the scaling behavior of the system [92, 131]. This exponent is commonly used to estimate equipment capital cost as a function of the system size. Once the scaling exponent is found, LCI data can be estimated for different sizes and LCA studies can be performed in a range of sizes.

It should be mentioned that, in some cases, two components of the same system may have different scaling exponents (e.g. the motor and generator components in a CHP system) as reported in the following. Therefore, the scaling is carried out for the LCI flows of each component of a system using

the corresponding scaling exponent. In this way, it is possible to distinguish between components of the system which are size-dependent and others which instead are size-independent, such as cables and electrical parts.

```
┌─────────────────────────────┐
│   Identify the size parameter   │
└─────────────────────────────┘
              │
              ▼
┌───────────────────────────────────┐
│  Use LCI data for system manufacturing  │
└───────────────────────────────────┘
              │
              ▼
┌─────────────────────────────────────────────────────────────┐
│ Find an exponent L that describes the scaling behaviour of the system (i.e. mass vs. size). │
│              Otherwise, use the cost exponent               │
└─────────────────────────────────────────────────────────────┘
              │
              ▼
┌──────────────────────────────────────────────┐
│  Use the power law to scale the LCI for different sizes  │
└──────────────────────────────────────────────┘
              │
              ▼
┌───────────────────────────────┐
│   Estimate cradle-to-gate LCA in a   │
│           range of sizes            │
└───────────────────────────────┘
```
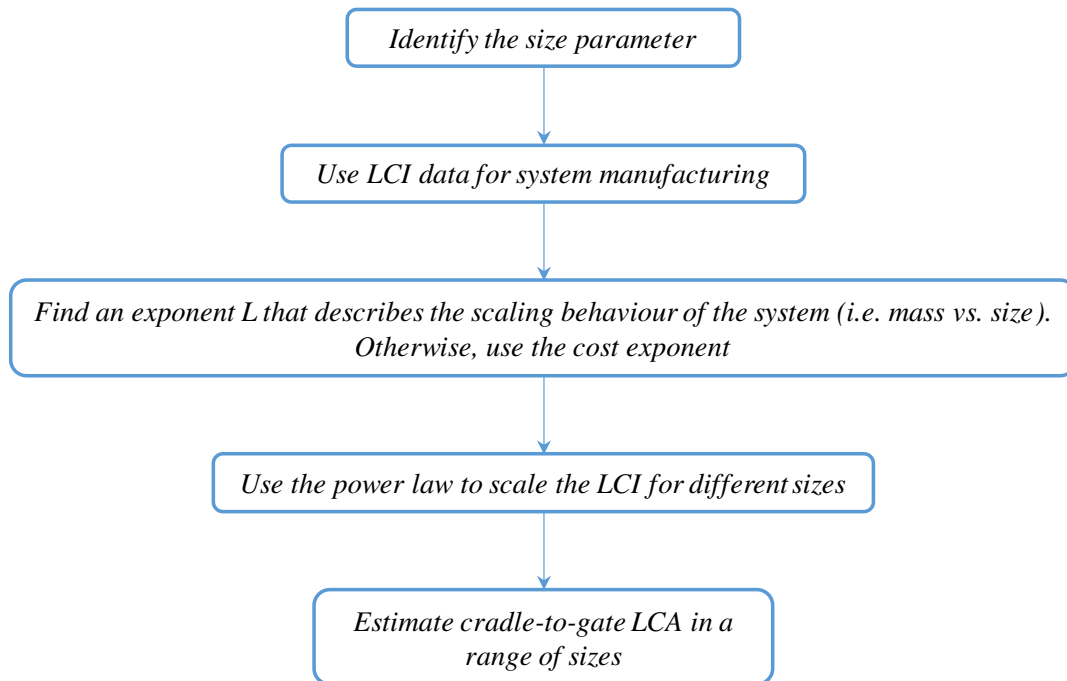
Fig. 6.2. Scaling procedure.

6.2.3 Inventory analysis and scaling of energy technologies

The LCI documents the material, water and energy balances for all stages listed above, to quantify the resources in mass units and energy units (electric energy in kWh and thermal energy in MJ). Regarding the LCI of the investigated energy systems, data were obtained from the Ecoinvent® database which contains a large number of production processes with a focus on the European market. Thus, the European energy mix is the reference for the calculation of the demanded energy carriers.

For all systems, the scaling range is fixed from 1 kW to 250 kW and systems with a nominal power of 1 kW, 5 kW, 10 kW, 20 kW, 50 kW, 100 kW, 150 kW, 200 kW and 250 kW are assessed within the scaling interval. These sizes are selected since systems with these capacities are available in the market. Regarding the STC and the PV systems, the area ranges are calculated in such a manner that the production of approximately 250 kW$_{th}$ (STC) or 250 kW$_p$ (PV) is obtained.

In the following, the main assumptions made for modeling and scaling the LCI of each technology are reported:

- *Solar thermal collector*

The studied STC is a flat plate collector type for multiple dwellings use [132]. As reported in Table 6.1, the collector consists of a frame, an absorber with a selective coating, single glazing materials, thermal insulation and a sealing.

For assessing the impacts of the STC as a function of the size, a reference functional parameter of 1 m^2 of solar collector is considered. The chosen functional parameter allows the linear scaling of the LCI as a function of solar thermal collector area. Therefore, the key properties of the scaled LCI are calculated by setting $L=1$ in Eq. (6.2).

Table 6.1. LCI data for the manufacturing of 1 m^2 of STC (from [132]).

	Amount	Unit
Materials and energy requirements		
Aluminum	3.93	[kg]
Copper	2.82	[kg]
Chromium steel 18/8, hot rolled	4.14	[kg]
Solar glass, low-iron	9.12	[kg]
Brazing solder, cadmium free	0.00368	[kg]
Propylene glycol, liquid	1.01	[kg]
Silicone product	0.0588	[kg]
Soft solder, Sn97Cu3	0.0588	[kg]
Stone wool, packed	2.43	[kg]
Synthetic rubber	0.732	[kg]
Corrugated board box	3.68	[kg]
Electricity, medium voltage	1.16	[kWh]
Water, completely softened	1.38	[kg]
Tap water	9.4	[kg]
Materials processes		
Sheet rolling, copper	2.82	[kg]
Selective coating of copper sheet, black chrome	1	[m2]
Anti-reflex-coating, solar glass	1	[m2]

- *Photovoltaic panel*

In this case, PV panels for grid-connected applications are investigated [133]. As shown in Table 6.2, the photovoltaic system is composed of the PV panels and the mounting structure. The PV panels consist of a number of solar cells which are enclosed by glass based laminates and are framed by an aluminum structure. As a type of cells, single crystalline silicon cells are used.

In this work, it is supposed that the PV panels are mounted for façade building applications. In this type of installations, panels are attached to the façade by an aluminum profile which is fixed to the building structure. A functional parameter of 1 m^2 of PV panels is considered.

Regarding the scaling of the PV system, the LCI for the PV panels and the mounting structure is scaled linearly with the PV area.

Table 6.2. LCI data for the manufacturing of 1 m² of photovoltaic panel (from [133]).

	Amount	Unit
Single-si solar panel		
<u>Materials and energy requirements</u>		
aluminum alloy, AlMg3	2.63	[kg]
Copper	0.113	[kg]
Solar glass, low iron	10.1	[kg]
photovoltaic cell, single-Si wafer	0.932	[m2]
glass fiber reinforced plastic, injection moulded	0.188	[kg]
1-propanol	0.00814	[kg]
acetone, liquid	0.013	[kg]
brazing solder, cadmium free	0.00876	[kg]
corrugated board box	1.1	[kg]
ethylvinylacetate, foil	1	[kg]
lubricating oil	0.00161	[kg]
methanol	0.00216	[Kg]
nickel, 99.5%	0.00016	[kg]
polyvinylfluoride, film	0.11	[kg]
silicone product	0.122	[kg]
vinyl acetate	0.00164	[kg]
polyethylene terephthalate, granulate, amorphous	0.373	[kg]
electricity, medium voltage	4.71	[kWh]
Heat	5.41	[MJ]
Tap water	21.3	[kg]
<u>Materials processes</u>		
wire drawing, copper	0.113	[kg]
Tempering, flat glass	10.1	[kg]
Mounting structure		
<u>Materials and energy requirements</u>		
steel, low-alloyed	1.8	[kg]
Aluminum	2.64	[kg]
Corrugated board box	0.04	[kg]
polyethylene, high density, granulate	0.00073	[kg]
polystyrene, high impact	0.00360	[kg]
<u>Materials processes</u>		
sheet rolling, steel	0.11	[kg]
Hot rolling, steel	1.8	[kg]
section bar rolling, steel	1.69	[kg]
section bar extrusion, aluminium	2.64	[kg]

- *Combined heat and power system*

As illustrated in Table 6.3, the CHP unit considered as a reference is based on internal combustion engine technology and provides 160 kW$_{el}$ and 360 kW$_{th}$. The CHP system is composed of an engine,

a generator, a heat exchanger, a sound insulation system, a control cabinet, electric parts and a catalytic converter [134].

For LCI scaling, the electrical power output $P_{CHP,el}$ is considered as the functional parameter of the CHP system. In this case, the components which depend on the size of the CHP unit such as the motor, generator, heat exchanger, sound insulation, air input/output supply, catalytic converter and the flows needed for motor/generator assembly were distinguished from the parts which are size-independent such as the control cabinet and the electric parts. The LCI flows of the parts which are size-independent are considered constant. Instead, for the size-dependent parts, different scaling exponents are used to extrapolate the LCI in the considered scaling range.

As reported in Table 6.4, the LCI input and output flows of the engine and the generator are related to the capacity of the CHP with scaling exponents of 0.64 and 0.68, respectively. The scaling exponents for the engine and generator are identified in [91] by considering different types of engines/generators and using a regression method to disclose the relationship between the mass [kg] and the power output [kW] of the engine/generator. It should be noted that an assumption was made about the scaling of electricity, heat and water flows. In fact, these were scaled in the same fashion as the raw material flows supposing that the same scaling behavior also applies here.

The LCI flows of the remaining parts (excluding the control cabinet and the electric parts, which were considered constant) were extrapolated by using a scaling exponent L of 0.66. This exponent was calculated from the relationship between the total weight of the CHP unit and the input power [134].

Table 6.3. LCI data for the manufacturing of 160 kW_{el} CHP unit (from [134]).

	Amount	Unit
Internal combustion engine		
Materials and energy requirements		
Cast iron	1250	[kg]
Reinforcing steel	125	[kg]
Chromium steel 18/8	125	[kg]
Steel, low-alloyed	250	[kg]
Electricity, medium voltage	201.25	[kWh]
Heat	19700	[MJ]
Water	2.625	[m3]
Materials processes		
Hot rolling, low-alloyed steel	250	[kg]
Hot rolling, chromium steel	125	[kg]
Generator		
Materials and energy requirements		
Cast iron	743.75	[kg]
Copper	318.75	[kg]

Electricity, medium voltage	231.25	[kWh]
Heat	22700	[MJ]
Water	1.6	[m3]

Assembly motor/generator

Materials and energy requirements		
Reinforcing steel	560	[kg]
Electricity, medium voltage	64.2	[kWh]
Heat	6300	[MJ]
Water	0.84	[m3]

Heat exchanger

Materials and energy requirements		
Reinforcing steel	737.5	[kg]
Steel, low-alloyed	737.5	[kg]
Water	2.2125	[m3]
Materials processes		
Hot rolling, low-alloyed steel	737.5	[kg]

Sound insulation

Materials and energy requirements		
Reinforcing steel	1920	[kg]
Stone wool	480	[kg]
Water	2.88	[m3]

Control cabinet

Materials and energy requirements		
Aluminum	0.15	[kg]
Copper	10.8	[kg]
Lead	0.76	[kg]
Nickel	0.34	[kg]
Platinum	0.00210	[kg]
Polyethylene, low density, granulate	78.5	[kg]
Polyvinylchloride, emulsion polymerised	0.95754	[kg]
Polyvinylchloride, suspension polymerised	6.54255	[kg]
Reinforcing steel	276	[kg]
Tin	1.62	[kg]
Zinc	0.25	[kg]
Electricity, medium voltage	1690	[kWh]
Heat	16.54	[MJ]
Water	0.434	[m3]

Air input/output supply

Materials and energy requirements		
Reinforcing steel	288	[kg]
Electricity, low voltage	2830	[kWh]
Electricity, medium voltage	33.3	[kWh]
Heat	33345	[MJ]
Water	0.432	[m3]

Electric parts

Materials and energy requirements		
Aluminum	0.1	[kg]
Copper	6.5	[kg]
Lead	0.47	[kg]
Nickel	0.21	[kg]

Platinum	0.0013	[kg]
Polyethylene, low density, granulate	47.4	[kg]
Polyvinylchloride, suspension polymerised	0.5	[kg]
Reinforcing steel	52.7	[kg]
Tin	0.997	[kg]
Zinc	0.154	[kg]
Electricity, medium voltage	5670	[kWh]
Heat	29355	[MJ]
Water	0.0914	[m3]
Catalytic three way converter		
Materials and energy requirements		
Corrugated board	2.75	[kg]
Palladium	0.041	[kg]
Platinum	0.2045	[kg]
rhodium	0.041	[kg]
Chromium steel	330	[kg]
Zeolite powder	19	[kg]
Electricity, medium voltage	955	[kWh]
Water	0.495	[m3]
Materials processes		
Hot rolling, chromium steel	330	[kg]
Assembly of CHP components		
Materials and energy requirements		
Electricity, low voltage	4940	[kWh]
Heat	27000	[MJ]

Table 6.4. Scaling exponents of the different components of the CHP unit (size parameter S=Pel).

	Scaling exponent L	Reference
Engine	0.64	[91]
Generator	0.68	[91]
Control cabinet	0 (Size-independent)	-
Electric parts	0 (Size-independent)	-
Other parts	0.66	[134]

- *Ground and air source heat pumps*

For both heat pumps, GSHP and ASHP, the reference system is characterized by a nominal thermal power of 10.25 kW$_{th}$ [135]. Moreover, it was supposed that the cooling mode of operation does not affect the amount of materials and energy required for the manufacturing of both systems. The LCI for the GSHP is illustrated in Table 6.5. In this study, the same list of materials used for the GSHP was supposed for manufacturing the ASHP. In fact, the LCI of the ASHP is calculated by multiplying the LCI of the GSHP by a factor of 1.6 [135], since the ASHP is characterized by a higher weight and refrigerant use compared to the GSHP [135]. The main components of both heat pumps are: the housing, the compressor, the evaporator, the condenser and the control system. Moreover, a borehole heat exchanger which consists of two U-tubes is considered for the GSHP system. The refrigerant R134 is the working fluid considered for both systems.

The functional parameter considered for scaling the LCI of both GSHP and ASHP systems is the thermal power ($P_{GSHP/ASHP,th}$) expressed in [kW$_{th}$].

The extrapolation of the LCI key properties for the GSHP and ASHP is conducted by using scaling exponents from literature which relate the total mass of the equipment to the system capacity. As can be seen from Table 6.6, scaling exponents of 0.60 and 0.67 were used to calculate the LCI of the GSHP and ASHP at different sizes, respectively [98]. Materials for electrical cables, i.e. copper and PVC, were considered size-independent for both cases (GSHP and ASHP). Moreover, the amount of refrigerant (in kg) is calculated by using a scaling exponent of 0.62 for the GSHP, while an exponent of 0.91 is used for the amount of refrigerant needed for the ASHP operation [98]. Finally, the borehole heat exchanger was considered size-independent by supposing that the length of the probes does not vary with the GSHP nominal power and the effect of the probes diameter is negligible.

Table 6.5. LCI data for the manufacturing of 10 kW$_{th}$ GSHP pump and 150 m borehole heat exchanger (from [135]).

	Amount	Unit
GSHP		
Materials and energy requirements		
Copper	22	[kg]
Reinforcing steel	75	[kg]
Steel low-alloyed, hot rolled	20	[kg]
Refrigerant R134a	3.09	[kg]
polyvinylchloride, bulk polymerized	1	[kg]
Lubricating oil	1.7	[kg]
Tube insulation, elastomere	10	[kg]
Electricity, medium voltage	140	[kWh]
Heat	1400	[MJ]
Water	0.708	[m3]
Borehole heat exchanger		
Materials and energy requirements		
Reinforcing steel	33	[kg]
Polyethylene low density granulate	180	[kg]
Ethylene glycol	102	[kg]
Cement	33	[kg]
Activated bentonite	8	[kg]
Water	10.2	[m3]

Table 6.6. Scaling exponents of the different components of the GSHP and ASHP unit (size parameter $S=P_{GSHP/ASHP,th}$).

	Scaling exponent	Reference
GSHP	0.60	[98]
ASHP	0.67	[98]
Refrigerant/GSHP	0.62	[98]
Refrigerant/ASHP	0.91	[98]
Borehole heat exchanger	0 (Size-independent)	-
Electrical cables	0 (Size-independent)	-

- *Absorption chiller*

The ABS unit inventoried in this study is a single-stage water/ammonia system with a cooling capacity of 100 kW [136]. A hybrid cooler is also included in the ABS boundary. Table 6.7 reports the LCI flows for the assessed system.

The functional parameter $P_{ABS,cool}$, i.e. the installed cooling power of the ABS, is used for LCI scaling. A cost exponent L of 0.54 is used to estimate the LCI flows of the ABS at different sizes, by considering the similarity between cost and LCA scaling. The cost exponent equal to 0.54 is obtained from the literature [137] and relates the investment cost of the equipment to its cooling power expressed in $[kW_c]$.

Table 6.7. LCI data for the manufacturing of 100 kW_c ABS unit (from [136]).

	Amount	Unit
Materials and energy requirements		
Aluminum	420	[kg]
Copper	480	[kg]
Chromium steel 18/8, hot rolled	480	[kg]
Reinforcing steel	3220	[kg]
Polyethylene, high density, granulate	40	[kg]
Ammonia liquid	72	[kg]
Electronics, for control units	60	[kg]
Ethylene glycol	150	[kg]
Stone wool	70	[kg]
Tube insulation, elastomere	90	[kg]
Electricity, medium voltage	133	[kWh]
Heat	950	[MJ]
Water	5.98	[m3]
Materials processes		
Sheet rolling, aluminum	420	[kg]
Wire drawing, copper	480	[kg]
Sheet rolling, chromium steel	480	[kg]
Sheet rolling, reinforcing steel	3220	[kg]
Zinc coating, coils	68	[m2]
Injection moulding, polyethylene	40	[kg]

- *Pellet boiler*

The PB unit considered as reference is a 12 kW_{th} unit which consists of steel body with a fully insulated cladding [138]. The system includes a pellet feeding system, a speed controlled vacuum fan for air supply regulation and a stainless steel burner. The LCI data for the considered system are reported in Table 6.8.

The functional parameter of the PB is represented by the nominal thermal power $P_{\text{PB,th}}$. The default cost exponent (L=0.6) is used to scale the LCI in the range from 1 kW$_{\text{th}}$ to 250 kW$_{\text{th}}$, as suggested in [131].

Table 6.8. LCI data for the manufacturing of 12 kW$_{\text{th}}$ PB unit [138].

	Amount	Unit
Materials and energy requirements		
Brass	0.659	[kg]
Copper	0.010	[kg]
Iron burner	29.51	[kg]
Steel pipes	1.974	[kg]
Galvanized steel	22.639	[kg]
Lead	0.280	[kg]
Chromium steel 18/8	117.761	[kg]
Low-alloyed steel	55.417	[kg]
Unalloyed steel	41.096	[kg]
Expanded vermiculite	2.560	[kg]
Glass fiber	0.517	[kg]
Rock wool	0.810	[kg]
Nylon 6-6	0.880	[kg]
Polyethylene low density granulate	0.030	[kg]
Silicone product	0.605	[kg]
Synthetic rubber	0.291	[kg]
Expanded vermiculite	2.560	[kg]
Glass fiber	0.517	[kg]
Rock wool	0.810	[kg]
Electronics for control units	1.880	[kg]
Packaging film low density LDPE	1.044	[kg]
Heat	647.136	[MJ]
Electricity, medium voltage	1375.164	[MJ]

- *Hot water storage*

The reference system is a storage unit with 2000 l of volume of water [132]. As illustrated in Table 6.9, the main input materials composing the system are low-alloyed steel and chromium steel. The functional parameter for the storage is the volume expressed in [l].

The scaling interval of the thermal water storage was fixed by calculating the volume of the storage required to store up to 250 kWh of thermal energy as reported in Eq. (6.3):

$$V_{\text{storage}} = \frac{E_{\text{storage}} \cdot 3600 \cdot 1000}{\rho_{\text{water}} \cdot c_{\text{water}} \cdot \Delta T} \qquad (6.3)$$

where V_{storage} is the volume of the storage expressed in [l], E_{storage} is the maximum storable energy expressed in [kWh], ρ is the density of water in [kg/m^3], c_{water} is water specific heat in [kJ/(kg.K)]

and ΔT is the temperature difference assumed equal to 35 K [126]. Thermal water storage is widely used for residential building applications where it can be coupled with both solar and CHP systems. For estimating the LCI of storage systems with different volumes a cost exponent of 0.81 is used in this study, according to the cost scaling relationships presented in [137].

Table 6.9. LCI data for the manufacturing of 2000 l storage system (from [132]).

	Amount	Unit
Materials and energy requirements		
Steel low-alloyed, hot rolled	305	[kg]
Welding gas steel	10	[m]
Chromium steel 18/8, hot rolled	35	[kg]
alkyd paint, white, in 60% solution state	1.7	[kg]
glass wool mat	25	[kg]
sawnwood, softwood, dried (u=20%)	0.06670	[m3]
Electricity, medium voltage	45	[kWh]
Electricity, low voltage	45	[kWh]
Heat	344	[MJ]

6.2.4 Impact assessment indicator

The presented cradle-to-gate analysis focuses on the widely used impact parameter CED of selected energy systems for residential applications. The CED of a system stands for the direct and indirect energy consumption in units of energy (MJ) throughout the life cycle. The total CED consists of the sum of the fossil, nuclear, biomass, water, wind and solar energy demand in the life cycle of the analyzed product [59] as reported in Eq. (6.4):

$$CED_T = CED_f + CED_n + CED_{bio} + CED_{wa} + CED_w + CED_{so} \qquad (6.4)$$

The fossil CED (CED_f) can be considered as an impact indicator as it represents the depletion of energy resources related to the life cycle of a certain product. It is mainly related to the amount of consumed and burned fossil fuels which in turn has a high impact on the environment.

In the following, the main assumptions made for modeling each technology, i.e. STC, PV panel, CHP system, ABS, ASHP and GSHP, are reported. In addition, the water storage of thermal energy is described.

6.3. Validation

Although several LCA studies dealing with energy systems suitable to residential applications were carried out, a homogeneous comparison of all the technologies presented in this research is difficult because of the different functional units, regional variations, inclusion/exclusion of different life cycle

stages and different life cycle impact assessment methodologies. Therefore, a comparison to other studies is made in this Section only for the technologies and sizes available in the literature. The comparison of the results obtained by means of the methodology developed in this work to published data shows a good agreement, thus validating the LCA scaling procedure developed in this work.

6.3.1   Validation of the scaling procedure for PBs of different sizes

Since linear scaling, i.e. L=1 according to Eq. (6.2), is commonly applied in LCA studies, the influence of using a linear approach instead of nonlinear scaling and the relevance of scaling by using power-law relationships is illustrated in this Section. The considered technology is a pellet boiler, since data from different sources and at different sizes were available only for this system. The size parameter S used for scaling the LCI for different sizes is the installed thermal power of the boiler.

In order to validate the proposed methodology, LCI data for the PB should be available, at least, for two different sizes. Thus, detailed LCI data are taken from different sources and for different sizes. In particular, LCI data for manufacturing a 12 kW_{th} PB are taken from Chiesa et al. [138], a second LCI dataset available for a 46 kW_{th} PB is reported by Cellura et al. [139] and finally the LCI of a 25 kW_{th} and a 300 kW_{th} boilers are found in [140].
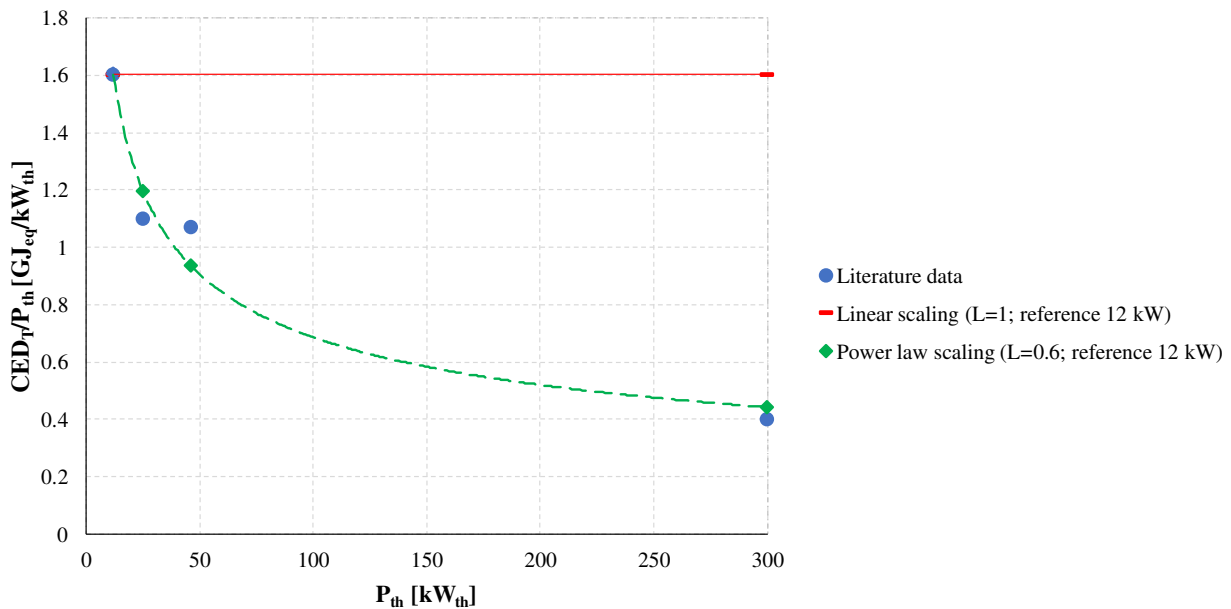

Fig. 6.3. Specific CED trend for a pellet boiler, using linear scaling and power law scaling and comparison to the CED calculated using LCI literature data.

Figure 6.3 compares the total CED per kW_{th} calculated by using literature LCI data available at different sizes of the pellet boiler to the values obtained by using linear scaling (specific CED

independent of the size) and the approach proposed in this research, i.e. LCI scaling with power law relationship.

As previously discussed, since no information about PB scaling is available, the nonlinear scaling with power law relationship is performed by using a costs exponent of 0.6, taken from the literature [131]. Moreover, linear scaling and scaling with power law relationship were both performed by using the 12 kW$_{th}$ pellet boiler as the reference.

Figure 6.3 demonstrates that scaling with power law relationship clearly provides more accurate results compared to the conventional LCI scaling which assume a constant CED per kW$_{th}$. In fact, considering the 300 kW$_{th}$ system, the total CED calculated by scaling the LCI with power law relationship and with linear scaling is equal to 132.7 and 480.8 GJ$_{eq}$, respectively, while the total CED calculated by using available LCI data is equal to 119.5 GJ$_{eq}$. The results show that linear scaling heavily over-estimate (in this case) the calculated impact (with a maximum error equal to 302%), while the proposed approach allows more accurate results with a maximum error of 12 %.

6.3.2   Validation of the scaling exponents to be used for CHP system scaling

Whiting et al. [70] used a similar scaling approach based on power law relationships to scale up the environmental impacts associated with the manufacturing of a CHP system and an aerobic digestion plant. For both systems, environmental impacts were scaled by using an exponent value of 0.6. Likewise, investment costs of a CHP plant were scaled by Lantz [94] following the economy of scale approach and using a costs exponent of 0.66. These two works show the validity of the power law for the LCA scaling and its analogy with the costs scaling. The analogy between LCI scaling and costs scaling was also demonstrated by Gerber et al. [93]. They recommend the use of power law relationship for LCI scaling instead of linear scaling. Moreover, they showed that, when no information about the scaling behavior is available (i.e. relationship between mass and equipment size), the use of costs exponents always allows better results than linear scaling. The same is also confirmed by Caduff et al. [98] that recommend the use of scaling factors in the range from 0.5 to 0.8 for the scaling of energy technologies.

6.3.3   Validation of the scaling procedure for STC, PV, ASHP and hot water storage

Table 6.10 shows the CED estimated in this study and CED values reported in the literature for the STC, PV panel, ASHP and hot water storage. As can be seen, the CED of the STC calculated in this study is slightly higher than the one calculated by Ardente et al. [73]. The small difference (about

11.5%) may be due to the different transport distances and energy mix assumed by the authors which used the Italian energy mix to model the production of electricity.

The results for the PV system agree well to the studies carried out by Kabakian et al. [78] and Tiwari et al. [101]. In their studies, the specific CED associated with the manufacturing of a PV system is 4.78 GJ_{eq}/m^2 and 4.96 GJ_{eq}/m^2, respectively. Thus, these results are fully consistent with the CED found in this study.

The CED for the production of a 10 kW ASHP is in agreement with the data published in [141]. Once again, this small difference may be due to the different assumptions made in both studies.

The CED of the hot water storage calculated in this work is compared to two other studies. The first study was carried out by Beccali et al. [142] and considers a 2000 l hot water storage, while the second study was carried out by Gürzenich et al. [143] and considers a 100 l storage. Comparisons show that the CED calculated in this work is fully comparable to the data published by Beccali et al. [142], since both studies assume the European mix. On the other hand, as expected, a slight variation is found compared to the work of Gürzenich et al. [143], since this study reflects the Indian situation. However, both comparisons show that results are fully consistent, by considering that LCA results are subject to different factors [54].

Table 6.10. Comparison between CED values reported in the literature and CED values estimated in this research.

STC	
This research	*Ardente et al. [73]*
1.53 GJ_{eq}/m^2	1.73 GJ_{eq}/m^2

PV panel		
This research	*Kabakian et al. [78]*	*Tiwari et al. [101]*
4.69 GJ_{eq}/m^2	4.78 GJ_{eq}/m^2	4.96 GJ_{eq}/m^2

ASHP (size: 10 kW$_{th}$)	
This research	*Beccali et al. [141]*
12 GJ_{eq}	12.5 GJ_{eq}

Hot water storage (capacity: 2000 l)	
This research	*Beccali et al. [142]*
14.18 GJ_{eq}	14.8 GJ_{eq}

Hot water storage (capacity: 100 l)	
This research	*Gürzenich et al. [143]*
1.27 GJ_{eq}	1.54 GJ_{eq}

6.4. Results and discussion

- *CED impact curves vs. technology size*

Figure 6.4 show the total CED and fossil CED calculated for the STC, PV, CHP, GSHP, ASHP, ABS, PB and hot water storage technologies. The full symbols represent the results of the systems considered as a reference, while the empty symbols represent the results of the scaled systems.

As highlighted from Figure 6.4, the impact indicators calculated for the STC and PV systems are characterized by a linear trend, which is due to the linear scaling approach adopted for both systems. It should be noted that, though the absolute values of the total CED and fossil CED diverge by increasing STC/PV area, the fraction of fossil energy demand of the total CED, for the manufacturing of the STC/PV system, remains constant independent of system functional parameter.

With regard to the specific impact expressed in [Units of impact/Units of functional parameter], it can be noted that the scaling effect is noticeable for the energy technologies of which a non-linear scaling approach is assumed, i.e. CHP, GSHP, ASHP, ABS, PB and hot water storage. For instance, by comparing the 1 kW_{el} and 250 kW_{el} CHP units, it is found that the specific total CED decreases from 292.8 GJ_{eq}/kW_{el} for a 1 kW_{el} CHP unit to 3.2 GJ_{eq}/kW_{el} for a 250 kW_{el} CHP, the fossil CED decreases from 191.1 GJ_{eq}/kW_{el} to 2.4 GJ_{eq}/kW_{el}. From these results, it can be stated that the higher the size of the CHP, the lower is the impact referred to the produced energy; this proves that linear scaling may under- or over- estimate LCA results (see Section 6.3). The same applies to the other energy technologies, with the exception of STC and PV systems. Moreover, unlike the non-linear scaling approach used for the abovementioned energy technologies, the linear scaling approach leads to a constant specific impact independent of system size. The impact reported in Figure 6.4 represent one of the main achievements of this work.
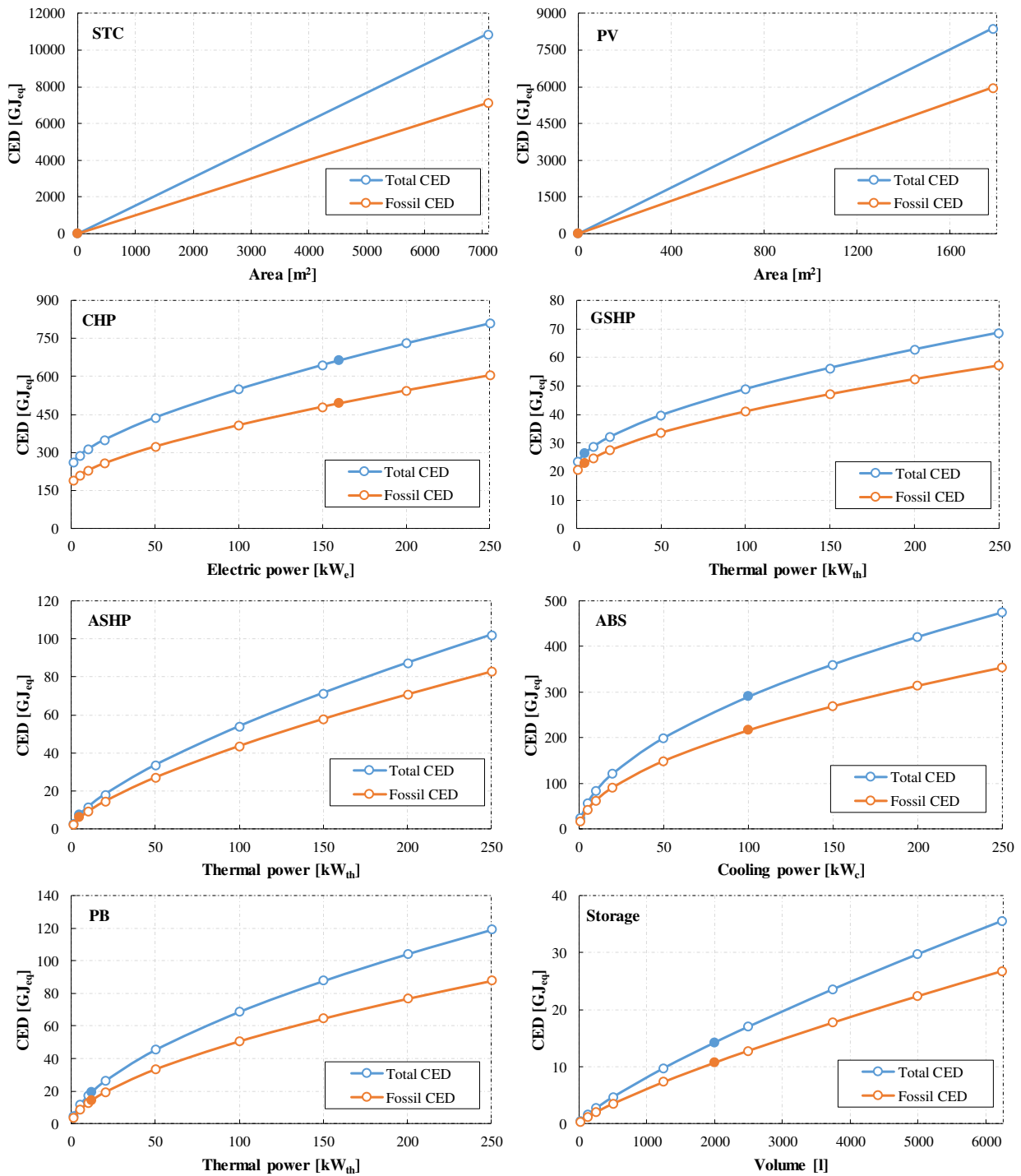
Fig. 6.4. Total CED and Fossil CED trend vs. technology size.

- *Comparison of different energy system configurations*

To highlight the effect of the scaling procedure developed in this study and identify the best option in order to meet a given energy demand, a comparison is made among by varying their capacity. In particular, Figure 6.5 reports a comparison between the CHP and the PV panels as a function of the installed electric power. It can be seen that the increase of the total CED is noticeable for the PV panel

as a function of the installed capacity, while the increase of the total CED of the CHP system is much lower compared to the PV system.
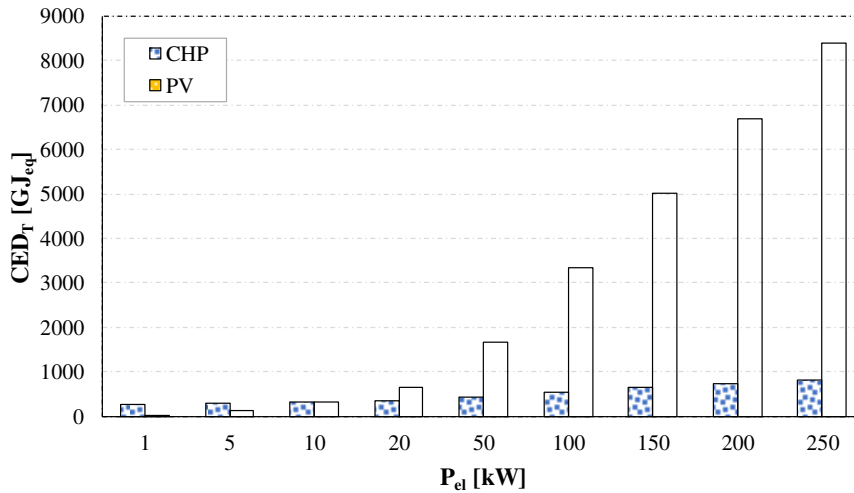

Fig. 6.5. Comparison of the total CED of the CHP and PV systems.

Figure 6.6 illustrates a comparison between the STC, GSHP and ASHP units as a function of the installed thermal power. As can be seen, the STC is the system which has the highest impact with the exception of the case of 1 kW$_{th}$ power capacity. It can also be noticed that, for sizes lower than 100 kW$_{th}$, the impact related to the production of the ASHP is lower than the impact of the GSHP, while this impact tends to be higher for sizes greater than 100 kW$_{th}$. This can be explained by the fact that the borehole heat exchanger impact of the GSHP weighs more for small sizes even if the ASHP requires more materials and energy. However, by considering that the borehole was assumed GSHP size-independent, the impact of the ASHP tends to be more predominant.
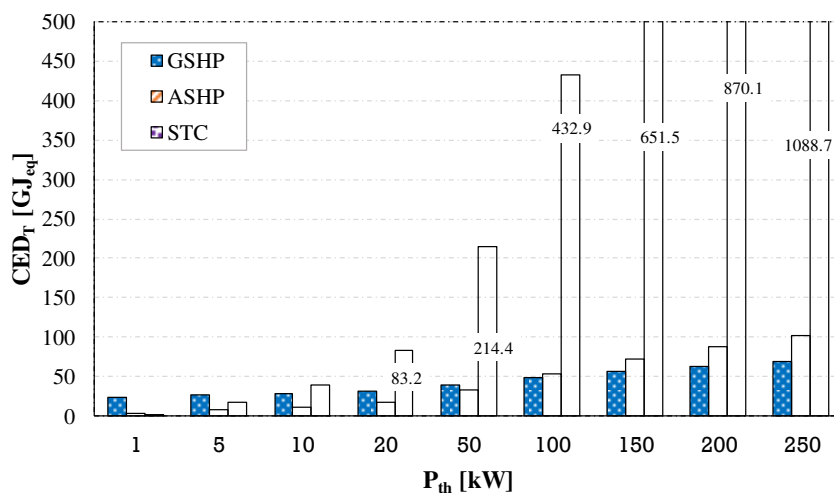

Fig. 6.6 Comparison of the total CED of the GSHP, ASHP and STC.

Whereas above each technology is compared solely, in the following hybrid systems, i.e. system combining electricity and heat generation, will be in the center of interest, comparing them with a CHP. The hybrid systems under investigation are PV for electricity generation with STC, GSHP and ASHP, respectively, for the heat supply.

In order to calculate the thermal power produced from the CHP system as a function of the nominal electric power, a market survey [29] was conducted on CHP systems based internal combustion engines, by analyzing the engines currently available in the range 1 kW_{el} - 294 kW_{el}. The result of this analysis is expressed by the following relationship:

$$P_{CHP,th} = 2.978 \cdot (P_{CHP,el})^{0.871} \tag{6.5}$$

The results of the comparison between CHP and hybrid systems are reported in Figure 6.7. In order to have a consistent comparison between the combined and separate scenario, it supposed that the electric power of the CHP can be produced from a PV system with an appropriate area, while the thermal power of the CHP can be produced from the STC, GSHP or ASHP. Figure 6.7 demonstrates that, for an installed electric power higher than 10 kW, the CHP based system requires less primary energy than the aggregate systems PV+GSHP and PV+ASHP, while this option tends to require more energy for lower capacities. It can also be noticed that for small electric power (approximately 1 kW), compared to the CHP option, the other options are more convenient. At 5 kW a mixed result can be observed. While PV with heat pumps demands less CED than a CHP, PV+STC systems realize higher CED values.

Moreover, the increase of the CED of the CHP system with its size is much smaller than the increase of the CED of the aggregate systems. However, it should be mentioned that this analysis only takes into account the manufacturing phase, while the operation phase is not included; this could influence the ranking of the different technologies.

Whereas the CED for PV+heat pump systems are dominated by the CED of PV systems – the share of CED of PV is higher than 90%, a different picture can be observed for PV+STC systems.
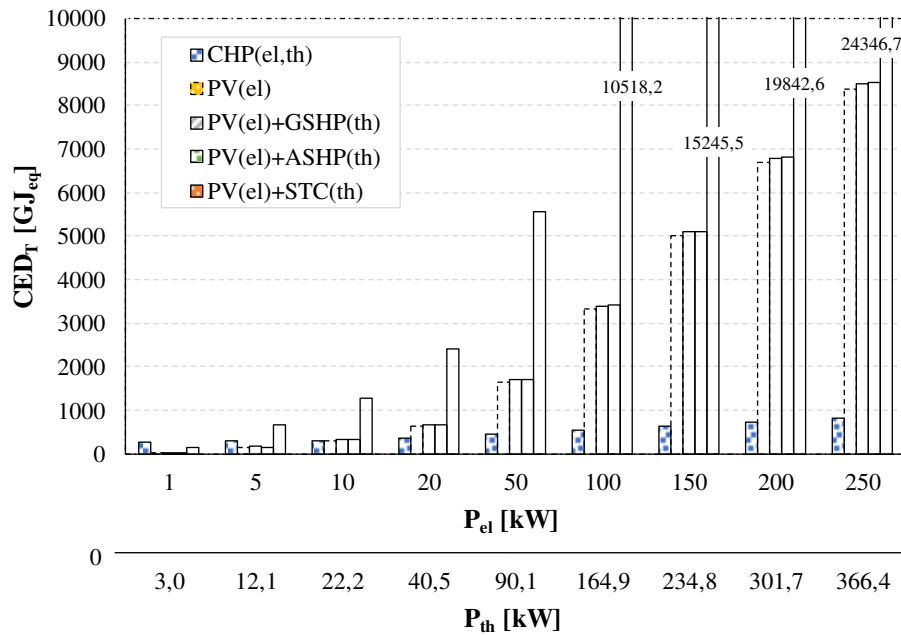
Fig. 6.7. Total CED of the CHP and the different aggregate systems as a function of the thermal and electrical installed capacity.

- *Dominance analysis*

In order to identify the processes and activities of the life cycle which are responsible for the greatest (dominant) environmental impact, a dominance analysis of the fossil CED with regard to the life cycle processes is performed (see Figure 6.8). In fact, environmental impacts are closely-related to the use of fossil energy. This type of analysis allows to identify where improvements are most needed. The dominance analysis is performed for all energy technologies by considering the same reference functional parameter used for scaling.

The analysis reveals that transports are of minor importance for all the assessed technologies. Figure 6.8a shows that aluminum and chromium are the most dominant production processes causing the greatest energy consumption for the manufacturing of the STC. From Figure 6.8b, it can be seen that the largest energy consumption for the manufacturing of PV panels is due to wafers production. The production of silicon products, such as silicon wafers for photovoltaics and electronic grade silicon, requires large amounts of electricity, so the electricity use is the most important factors. Thus, the production of silicon products usually takes place in countries with low prices and a secure supply. As highlighted in Figure 6.8c, the major contributor process to the fossil CED of the CHP system is the control cabinet, which is mainly due to the use of fossil energy sources, such as hard coal (7.4 %) and natural gas (9.7 %). Since the control cabinet is considered a size-independent component, the contribution of the latter to the total fossil CED is expected to decrease by considering a larger size compared to the reference (160 kW_{el}). Indeed, by considering the CHP unit with 250 kW_{el}, the share

118

of the control cabinet decreases to 20.6 %, which is still important. However, this demonstrates how scaling and distinction between size-dependent and size-independent components may affect the final results and consequently the action of decision makers. Regarding the GSHP (Figure 6.8d), the 75.5% of the overall fossil CED is caused by the borehole heat exchanger process, which in turn is coming out from the production of polyethylene and ethylene glycol with about 51.3 % and 19.6 % of the total fossil CED, respectively. Thus, opportunities to reduce the demanded energy throughout the life cycle of GSHP systems lie in enhancing the energy efficiency of industrial sectors such as polymerization where high temperatures are required for the cracking of naphtha, which is the most important raw material for polymer production. From Figures 6.8e through 6.8h, it is possible to observe that the major contributors to the fossil CED are metals and this reflects the functional unit composition of the ASHP, ABS, PB and hot water storage which are mainly made of steel. The relatively high consumption of fossil fuels is mainly due to processes which require high temperatures, such as blast furnace process for the production of hot metal and blast oxygen furnace converter process which is used for steel making.
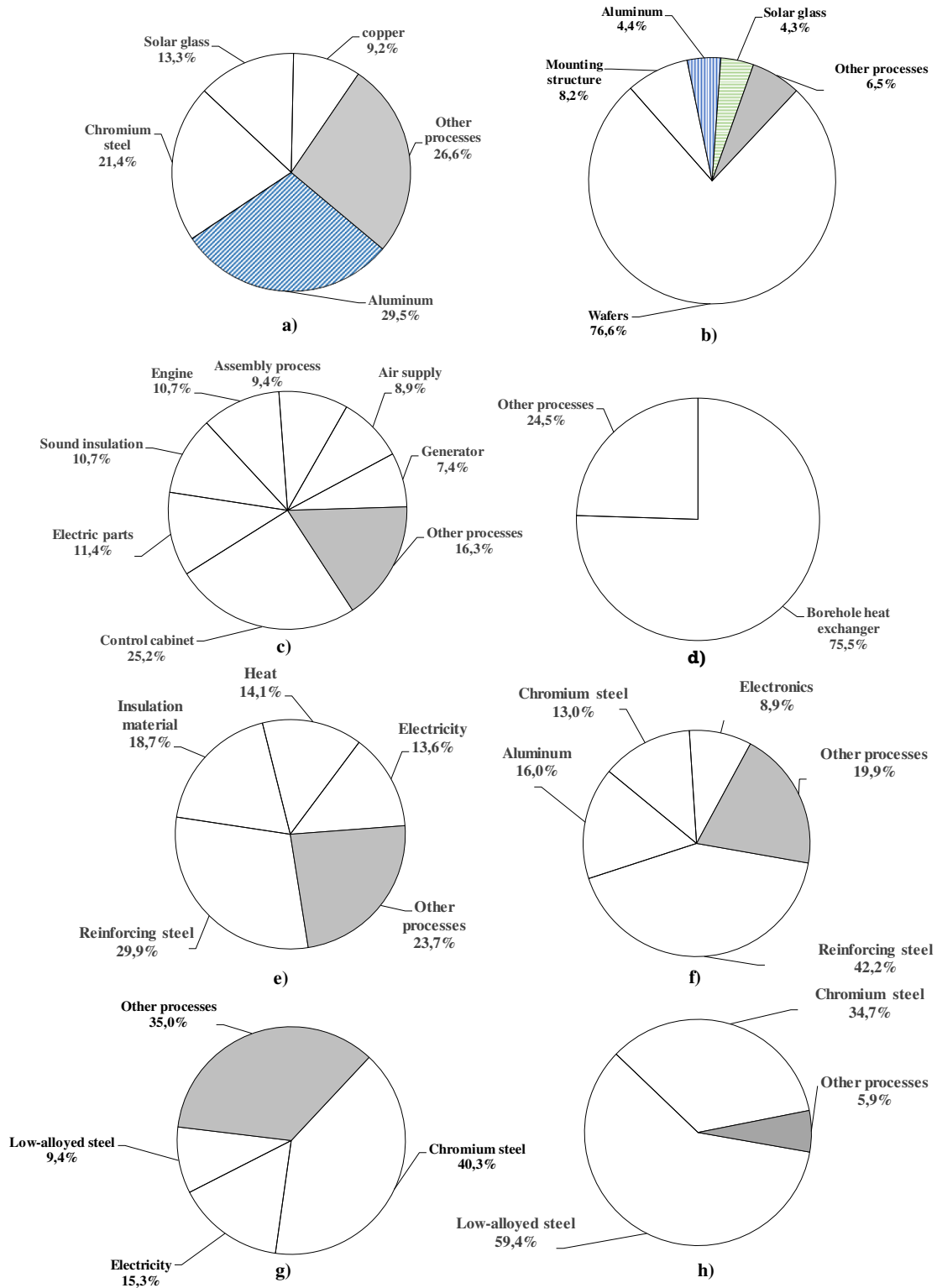
Fig. 6.8. Dominance analysis of the fossil CED of the STC a), PV b), CHP c), GSHP d), ASHP e), ABS f), PB g) and hot water storage h).

7. Optimization of a hybrid energy plant by accounting for on-site and off-site primary energy consumption

The following sections of this chapter deal with the sizing optimization of HEPs by accounting for the life cycle energy demand. The optimization is carried out by using a GA and a case study is considered to demonstrate the effectiveness of the proposed procedure.

7.1. Introduction

In order to achieve an optimal design of the HEP, on-site and off-site environmental impacts, primary energy consumption or costs have to be accounted for, especially when considering renewable energy systems. Off-site primary energy consumption may be quantified by using LCA, while on-site energy demand may be evaluated by simulating plant operation throughout its useful life.

The work in this chapter presents a procedure for optimizing the size of a complex HEP by taking into account of the non-linear LCI scaling of energy systems. The HEP is composed of renewable and non-renewable energy systems and the optimization is conducted with the aim of minimizing the primary energy consumed during the manufacturing, transportation and operation phases. Finally, a case study is considered to demonstrate the effectiveness of the proposed procedure. Two approaches are considered to assess the influence of the integration of LCA into the optimization process. The first approach consists of solving the sizing optimization problem by minimizing on-site primary energy consumption, i.e. only during the operation phase, while in the second approach on-site and off-site primary energy consumption are minimized by integrating the LCA into the optimization process.

7.2. Model development

The optimal design of the HEP is made by considering an energy-based criterion, i.e. the primary energy demanded throughout the manufacturing and operation phases is minimized. However, a different objective function, such as pollutant emission production or total cost, may be implemented in the model developed in this research. Sizing optimization is conducted by using a GA because of its ability to deal with discrete spaces and solve nonlinear problems [50]. In fact, this kind of evolutionary algorithm does not require limiting assumptions about the underlying objective function. The optimization is conducted by simulating the HEP throughout one year and the analysis is carried out on an hourly basis. For the simulation of the HEP, a model is developed in Matlab®.

7.2.1 Hybrid energy plant

Figure 7.1 shows a scheme of the HEP considered in this research. It is composed of different technologies which use renewable and non-renewable energy sources. In particular, STC, PV, CHP, ABS, ASHP, GSHP and hot water storage are considered.
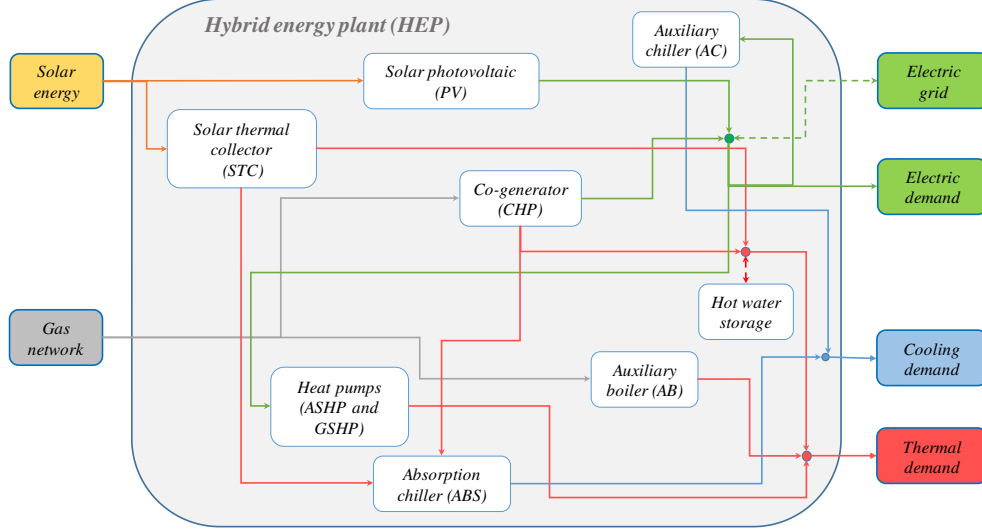

Fig. 7.1. Scheme of the HEP.

In addition, an AB and an AC are also considered as auxiliary systems in order to meet thermal and cooling demands in case that they are not fulfilled by the abovementioned systems. Heat pumps are assumed reversible, i.e. they can produce thermal energy in winter and cooling energy in summer.

Equations (7.1), (7.2) and (7.3) express the balance of thermal energy, cooling energy and electric energy demands to be met by the different technologies of the HEP:

$$E_{\text{AB,th}}(i) = E_{\text{th}}(i) - \left(E_{\text{STC,th}}(i) + E_{\text{CHP,th}}(i) + E_{\text{GSHP,th}}(i) + E_{\text{ASHP,th}}(i) + E_{\text{storage,th}}(i) \right) \tag{7.1}$$

$$E_{\text{AC,cool}}(i) = E_{\text{cool}}(i) - \left(E_{\text{ABS,cool}}(i) + E_{\text{GSHP,cool}}(i) + E_{\text{ASHP,cool}}(i) \right) \tag{7.2}$$

$$E_{\text{el}}(i) + E_{\text{GSHP,el}}(i) + E_{\text{ASHP,el}}(i) + E_{\text{AC,el}}(i) = E_{\text{PV,el}}(i) + E_{\text{CHP,el}}(i) + E_{\text{grid,el}}(i) \tag{7.3}$$

As can be seen, these equations ensure the fulfilment of the thermal, cooling and electric energy demands at each time step i (equal to one hour) of the entire simulation period of one year. In particular, from Eq. (7.1), E_{th}, which represents the space heating and hot water demand, can be met by the STC, CHP, GSHP and ASHP systems. The AB ensures the fulfillment of the thermal demand in case it is not met by the other systems. From Eq. (7.2), E_{cold}, which represents the cooling demand, is fulfilled by the ABS, GSHP and ASHP systems. The AC ensures the fulfillment of the cooling

demand if not fulfilled by the other systems. As reported in Eq. (7.3), the electric energy demand (E_{el}), the electricity required by the heat pumps ($E_{GSHP,el}$ and $E_{ASHP,el}$) and the AC ($E_{AC,el}$) are provided by the PV ($E_{PV,el}$) and CHP ($E_{CHP,el}$) systems. If these systems are not able to fulfill the demand of electric energy, the remaining part, which is represented by $E_{grid,el,taken}$, is imported from the grid. Otherwise, the excess of the produced electric energy from the CHP system and the PV panel is delivered to the grid.

Equation (7.4) defines the primary energy used during the operation phase. It is defined as the sum of primary energy consumption of the CHP, AB and the primary energy referred to the electricity exchanged with the grid.

$$PE_{op} = PE_{fuel, CHP} + PE_{fuel, AB} + PE_{E_{el,taken}} - PE_{E_{el,sent}} \tag{7.4}$$

7.2.2 Energy systems

The technologies considered in this work are selected according to two criteria. The first criterion is that the candidate technologies are market available (in quite a wide range of sizes) and suitable for residential users as both single components and aggregate systems. Though ORC systems may be a promising alternative as the prime movers of micro-CHP systems in addition to internal combustion engines, they still present some challenges for real applications, as discussed by Ziviani et al. in [144]. Because of the purpose of the analyses carried out in this work, the second criterion used to select the technologies is the availability of quantitative LCA data.

The technologies which are considered in this study are modelled by following a gray-box modelling approach. In particular, systems are defined by power and efficiency curves. It should be noted that the efficiency of all the energy technologies, with the exception of STC and PV panels of which performance only depends on ambient conditions, vary with the load. The basic correlations for each technology comprising the HEP are reported in the following.

Photovoltaic panel

Regarding the PV panels, single-crystalline silicon solar cells are considered. The efficiency of the PV system takes into account the efficiency of the inverter and electrical connections considering a Balance of System (η_{BoS}) equal to 0.9 [115]:

$$\eta_{PV} = \eta_{M} \cdot \eta_{BoS} \tag{7.5}$$

With;

$$\eta_M = \eta_{M,ref} \cdot \left[1 - \beta \cdot \left(T_c - T_{ref}\right)\right]$$

where $\eta_{M,ref}$ is the efficiency of the PV at reference conditions, β a temperature penalty coefficient, T_c the operating temperature of the cell and T_{ref} the reference temperature of the cell. The operating temperature (T_c) of the cell depends on the external air temperature and solar radiation.

Solar thermal collector

The STC efficiency is estimated by means of the following equation reported in [105]:

$$\eta_{STC} = \eta_o - a_1 \cdot \left(\frac{T_{av} - T}{R}\right) - a_2 \cdot \left(\frac{T_{av} - T}{R}\right)^2 \qquad (7.6)$$

where η_o is the optical efficiency, a_1 and a_2 are correction factors, T the hourly external ambient temperature, T_{av} the average temperature and R the solar radiation. The collector efficiency varies during the year because it depends on both the external ambient temperature and the global solar radiation. The average temperature is assumed equal to 80 °C during summer, and 50 °C during winter.

Combined heat and power system

The CHP system considered in this study is based on an internal combustion engine. The size of the CHP system is defined by the nominal electric power. The electric efficiency and the nominal thermal power are calculated as a function of the nominal electric power as reported in [29]:

$$\eta_{CHP,el,nom} = 0.232 \cdot \left(P_{CHP,el,nom}\right)^{0.084} \qquad (7.7)$$

$$P_{CHP,th,nom} = 2.5 \cdot \left(P_{CHP,el,nom}\right)^{0.91} \qquad (7.8)$$

The performance of the CHP varies with the ambient temperature and load variation which is defined as the ratio between the actual thermal power and nominal power [29]. The minimum load is assumed equal to 10 % of the nominal thermal load [116]. Moreover, CHP system start-up is modelled by adding a penalty equal to the fuel consumption for five minutes at nominal conditions.

Heat pumps

The nominal cooling power is calculated as a function of the nominal thermal power by following the same approach reported in [29]:

$$P_{GSHP,cool,nom} = 0.82 \cdot P_{GSHP,th,nom} \qquad (7.9)$$

$$P_{ASHP,cool,nom} = 0.88 \cdot P_{ASHP,th,nom} \qquad (7.10)$$

For both heating and cooling modes, the performance of the heat pumps varies depending on the temperature of the external heat exchanger, internal heat exchanger and the load. The minimum load is assumed equal to 10 % of the nominal load [29, 117].

Absorption chiller

A single-effect H_2O-BrLi ABS is considered. The nominal efficiency of the ABS, represented by the energy efficiency ratio (*EER*), is assumed equal to 0.7 [29]. The capacity of the ABS system is defined by the nominal thermal power. The nominal cooling power is calculated as follows:

$$P_{ABS,cool,nom} = P_{ABS,th,nom} \cdot EER_{ABS,nom} \qquad (7.11)$$

The part load operation can affect the performance of the ABS. The minimum load is fixed equal to 25 % of the nominal load [145].

Auxiliary systems

A condensing boiler powered by natural gas and an electric chiller are considered as auxiliary generation systems. The nominal thermal efficiency (on an LHV basis) of the AB is assumed equal to 1.06, while the *EER* of the AC is assumed equal to 2.7. Both systems are considered as modulating systems. The minimum load of the AC is assumed equal to 10% [146], while the AB can modulate between 0 and 100 %. Moreover, a variation of the performance with load is assumed for both systems.

7.2.3   The control logic

The control logic of the different technologies is defined by Switch-On Priority (SOP) mapping, which defines the starting order and allows the minimization of on-site primary energy consumption during the considered period. The mapping is developed by considering the demands for winter and mid-season and the summer season separately, and the SOP control logic is defined by maximizing the efficiency of the system depending on the nominal capacity and the types of systems utilized. Renewable energy systems, such as STC and PV are not considered in the mapping, since they are not controllable and must be activated first. Furthermore, the AB and AC are not considered in the mapping because they are considered as auxiliary systems and their size is set equal to the peak of the thermal and cooling energy demand, respectively. The CHP size ranges between (50 to 500) kW, with a step of 50 kW and the ASHP and GSHP capacities range between (30 to 300) kW with a step

of 30 kW. The nominal thermal power of the ABS is defined equal to the CHP thermal nominal power.

In order to develop the SOP mapping, for each combination of component sizes, the on-site primary energy consumption is calculated and the best SOP control logic is evaluated. For the considered components, the developed SOP mapping consists of a 3D matrix which contains 1000 size combinations. At each iteration of the optimization process, the developed SOP mapping is used by the optimization algorithm to define the proper SOP which minimizes the on-site primary energy consumption.

7.2.4   Life cycle assessment model

In order to evaluate the primary energy consumed during the manufacturing phase of the PV, STC, CHP, GSHP, ASHP, ABS and the storage, a cradle-to-gate LCA is carried out (See Chapter 6). AB and AC are not assessed, since they are considered as auxiliary systems and they are not involved in the optimization process.

The LCIs of the investigated systems are presented in Chapter 5. The CED is considered as the impact indicator. To calculate the CED of a system in a range of sizes, LCI data were scaled by carrying out the scaling procedure described in Chapter 5.

It should be mentioned that, nonlinear scaling was only carried out for the CHP, GSHP, ASHP, ABS and storage equipment, while the LCI of STC and PV systems was scaled linearly (i.e. k=1) as a function of the respective area. Scaling exponents k for the CHP, GSHP, ASHP, ABS were obtained from literature or by assuming the economy of scale. Moreover, in order to calculate the primary energy associated with the manufacturing of the grid, the Italian grid was also modelled by using the Ecoinvent® database. The *CED* associated with the cradle-to-gate life cycle of the optimized technologies is calculated as in Eq. (7.12):

$$CED = \sum_z \frac{CED_z(P_z)}{lifetime(z)} + CED_{grid}(El_{taken}) \tag{7.12}$$

where *CED* represents the total *CED* expressed in MJ_{eq} per year, the first term on the right hand-side is the sum of the primary energy associated with the cradle-to-gate life cycle of the optimized systems and *CED*$_{grid}$ represents the primary energy associated with the life cycle of the Italian grid and depends on the electricity taken from the grid per year of operation. Finally, for each system, the variables N_z and P_z represent the useful lifetime and the decision variable (or the size), respectively.

7.2.5 Optimization model

The methodology for sizing optimization of HEPs is outlined in Fig. 7.2. The GA is initialized by generating a random population of individuals in the design space and each individual represents a combination of sizes of the technologies composing the HEP.

For each individual of the population, the primary energy PE_{op} consumed during the operation phase is calculated from the simulation model of the HEP as reported in Eq. (7.4), while the CED is calculated from the LCA model according to Eq. (7.12).
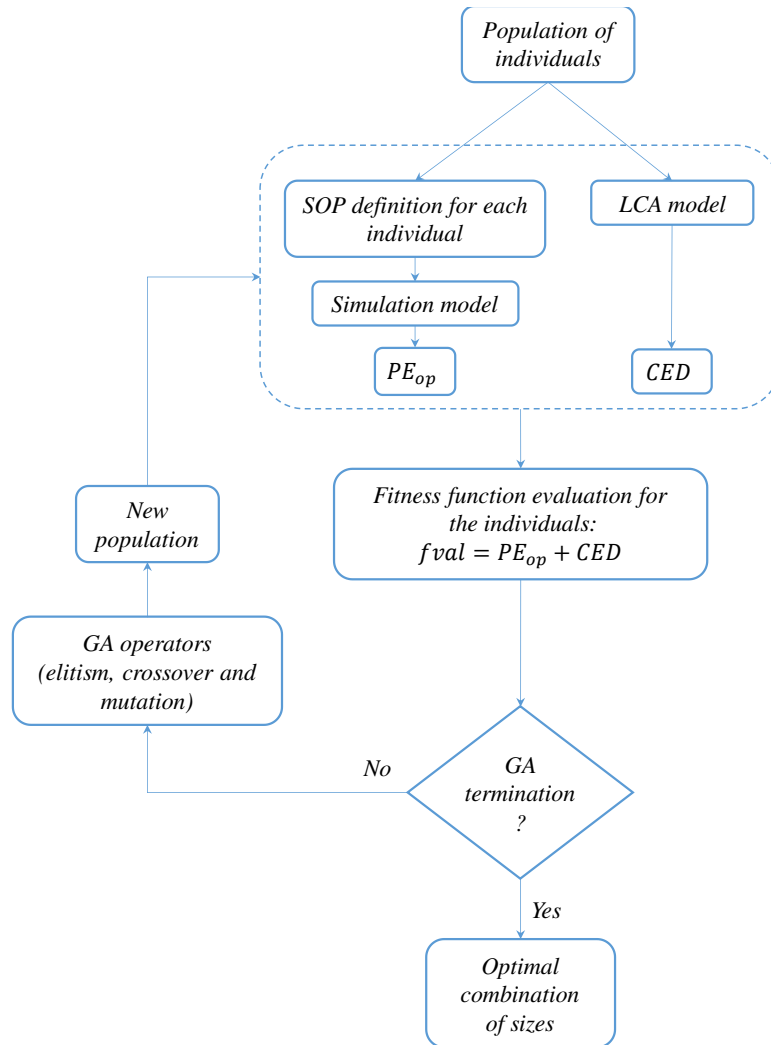

Fig. 7.2. GA optimization flowchart

Consequently, the GA evaluates the fitness function of each individual in the current population as follows:

$$fval = f(P) = PE_{op} + CED \tag{7.13}$$

Then, based on the values of the individuals in the current population, the GA creates a new population by applying three operators (elitism, crossover and mutation). These mechanisms are repeated by the GA until a certain criterion is met and the best individual, which represents the optimal combination of sizes, is selected.

The decision variables P which represent the sizes of the technologies to be optimized are $P_{CHP,el,nom}$, $P_{GSHP,th,nom}$, $P_{ASHP,th,nom}$, $P_{ABS,th,nom}$, A_{STC} and A_{PV}. The volume of the storage $V_{storage}$ is calculated according to [126] as a function of CHP and STC decision variables, while the size of AB and AC are imposed equal to the peak of the thermal and cooling energy demands, respectively.

7.3. Case study

A tower composed of thirteen floors, located in the northern Italy, is considered as a case study. In the tower, 1189 m^2, corresponding to a volume of 5735 m^3, are used as commercial premises, while 4457 m^2, corresponding to a volume of 20187 m^3, are used as offices.

7.3.1 Environmental data

The ambient temperature and solar radiation for the considered case study is calculated by using the procedure recommended in the standard [147]. This standard identifies one representative day of each month. Then, the hourly profiles of temperature and total solar radiation are calculated for the Italian climatic zone "A", where the considered building is situated, according to the standard [148]. The monthly air temperature and total solar radiation values are reported in Fig. 7.3a and Fig. 7.3b, respectively.
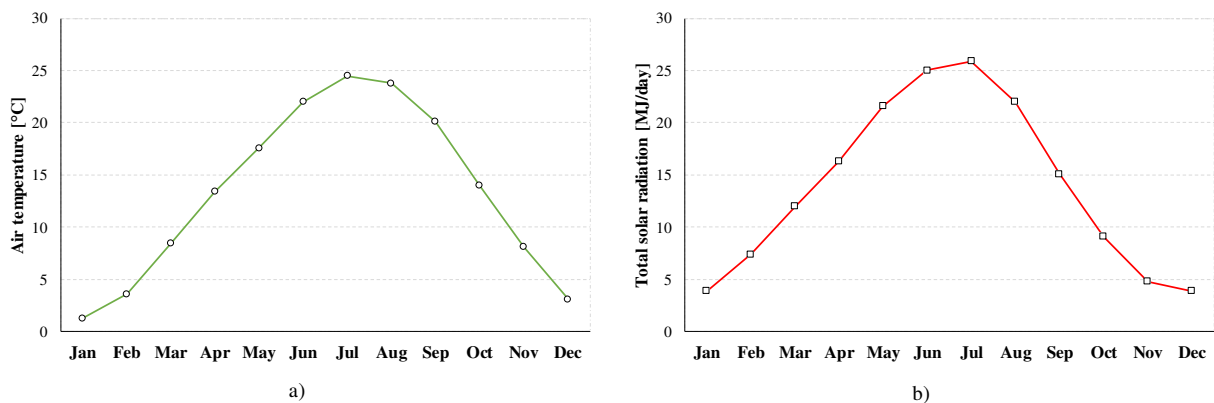

Fig. 7.3. Average air temperature (a) and daily total solar radiation (b).

7.3.2   Energy demands

Figures 7.4a through 7.4d report the monthly energy demand for space heating, hot water, space cooling and electricity, respectively. The monthly energy demands were characterized for three different zones and calculated by using the EdilClimaEC700® software. Zone 1 is for business use, Zone 2 is for offices and the Off Zone comprises elevators, lighting, parking lots, and the outdoor lighting basement. The energy demand is estimated equal to 207.17 MWh/year for space heating (Fig. 7.4a), 8.75 MWh/year for domestic hot water (Fig. 7.4b), 154.83 MWh/year for space cooling (Fig. 7.4c), and 410.92 MWh/year for electricity (Fig. 7.4d). The hourly demand presents a power peak of 234 kW for space heating and hot water, 294 kW for space cooling and 103 kW for electricity.

The energy demands were evaluated by considering 292 days of occupancy. The heating period for the climatic zone in which the building is located begins on 15th October and ends on 15th April, while the cooling period goes from 15th June to 15th September. Energy demands for domestic hot water and electricity are present throughout the whole year. In order to obtain hourly profiles of the energy demands, monthly energy demands are converted into hourly energy demands by using non-dimensional profiles which consider the types of users [149].
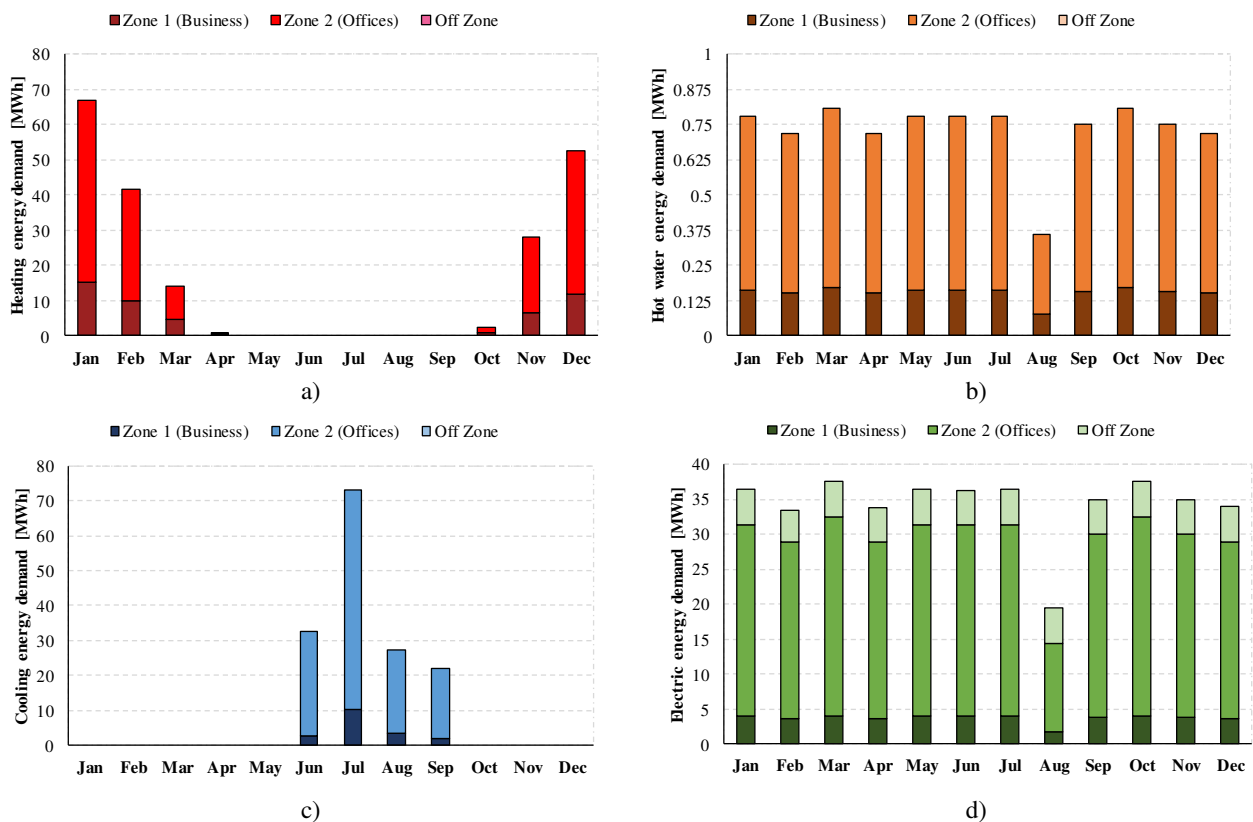

Fig. 7.4. Monthly energy demand for a) heating, b) hot water, c) cooling and d) electricity.

7.3.3 System variables and optimization algorithm set-up

The sizing optimization problem of the HEP is carried out based on the efficient matching between building energy demands and the energy supplied by the considered technologies, with the aim of minimizing the objective function represented by Eq. (7.13). The optimization aims at optimizing the STC and PV area (A_{STC} and A_{PV}) which can cover the available total area (328 m^2), the CHP nominal electric power ($P_{CHP,el,nom}$), which is an integer in the range (0 to 500) kW$_e$, the GSHP and ASHP nominal thermal power ($P_{GSHP,th,nom}$ and $P_{ASHP,th,nom}$) in the range (0 to 300) kW$_{th}$ and the ABS nominal thermal power ($P_{ABS,th,nom}$) in the range (0 to 400) kW$_{th}$. Regarding the GA set-up, 100 generations with a population of 300 individuals for each generation are evaluated and the elite count (i.e. the number of individuals with the best fitness values that survive to the next generation) is set equal to 10.

7.4. Results and discussion

Table 7.1 shows the optimization results of the two approaches considered in this study. In the first approach (LCA not integrated), LCA is not integrated into the optimization process, i.e. only the primary energy used during the operation phase is taken into account, while the second approach (LCA integrated) optimizes the sizes of the technologies considering the primary energy demanded throughout the cradle-to-gate life cycle and the operation phase of these systems.

As can be seen, the integration of LCA may lead to a different combination of sizes. In fact, by adding the off-site primary energy consumption evaluated by the LCA method, the area of the PV system increases in favor of the STC of about 37 m^2, the size of the CHP is increased from 93 kW$_e$ to 114 kW$_e$, the size of the GSHP is decreased from 298 kW$_{th}$ to 120 kW$_{th}$, the size of the ASHP decreases from 121 to 32 kW$_{th}$ and the ABS nominal power increases from 153 to 235 kW$_{th}$. It should be noted that a sensitivity analysis was carried out by increasing the available total area which can be covered by STC and PV panels (increased up to three times). The analysis revealed that, in the optimal solution, almost the entire available area is covered by PV panels.

Table 7.1. Optimal sizes of the technologies.

Optimization decision variables (P)	A_{STC} [m^2]	A_{PV} [m^2]	$P_{CHP,el,nom}$ [kW$_e$]	$P_{GSHP,th,nom}$ [kW$_{th}$]	$P_{ASHP,th,nom}$ [kW$_{th}$]	$P_{ABS,th,nom}$ [kW$_{th}$]	$V_{storage}$ [l]
LCA not integrated	40.3	287.5	93	298	121	153	892.6
LCA integrated	2.7	324.7	114	120	32	235	935.5

Figure 7.5 reports the annual CEDs associated with the cradle-to-gate life cycle of the two combinations of technology sizes (see Table 7.1) per one-year lifetime obtained by applying the two approaches. With reference to the CED of the GSHP, it can be noted that, even if the size of the GSHP is more than halved by passing from the "LCA not integrated" approach to the "LCA integrated" approach, the value of the CED does not decrease proportionally. This is due to the nonlinear scaling approach adopted in this research. Indeed, this justifies that linear scaling may under- or over-estimate LCA results and affect the optimization results.
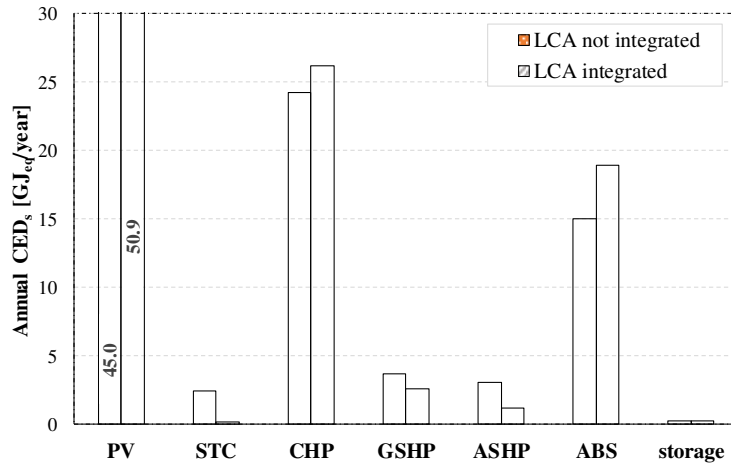

Fig. 7.5. Annual CED of the different technologies.

Figure 7.6 shows the primary energy associated with the grid (CED_{grid}), the cradle-to-gate life cycle of the whole plant (CED_{HEP}), the operation phase (PE_{op}) and the total primary energy consumption (*fval*). It can be seen that CED_{grid} most heavily affects the optimization results.

It should be mentioned that CED_{grid} can be evaluated only by considering both LCA and the operation. This is due to the fact that CED_{grid} is related to the electricity taken from the grid which depends on the operation policy of the different technologies. Furthermore, by integrating LCA into sizing optimization, the GA algorithm tends to increase the PV area in favor of the STC and also increases the size of the CHP, in order to minimize the amount of electricity taken from the grid. Moreover, the integration of LCA leads to a primary energy saving of about 12.5 %.
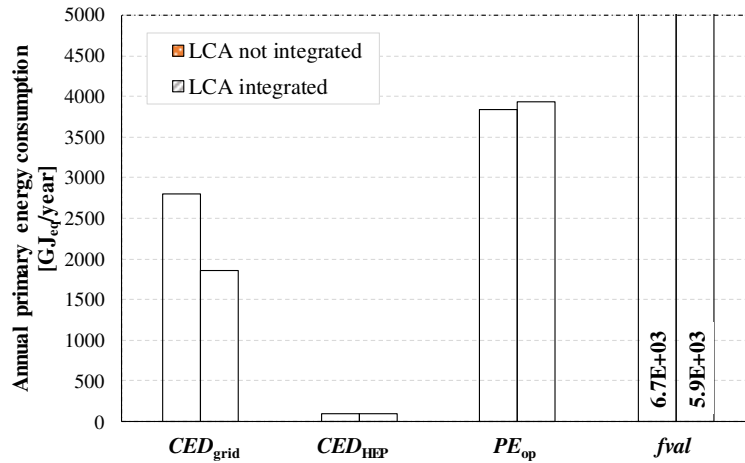
131

Fig.7.6. Contribution of the grid, HEP and operation phase to primary energy consumption.

Figures 7.7a through 7.7c show the production of thermal energy, cooling energy and electric energy from the different technologies, respectively. As can be noted from Fig. 7.7a, the system which fulfills most of the thermal energy demand is the CHP followed by the GSHP while ASHP and AB are not used for the production of thermal energy. By considering the case of "LCA integrated", the CHP produces about twice the thermal energy fulfilled by the same technology when LCA is not integrated into the optimization process. Indeed, about 40 % of the energy produced from the CHP (in the "LCA integrated" approach) is used to operate the ABS which is used to produce cooling energy. So, the integration of LCA makes the thermal energy to be met higher because, in addition to building thermal energy demand, the thermal energy required by the ABS also has to be fulfilled. But, even if the thermal energy demand is increased, the reversible GSHP is not used for the fulfillment of the thermal energy demand, while the thermal energy produced by the STC is lower because it is characterized by a smaller size.
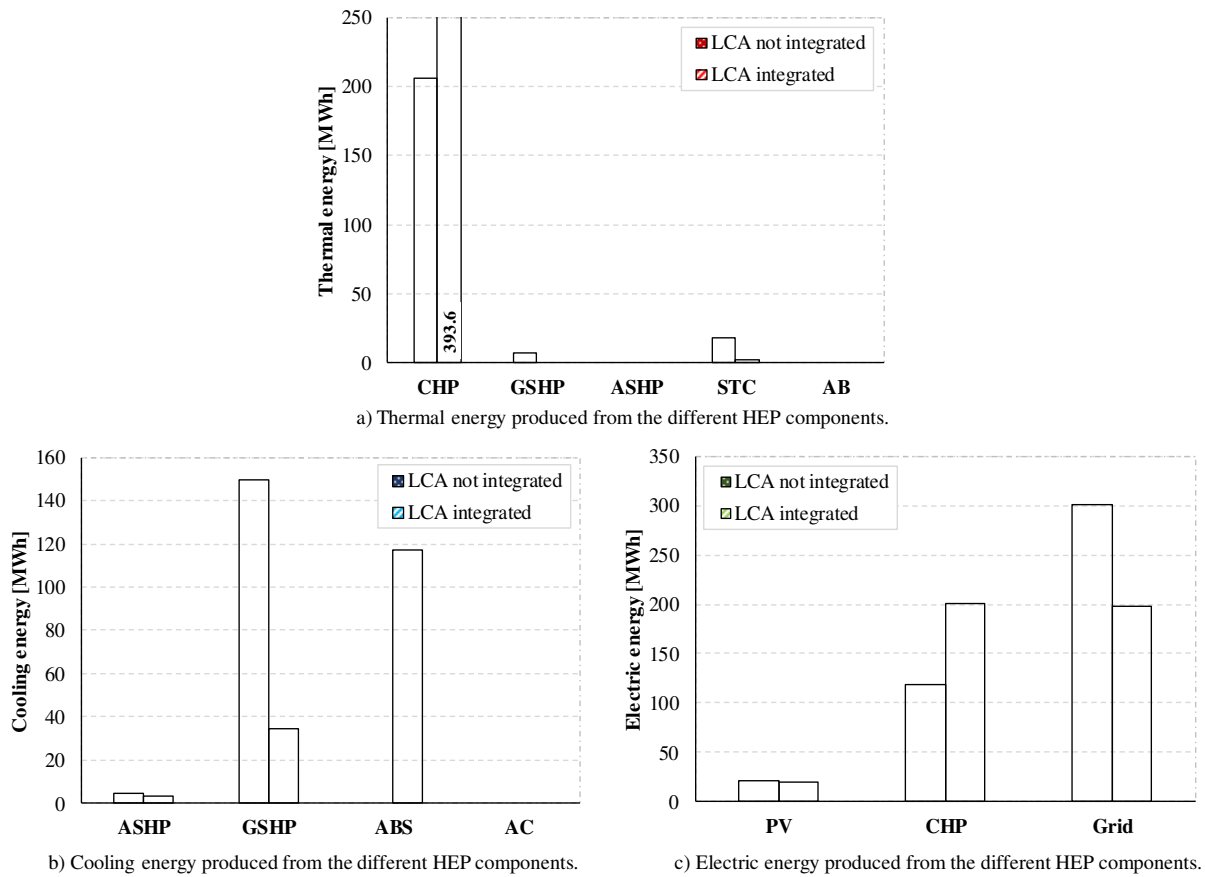
a) Thermal energy produced from the different HEP components.

b) Cooling energy produced from the different HEP components.

c) Electric energy produced from the different HEP components.

Fig. 7.7. Energy production from the different HEP components.

By analyzing the cooling energy production of the different systems, Fig. 7.7b shows that, if LCA is not integrated, the cooling energy demand is mostly fulfilled by the GSHP (about 90 %) followed by the ASHP (about 10 %), while the ABS is not used. However, by integrating LCA, most of the cooling energy demand is fulfilled by the ABS (about 68 %) followed by the GSHP unit which produces about 25 % of the energy produced by the same machine when LCA is not accounted for (Fig. 7.7b). As reported before when analyzing the thermal energy production of the "LCA integrated" approach, a certain amount of thermal energy produced by the CHP is used by the ABS which in turn fulfills a large portion of the cooling energy demand.

Figure 7.7c shows the electric energy produced by the PV, CHP system and the electricity taken from the grid for both approaches. The produced electricity is used to fulfill building electric demand and to operate the heat pumps. It can be seen that, by considering LCA into optimization, the solution identified by the GA tends to produce more electricity (and consequently more thermal energy) from the CHP system and tends to decrease the amount of electricity taken from the grid. This result is explained by the fact that the life cycle of the grid has a higher weight on the primary energy demanded throughout the life cycle (see Fig. 7.6). Moreover, by integrating LCA, the solution found by the algorithm tries to fulfill the cooling energy demand by using more heat driven technologies,

133

such as the ABS, and to limit the production of energy (both thermal and cooling energy) from the electricity driven technologies.

Figures 7.8 and 7.9 highlight how the HEP components are managed during a typical winter and summer day in order to meet the thermal and cooling energy demand. In Fig. 7.8, "Storage In" represents the energy produced by the CHP system and STC and stored in the storage, "Storage Out" stands for the stored energy used to meet the thermal energy demand, while "Storage State of Charge" is the thermal energy available in the storage. As can be noted from Figs. 7.8a and 7.8b, the integration of LCA affects the operational results of the different technologies comprising the HEP. In particular, when LCA is not integrated (Fig. 7.8a), the thermal energy demand is met by the STC, CHP system, GSHP and hot water storage. In particular, in each hour, the storage is the first system that contributes to meeting the thermal energy demand.

The CHP system is directly used to meet the demand, if the stored energy is not sufficient, and the excess thermal energy is stored. The GSHP is activated during peak hours when the stored energy and the CHP system are not able to meet the energy demand.

With regard to the "LCA integrated" approach (Fig. 7.8b), the same also applies here, i.e. the thermal energy demand is first met by the storage, supported by the CHP system and the STC. Instead, the GSHP is no longer used and the activation of electric driven technologies is avoided. In fact, the integration of LCA suggests increasing the size of both the CHP system and hot water storage. Consequently, the demand is fully met by these two technologies. For both approaches, the thermal demand met by the STC is negligible. However, when LCA is not integrated, the demand met by the STC is slightly higher, since the area of the STC is larger than in the case of the "LCA integrated" approach.

Figure 7.9 shows the contribution of each component to meet the cooling energy demand for the "LCA not integrated" approach (Fig. 7.9a) and "LCA integrated" approach (Fig.7.9b). When LCA is not integrated, the system which mostly contributes is the GSHP followed by the ASHP, while the ABS and AC are not used. This is mainly due to the fact that the GSHP requires lower energy consumption than ASHP and ABS. However, by integrating LCA (Fig. 7.9b), the rank of the different energy technologies is changed and the cooling demand is mostly met by the ABS. Furthermore, the GSHP and ASHP systems are used during peak loads or when cooling demand is lower than the minimum load of the ABS. This outcome confirms that, when LCA is integrated, it is advisable to first meet the cooling energy demand by using the CHP system coupled with the ABS.
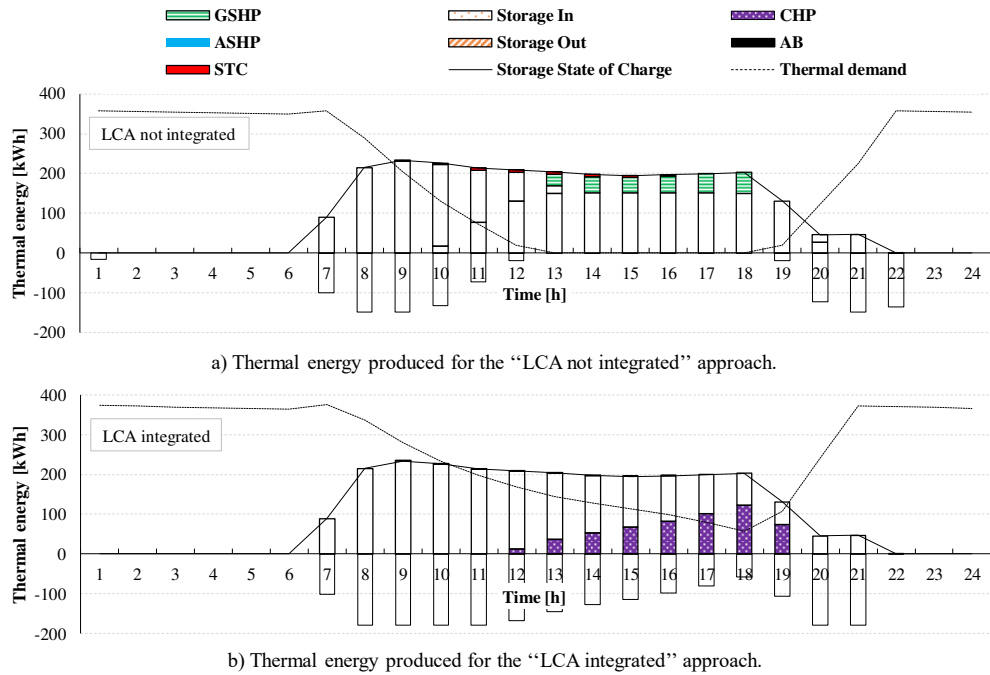
Fig.7.8. Contribution to thermal energy demand of the CHP system, GSHP, ASHP, STC, AB and storage during a winter day.
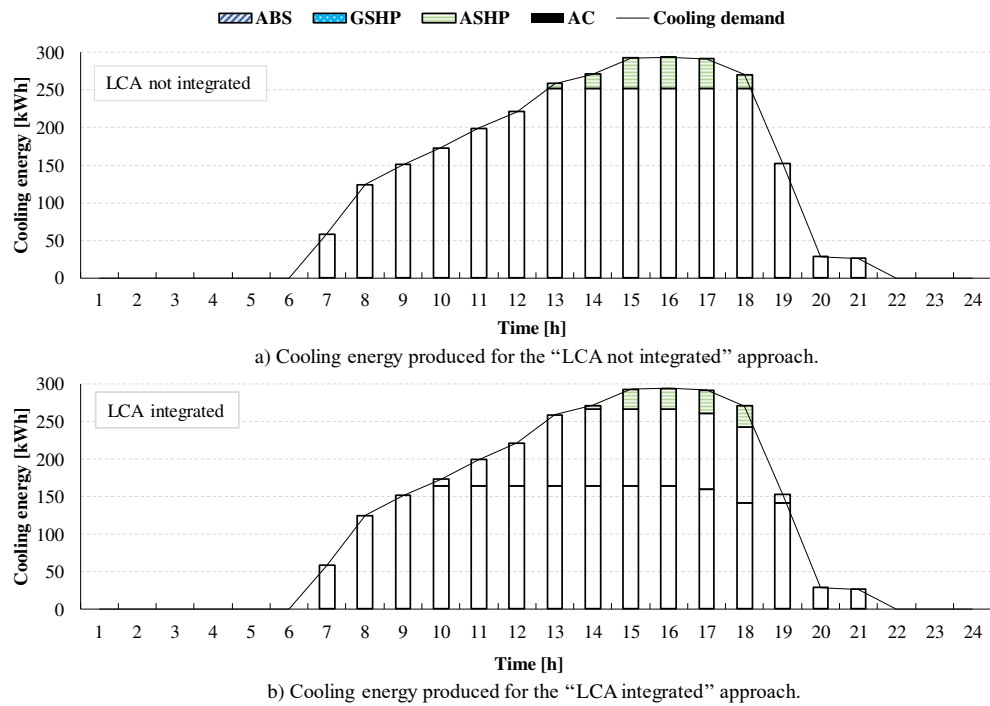

Fig.7.9. Contribution to cooling energy demand of ABS, GSHP, ASHP and AC during a summer day.

135

8. Conclusions and future work

In this research, original methods and guidelines for sizing and operating optimization of HEPs by accounting for on-site and off-site primary energy consumption were developed and applied. In particular, the HEPs considered may be composed of renewable and non-renewable energy systems and used for residential applications. Once that the concept of HEPs is introduced and the optimization models of HEPs used in literature and the challenge of integrating LCA into optimization are reviewed, original methods and procedures for the optimization of HEPs by accounting for the life cycle energy demand were developed and applied on a case study.

In this research, the topic of optimization of HEPs by accounting for the life cycle energy demand was divided into three connected parts. The first part treated the problem of optimization of HEPs by accounting for on-site primary energy consumption, the second part discussed the problem of quantification of off-site energy consumption associated with the life cycle of the HEP and the last part addressed the issue of optimization of HEPs by accounting for on-site and off-site primary energy consumption.

The first application presented a new general methodology for the optimization of sizing and operation of HEPs. The proposed methodology is based on the DP method. The study attempted to enlarge the use of DP techniques, which are mainly used for optimal control problems, by their application for both the sizing and operating optimization of HEPs. Since the aim of the first part is to optimize both size and operation, the proposed methodology may be applied on controllable technologies and for the optimization of exploitation of on-site energy resources. The developed optimization framework is successfully applied on a HEP which involves the employment of PV, STC, CHP, GSHP, ASHP, thermal storage and AB to fulfill the energy demands of a case study in winter and mid-season.

The superiority of the proposed method is demonstrated through a comparison with a traditional commonly used optimization method based on genetic algorithm. The optimal combinations of sizes found by the two methodologies are different. This is due to the different characteristics and working procedure of the genetic algorithm and dynamic programming. It may be that the objective function that is minimized has a shallow minimum around which many configurations are nearly equivalent.

Optimization results showed that the proposed method is superior and requires relatively lower computation time compared to a traditional method based on genetic algorithm. Moreover, compared to the genetic algorithm based method, the optimization method developed in this research allows

primary energy saving and computation time saving of about 5.3% and 41%, respectively. Compared to the consumption of a traditional plant composed of a boiler and the electric grid, the optimization model developed in this paper allows about 24.7% of energy saving to be achieved.

Moreover, compared to a traditional GA based method, the presented methodology proved to be more effective, easier to implement, computationally less expensive and also provides better results. The presented methodology may be used for the optimization of the controllable technologies involved in the HEP. Since renewable energy technologies are not controllable and are usually activated first, their optimization does not rely on energy criteria as applied in this research.

Successively, comprehensive LCA for technologies, such as STC, PV, CHP, ABS, ASHP, GSHP, PB and hot water storage which are widely used in residential applications, is carried out. The study applied an LCA methodology to evaluate the cumulative energy demand (CED) of the considered systems by taking into account scaling effects by means of a power law. The relevance of the proposed scaling approach is illustrated by the case of a pellet boiler and results show that power law scaling is by far more accurate than linear scaling, thus validating the assumption of power law scaling and its analogy with costs scaling. Further validation of the scaling procedure proposed in this paper was also conducted on other technologies and sizes available in the literature. The analyses carried out allow the following conclusions:

- The specific impact decreases when the size increases, i.e. the higher the size, the lower is the impact per unit of produced energy. This clearly demonstrates that linearization could dramatically over- or under- estimate the environmental impacts;

- The fact that components can be size-dependent or size-independent leads to a change of the contribution of the components to the total impact; this has relevant consequences on the reliability of LCA studies;

- By comparing the CHP system and PV with the same installed electric power, the total CED related to the production of the CHP is higher than the CED of the PV up to electric power of 10 kW, while the impact of the PV tends to be noticeably higher than the CHP for higher installed power;

- From the comparison between the CHP and the aggregate system composed of STC+PV, GSHP+PV and ASHP+PV, the option of producing electric and thermal energy by using a CHP unit is more convenient than the other options for sizes greater than 10 kW electric;

- For a given installed thermal power of the STC, GSHP and ASHP, the highest impact is related to the STC (with the exception of the case of 1 kW$_{th}$ power capacity). By comparing the GSHP and ASHP units, the results showed that GSHP systems are more environmentally friendly than ASHP systems for sizes larger than 100 kW$_{th}$.

The main achievements of the research are represented by:

- a scaling procedure, which can be adapted to other technologies and environmental impacts;

- impact curves of different technologies covering the range of power output suitable to residential users.

The scaling procedure and impact curves, which are novel in the literature, can be used for optimization purposes, to overcome the problem of lacking data and compare technologies of different capacities from a comprehensive point of view.

Finally, the last application addressed the problem of integration of LCA into design optimization and investigated the effect of considering the up-stream impacts on the optimal size of a hybrid energy plant. The work covered the evaluation of off-site primary energy consumption by using the LCA methodology, the challenge of LCA scaling of renewable and non-renewable energy technologies and the problem of integration of LCA in system design and optimization.

A methodology based on a genetic algorithm is used for the optimization of hybrid energy plants and two approaches were conducted in order to evaluate the influence of the integration of life cycle assessment on the optimal size and plant configuration. For both approaches ("LCA not integrated" and "LCA integrated"), the system which fulfills most of the thermal energy demand (more than 90 %) is the CHP system. If the life cycle assessment is not integrated, the cooling energy demand is mostly fulfilled by the ground source heat pump (about 90 %) followed by the air source heat pump (about 10 %), while the absorption chiller is not used. However, by integrating life cycle assessment, the thermal energy produced by the CHP system is almost doubled and about 40 % of the thermal energy produced by the CHP system is used to operate the absorption chiller which fulfills most of the cooling energy demand (about 68 %).

The life cycle of the grid has a major weight on the primary energy demanded throughout the life cycle, when considering life cycle assessment into optimization, the amount of electricity taken from the grid is decreased and more electricity is produced from the CHP. Moreover, by integrating the life cycle assessment, the cooling energy demand is fulfilled by using more heat driven technologies,

such as the absorption chiller, and the production of cooling energy from the electric driven technologies, such as the ground source heat pump and air source heat pump, is limited. Finally, when considering off-site primary energy consumption may lead to a different configuration of the hybrid energy plant and to higher primary energy saving (about 12 %); this in turn results in a lower depletion of energy resources and lower environmental impact.

This research provided general methods and guidelines for the design and optimization of HEPs by accounting for on-site and off-site primary energy consumption. The work covered the sizing and operating optimization of HEPs by accounting for only on-site primary energy consumption, the evaluation of off-site primary energy consumption by using the LCA methodology, the challenge of LCA scaling of renewable and non-renewable energy technologies and the problem of integration of LCA into system design and optimization. The proposed procedures and guidelines were also demonstrated by some case studies. These applications are novel in literature.

Future works that can be conducted in this field of research include the simultaneous optimization of the size and operation of HEPs by developing a one-step optimization method by taking into account on-site and off-site primary energy consumption or emissions. Different objective functions lead to different optimization results. Therefore, the selection of different objective functions, such as economy or environmental, can be of interest to investigate how the selection of a different objective function affects the sizing and operational results of the energy converters. A multi-objective function can also be adopted by combining in some manner more than one objective function. Moreover, given the number of optimization methods available in the literature, a further study on the best optimization algorithm, may be performed.

Furthermore, other energy technologies or systems under development may be modelled and integrated in the HEP and new configurations may be investigated. For instance, hybrid PV-STC solar collectors or other CHP configurations. In fact, instead of the use of an ICE based CHP, ORC engines, micro gas turbines or fuel cell technology may be considered in the HEP.

Another upgrade may concern the assessment of the end of life of the various technologies and the evaluation of the effect of the different disposal strategies, such as recycling, land filling and incineration, on LCA results. A future work may also interest LCA scaling by taking into account the disposal phase.

References

[1] Impact Assessment of Energy Efficiency Directive, SEC (2011) 779 del 22-06-2011.

[2] Direttiva 2009/29/CE del Parlamento Europeo e del Consiglio del 23 aprile 2009 sulla promozione dell'uso dell'energia da fonti rinnovabili, recante modifica e successiva abrogazione delle direttive 2001/77/CE e 2003/30/CE.

[3] Piano d'Azione Italiano per l'Efficienza Energetica (2011).

[4] Chwieduk D. Towards sustainable-energy buildings. Applied Energy, 76 (2003), pp. 211-217.

[5] Directive 2010/31/EU of the European Parliament and of the Council of 19 May 2010, "On the energy performance of buildings".

[6] Ogunjuyigbe A.S.O., Ayodele T.R., Akinola O.A. Optimal allocation and sizing of PV/Wind/Split-diesel/Battery hybrid energy system for minimizing life cycle cost, carbon emission and dump energy of remote residential building. Appl Energy, 171 (2016), pp. 153-171.

[7] Wu D.W., Wang R.Z. Combined cooling, heating and power: a review. Progress in Energy and Combustion Science, 32 (2006), pp. 459-95.

[8] Chicco G., Mancarella P. Distributed multi-generation: a comprehensive view. Renewable and Sustainable Energy Reviews, 13 (2009), pp. 535-551.

[9] Jing Y.-Y., Bai H., Wang J.-J. Multi-objective optimization design and operation strategy analysis of BCHP system based on life cycle assessment. Energy, 37 (1) (2012), pp. 405-416.

[10] Manwell J.F. Hybrid energy systems. In: Cleveland, C.J. (ed.), Encyclopedia of Energy, vol. 3, pp. 215-229, London (2004).

[11] Fabrizio E., Corrado V., Filippi M. A model to design and optimize multienergy systems in buildings at the design concept stage. Renewable Energy, 35 (2010), pp. 644-665.

[12] Sontag R., Lange A. Cost effectiveness of decentralized energy supply system taking solar and wind utilization plants into account. Renewable Energy, 28 (2003), pp. 1865-1880.

[13] Moghaddam I.G., Saniei M., Mashhour E. A comprehensive model for self-scheduling an energy hub to supply cooling, heating and electrical demands of a building. Energy, 94 (2016), pp. 157-170.

[14] Cozzolino R., Tribioli L., Bella G. Power management of a hybrid renewable system for artificial islands: A case study. Energy 106 (2016), pp. 774-789.

[15] Lee K.H., Lee D.W., Baek N.C., Kwon H.M., Lee C.J. Preliminary determination of optimal size for renewable energy resources in building using RET Screen. Energy, 47 (2012), pp. 83-96.

[16] Wu Q., Zhou J., Liu S., Yang X., Ren H. Multi-objective optimization of integrated renewable energy system considering economics and CO2 emissions. Energy Procedia, 104 (2016), pp. 15-20.

[17] Mancarella P. MES (multi-energy systems): An overview of concepts and evaluation models. Energy, 65 (2014), pp. 1-17.

[18] Dincer I., Zamfirescu C. Sustainable Energy Systems and Applications. Springer, New York (2011).

[19] Manwell, Hybrid energy system. In: Cleveland (ed.), Encyclopedia of Energy, London (2004), Vol.3 pp. 215-229.

[20] E. Fabrizio, V. Corrado, M. Filippi. A model to design and optimize multienergy systems in buildings at the design concept stage, Renew. Energy 35 (2010) 644-665.

[21] Shaopeng G., Qibin L., Jie S., Hongguan J. A review on the utilization of hybrid renewable energy. Renewable and Sustainable Energy Reviews, 91 (2018), pp. 1121-1147.

[22] Nayar C.V., Lawrance W.B., Phillips S.J. Solar/wind/diesel hybrid energy systems for remote areas. Proceedings of energy conversion engineering conference, Washington DC, USA, 6–11 August (1989).

[23] Markvart T. Sizing of hybrid photovoltaic-wind energy systems. Solar Energy, 57 (1996), pp. 277-281.

[24] Chasapis D., Drosou V., Papamechael I., Aidonis A., Blanchard R. Monitoring and operational results of a hybrid solar-biomass heating system. Renewable Energy, 33 (2008), pp. 1759-1767.

[25] Ozgener O., Hepbasli A. A review on the energy and exergy analysis of solar assisted heat pump systems. Renew Sust Energy Rev, 11 (2007), pp. 482-496.

[26] Prasartkaew B., Kumar S. Experimental study on the performance of a solar-biomass hybrid air-conditioning system. Renew Energy, 57 (2013), pp. 86-93.

[27] Servert J., San Miguel G., Lopez D. Hybrid solar-biomass plants for power generation; Technical and economic assessment. Global Nest Journal, 13 (2011), pp. 266-276.

[28] J. Soares A.C.O. Numerical simulation of a hybrid concentrated solar power/biomass mini power plant. Appl Therm Eng, 111 (2016), pp. 1378-1386.

[29] Barbieri E.S., Dai Y.J., Morini M., Pinelli M., Spina P.R., Sun P., Wang R.Z. Optimal sizing of a multi-source energy plant for power heat and cooling generation. Applied Thermal Engineering, 71 (2014), pp. 736-750.

[30] Hung-Cheng C. Optimum capacity determination of stand-alone hybrid generation system considering cost and reliability. Applied Energy, 103 (2013), pp. 155-164.

[31] Gonzalez A., Riba J., Rius A. Combined heat and power design based on environmental and cost criteria. Energy, 116 (2016), pp. 922-932.

[32] Yousefi H., Ghdusinejad M.H., Noorollahi Y. GA/AHP-based optimal design of a hybrid CCHP system considering economy, energy and emission. Energy and Buildings 138 (2017), pp. 309-317.

[33] Yu Z., Chen J., Sun Y., Zhang G. A GA-based system sizing method for net-zero energy buildings considering multi-criteria performance requirements under parameter uncertainties. Energy and Buildings, 129 (2016), pp. 524-534.

[34] Sharafi M., EL Mekkawi T.Y. Multi-objective optimal design of hybrid renewable energy systems using PSO-simulation based approach. Renewable Energy, 68 (2014), pp. 67-79.

[35] Wei F., Wu Q.H., Jing Z.X., Chen J.J., Zhou X.X. Optimal unit sizing for small-scale integrated energy systems using multi-objective interval optimization and evidential reasoning approach. Energy, 111 (2016), pp. 933-946.

[36] Shirazi A., Taylor R.A., Morrison G.L., White S.D. A comprehensive, multi-objective optimization of solar-powered absorption chiller systems for air-conditioning applications. Energy Conversion and Management, 132 (2017), pp. 281-306.

[37] Marano V., Rizzo G., Tiano F.A. Application of dynamic programming to the optimal management of a hybrid power plant with wind turbines, photovoltaic panels and compressed air energy storage. Applied Energy, 97 (2012), pp. 849–859.

[38] Bianchi M., Branchini L., Cavina N., Cerofolini A., Corti E., De Pascale A., Orlandini V., Melino F., Moro D., Peretto A., Ponti F. Managing wind variability with pumped hydro storage and gas turbines. Energy Procedia, 45 (2014), pp. 22-31.

[39] Facci A.L., Andreassi L., Ubertini S. Optimization of CHCP (combined heat power and cooling) systems operation strategy using dynamic programming. Energy, 66 (2014), pp. 387–400.

[40] Wang H., Yin W., Abdollahi E., Lahdelma R., Jiao W. Modelling and optimization of CHP based district heating system with renewable energy production and energy storage. Applied Energy, 159 (2015), pp. 401-421.

[41] Ondeck A.D., Edgar T.F., Baldea M. Optimal operation of a residential district-level combined photovoltaic/natural gas power and cooling system. Applied Energy, 156 (2015), pp. 593-606.

[42] Carpaneto E., Lazzeroni P., Repetto M. Optimal integration of solar energy in a district heating network. Renewable Energy, 75 (2015), pp. 714-721.

[43] Ju L., Tan Z., Li H., Tan Q., Yu X., Song X. Multi-objective operation optimization and evaluation model for CCHP and renewable energy based hybrid energy system driven by distributed energy resources in China. Energy, 11 (2016), pp. 322-340.

[44] Sakawa M., Kato K., Ushiro S. Operational planning of district heating and cooling plants through genetic algorithms for mixed 0–1 linear programming. European Journal of Operational Research, 137 (2002), pp. 677-687..

[45] Evins R. Multi-level optimization of building design, energy system sizing and Operation. Energy 90 (2015), pp. 1775-1789.

[46] Fazlollahi S., Mandel P., Becker G., Maréchal F. Methods for multi-objective investment and operating optimization of complex energy systems. Energy, 45 (2012), pp. 12-22.

[47] Morvaj B., Evins R., Carmeliet J. Optimizing urban energy systems: Simultaneous system sizing, operation and district heating network layout. Energy, 116 (2016), pp. 619-636.

[48] N. Destro, A. Benato, A. Stoppato, A. Mirandola. Components design and daily operation optimization of a hybrid system with energy storages. Energy, 117 (2016), pp. 569-577.

[49] Stoppato A., Benato A., Destro N., Mirandola A. A model for the optimal design and management of a cogeneration system with energy storage. Energy and Buildings, 124 (2016), pp. 241-247.

[50] Messac A. Optimization in Practice with MATLAB®. Cambridge University Press, (2015).

[51] Lew A., Mauch H. Introduction to Dynamic Programming, Springer. Studies in Computational Intelligence, 38 (2007), pp. 3–43.

[52] Bravo R., Friedrich D. Two-stage optimization of hybrid solar power plants. Solar Energy, 164 (2018), pp. 187-199.

[53] Feng Z., Niu W., Cheng C., Wu X. Optimization of hydropower system operation by uniform dynamic programming for dimensionality reduction. Energy, 134 (2017), pp. 718-730.

[54] Varun, Bhat I.K., Prakash R. LCA of renewable energy for electricity generation systems - A review. Renewable and Sustainable Energy Reviews, 13 (2009); pp. 1067-1073.

[55] ISO 14040. Environmental Management – Life Cycle Assessment – Principles and Framework, (1997).

[56] Patel M. Cumulative energy demand (CED) and cumulative CO_2 emissions for products of the organic chemical industry. Energy, 28 (2003), pp. 721-740.

[57] Huijbregts M.A.J., Hellweg S., Frischknecht R., Hendriks H.W.M., Hungerbuhler K., Hendriks A.J. Cumulative energy demand as predictor for the environmental burden of commodity production. Environmental Science and Technology. 44 (2010), pp. 2189-2196.

[58] Klopffer W. In defense of the cumulative energy demand. Int. J. LCA, Editorial, (1997).

[59] Frischknecht R., Wyss F., Knopfel S.B., Lutzkendorf T., Balouktsi M. Cumulative energy demand in LCA: the energy harvested approach. International Journal of LCA, 20 (2015), pp. 957-969.

[60] Frischknecht R., Heijungs R., Hofstetter P. Einstein's lessons for energy accounting in LCA. International Journal of LCA, 5 (1998), pp. 266-272.

[61] Mirò L., Orò E., Boer D., Cabeza L.F. Embodied energy in thermal energy storage (TES) systems for high temperature applications. Applied Energy, 137 (2015), pp. 793-799.

[62] Huijbregts M.A.J., Rombouts L.J.A., Hellweg S., Frischknecht R., Jan Hendriks A., Van De Meent D., Ragas M.J., Reijnders L., Struijs J. Is cumulative fossil energy demand a useful indicator for the environmental performance of products? Environmental Science and Technology, 40 (2006), pp. 3.

[63] Moore A.D., Urmee T., Bahri P.A., Rezvani S., Baverstock G.F. Life cycle assessment of domestic hot water systems in Australia. Renew Energ, 103 (2017), pp. 187-196.

[64] Colclough S., McGrath T. Net energy analysis of a solar combi system with seasonal thermal energy store. Appl Energy, 147 (2015), pp. 611-616.

[65] Gurzenich D., Mathur J., Bansal N.K., Wagner H.J. Cumulative energy demand for selected renewable energy technologies. International Journal of LCA, 3 (1999), pp. 143-149.

[66] Xu L., Pang M., Zhang L., Poganietz W.-R., Marathe S.D. Life cycle assessment of onshore wind power systems in China. Resour Conserv Recy, 132 (2018), pp. 361-368.

[67] Huang Y.F., Gan X.J., Chiueh P.T. Life cycle assessment and net energy analysis of offshore wind power systems. Renewable Energy, 102 (2017), pp. 98-106.

[68] Wagner H.J., Pick E. Energy yield ratio and cumulative energy demand for wind energy converters. Energy, 29 (2004), pp. 2289-2295.

[69] Mert G., Linke B.S., Aurich J.C. Analyzing the cumulative energy demand of product-service systems for wind turbines. Procedia CIRP, 59 (2017), pp. 214-219.

[70] Whiting A., Azapagic A. Life cycle environmental impacts of generating electricity and heat from biogas produced by anaerobic digestion. Energy. 70 (2014), pp. 181-193.

[71] Staffell I., Ingram A. Life cycle assessment of an alkaline fuel cell CHP system. International Journal of Hydrogen Energy, 35 (2010), pp. 2491-2505.

[72] Kelly K.A., McManus M.C., Hammond G.P. An energy and carbon life cycle assessment of industrial CHP (combined heat and power) in the context of a low carbon UK. Energy, 77 (2014), pp. 812-821.

[73] Ardente F., Beccali G., Cellura M., Lo Brano V. Life cycle assessment of a solar thermal collector: sensitivity analysis, energy and environmental balances. Renewable Energy, 30 (2005), pp. 109-130.

[74] Longo S., Palomba V., Beccali M., Cellura M., Vasta S. Energy balance and life cycle assessment of small size residential solar heating and cooling systems equipped with adsorption chillers. Solar Energy, 158 (2017), pp. 543-558.

[75] Comodi G., Bevilacqua M., Caresana F., Paciarotti C., Pelagalli L., Venella P. Life cycle assessment and energy-CO_2-economic payback analyses of renewable domestic hot water systems with unglazed and glazed solar thermal panels. Appl Energy, 164 (2016), pp. 944-955.

[76] Nishimura A., Hayashi Y., Tanaka K., Hirota M., Kato S., Ito M., Araki K., Hu E.J. Life cycle assessment and evaluation of energy payback time on high-concentration photovoltaic power generation system. Applied Energy, 87 (2010), pp. 2797-2807.

[77] Fu Y., Liu X., Yuan Z. Life-cycle assessment of multi-crystalline photovoltaic (PV) systems in China. Journal of Cleaner Production, 86 (2015), pp. 180-190.

[78] Kabakian V., McManus M.C., Harajli H. Attributional life cycle assessment of mounted 1.8 kWp monocrystalline photovoltaic system with batteries and comparison fossil energy production system. Appl Energy, 154 (2015), pp. 428-437.

[79] Desideri U., Proietti S., Zepparelli F., Sdringola P., Bini S. Life cycle assessment of a ground-mounted 1778 kWp photovoltaic plant and comparison with traditional energy production systems. Appl Energy, 97 (2012), pp. 930-943.

[80] Koroneos C.J., Nanaki E.A. Environmental impact assessment of a ground source heat pump system in Greece. Geothermics, 65 (2017), pp. 1-9.

[81] Huang B., Mauerhofer V. Life cycle sustainability assessment of ground source heat pump in Shanghai, China. Journal of Cleaner Production, 119 (2016), pp. 207-214.

[82] Keoleian G.A., Menerey D. Life cycle design guidance manual. Environmental requirements and the product system. Final report (1993).

[83] Keoleian G.A. The application of life cycle assessment to design. J Clean Prod, 1 (3-4) (1993), pp. 143-149.

[84] Gasafi E., Meyer L., Schebek L. Using life-cycle assessment in process design: Supercritical water gasification of organic feedstocks. J Ind Ecol, 7 (3-4) (2004), pp. 75-91.

[85] Lu B., Gu P., Spiewak S. Integrated life cycle design approach for sustainable product development. Proceedings of the Canadian Engineering Education Association, 2011, doi:10.24908/pceea.v0i0.3990.

[86] Stefanis S.K., Livingston A.G., Pistikopoulos E.N. Minimizing the environmental impact of process plants: A process systems methodology. Comput Chem Eng, 19 (1995), pp. 39-44.

[87] Kniel G., Delmarco K., Petrie J. Life cycle assessment applied to process design: Environmental and economic analysis and optimization of a nitric acid plant. Environmental Progress, 15 (1996), pp. 221–228.

[88] Mann M.K., Spath P.L., Craig K. R. Economic and life-cycle assessment of an integrated biomass gasification combined cycle system. 31st Intersociety Energy Conversion Engineering Conference, (1996).

[89] Azapagic A., Clift R. The application of life cycle assessment to process optimization. Computers and Chemical Engineering, 23 (1999), pp. 1509–1526.

[90] Dufo-Lòpez R., Bernal-Agustìn J.L., Yusta-Loyo J.M., Domìnguez-Navarro J.A., Ramìrez-Rosado I.J., Lujano J., Aso I. Multi-objective optimization minimizing cost and life cycle emissions of stand-alone PV-wind-diesel systems with batteries storage. Applied Energy, 88 (2011), pp. 4033-4041.

[91] Caduff M., Huijbregts M.A.J., Althaus H.-J., Hendriks A.J. Power-law relationships for estimating mass, fuel consumption and costs of energy conversion equipments. Environ Sci Technol, 45 (2) (2011), pp. 751-754.

[92] Moore, F. T. Economies of scale: Some statistical evidence. Q. J. Econ. 1959; 73 (2): 232–245.

[93] Gerber L., Gassner M., Maréchal F. Systematic integration of LCA in process systems design: Application to combined fuel and electricity production from lignocellulosic biomass. Comput Chem Eng, 35 (7) (2011), pp. 1265-1280.

[94] Lantz M. The economic performance of combined heat and power from biogas produced from manure in Sweden - A comparison of different CHP technologies. Appl Energy, 98 (2012), pp. 502-511.

[95] Eicker U., Pietrushka D. Design and performance of solar powered absorption cooling system in office buildings. Energ Buildings, 41 (2009), pp. 81-91.

[96] Gavagnin G., Sanchez D., Matinez G.S., Rodriguez J.M., Munoz A. Cost analysis of solar thermal power generators based on parabolic dish and micro gas turbine: Manufacturing, transportation and installation. Applied Energy, 194 (2017), pp:108-122.

[97] Caduff M., Huijbregts M.A.J., Althaus H.-J., Koehler A., Hellweg S. Wind power electricity: The bigger the turbine, the greener the electricity? Environ Sci Technol, 46 (9) (2012), pp. 4725-4733.

[98] M. Caduff, M. A.J. Huijbregts, A. Koehler, H.J. Althaus, S. Hellweg. Scaling Relationships in Life Cycle Assessment: The case of heat production from biomass and heat pumps. Journal of Industrial Ecology. 2014; 18:393–406.

[99] Caduff M., Huijbregts M.A.J., Althaus H.-J., Hendriks A.J. Power-law relationships for estimating mass, fuel consumption and costs of energy conversion equipments. Environ Sci Technol, 45 (2) (2011), pp. 751-754.

[100] Bauman H., Tillman A.M. The Hitch Hiker's Guide to LCA - An orientation in life cycle assessment methodology and application. The authors and Studentlitteratur (2004).

[101] Tiwari G.N., Tiwari A.S. Flat plate collectors. In: Handbook of Solar Energy. Energy Systems in Electrical Engineering, Springer, Singapore, (2016).

[102] Gish T.K., Prelas M.A. Evacuated tube collectors. In: Energy Resources and Systems. Springer, Dordrecht, (2011).

[103] Cabrera F.J., Fernández-García A., Silva R.M.P., Pérez-García M. Use of parabolic trough solar collectors for solar refrigeration and air-conditioning applications. Renewable and Sustainable Energy Reviews, 20 (2013), pp. 103-118.

[104] Breeze P. Power Generation Technologies (Second Edition). Newnes, (2014), pp. 259-286.

[105] Rubini L., Sangiorgio S. Le energie rinnovabili. Hoelpi, Milano (2012).

[106] Beith R. Small and micro combined heat and power (CHP) systems: advanced design, performance, materials and applications. UK: Woodhead Publishing (2011).

[107] Deethayat T., Kiatsiriroat T., Thawonngamyingsakul C. Performance analysis of an organic Rankine cycle with internal heat exchanger having zeotropic working fluid. Case Studies in Thermal Engineering, 6 (2015), pp. 155-161.

145

[108] Barbieri E.S. Sviluppo di un modello per il dimensionamento ottimizzato di sistemi multienergia per soddisfacimento dei fabbisogni energetici dell'edificio. PhD Thesis, (2014).

[109] Petchers N. Combined heating, cooling and power handbook: technologies and application: an integrated approach to energy conservation/resource optimization. USA: The Fairmont (2003).

[110] Libro bianco sulle pompe di calore. COAER (2008).

[111] Hasnain S.M. Review on sustainable thermal energy storage technologies, Part 1: heat storage materials and techniques. Energy Conservation and Management, 39 (1998), pp. 1127-1138.

[112] Bellman R.E., Dynamic Programming, Princeton University Press, NJ, 1957.

[113] Bertsekas D.P. Dynamic Programming and Optimal Control, Athena Scientific, Belmont, Massachusetts, Vol. 1, 3rd edition, 2005.

[114] Chen X.P., Hewitt N., Li Z.T., Wu Q.M., Yuan X., Roskilly T. Dynamic programming for optimal operation of a biofuel micro CHP-HES system. Applied Energy, 208 (2017), pp. 132-141.

[115] Cocco D., Palomba C., Puddu P. Tecnologie delle energie rinnovabili. SG Editoriali, Padova (2008).

[116] Saleh H.E. Effect of variation in LPG composition on emissions and performance in a dual fuel diesel engine. Fuel, 87 (2008), pp. 3031-3039.

[117] Waddicor D.A., Fuentes E., Azar M., Salom J. Partial load efficiency degradation of a water-to-water heat pump under fixed set-point control. Applied Thermal Engineering, 106 (2016), pp. 275-285.

[118] Steen D., Stadler M., Cardoso G., Groissbock M., De Forest N., Marnay C. Modeling of thermal storage systems in MILP distributed energy source models. Applied Energy, 137 (2015), pp. 782-792.

[119] Chinnek,J.W., 2001, Practical Optimization: a Gentle Introduction,

[120] Sundstrom O., Guzzella L. A Generic Dynamic Programming Matlab Function. In Proceedings of the 18th IEEE International Conference on Control Applications, Saint Petersburg, Russia, 2009, pp. 1625-1630,

[121] Commission decision 2007/74/EC, Off. J. Eur. Union (2006).

[122] Ministero Sviluppo Economico, Decreto Ministeriale DM 4/08/2011 (In Italian).

[123] Barbieri E.S., Morini M., Munari E., Pinelli M., Spina P.R., Vecci R. Concurrent optimization of size and switch-on priority of a multi-source energy system for a commercial building application. Energy Procedia, 81 (2015), pp. 45-54.

[124] Holland J.H. Adaption in Natural and Artificial System, University of Michigan Press, Ann Arbor, 1975.

[125] Peacock A.D., Newborough M. Impact of micro-CHP systems on domestic sector CO2 emissions. Appl. Therm Eng, 25 (2005), pp. 2653-2676.

[126] Ente Italiano di Normazione, UNI 8477-2 (1985) (In Italian).

[127] ISO 14044: 2006. Environmental management – life cycle assessment – requirements and guidelines.

[128] Bahlawan H., Morini M., Pinelli M., Poganietz W.R., Spina P.R., Venturini M. Optimal design of a hybrid energy plant by accounting for the cumulative energy demand. ICAE, 22-25 August 2018, Hong Kong, China. Paper 715.

[129] EMPA. EcoInvent. Switzerland: EcoInvent; 2007.

[130] OpenLCA 1.6.3, GreenDelta.

[131] Ulrich G. D. A guide to chemical engineering process design and economics. New York, Wiley (1996).

[132] Jungbluth, N. 2007: "Sonnenkollektor-Anlagen." In Dones, R. (Ed.) et al., Sachbilanzen von Energiesystemen: Grundlagen für den ökologischen Vergleich von Energiesystemen und den Einbezug von Energiesystemen in Ökobilanzen für die Schweiz. ecoinvent report No. 6-XI, Swiss Centre for Life Cycle Inventories, Dübendorf, CH.

[133] Jungbluth N., Stucki M. and Frischknecht R. (2009) Photovoltaics. In Dones, R. (Ed.) et al., Sachbilanzen von Energiesystemen: Grundlagen für den ökologischen Vergleich von Energiesystemen und den Einbezug von Energiesystemen in Ökobilanzen für die Schweiz. Swiss Centre for Life Cycle Inventories, Dübendorf, CH, 2009.

[134] Heck T. (2007) Wärme-Kraft-Kopplung. In: Dones, R. (Ed.) et al., Sachbilanzen von Energiesystemen: Grundlagen für den ökologischen Vergleich von Energiesystemen und den Einbezug von Energiesystemen in Ökobilanzen für die Schweiz. Final report ecoinvent No. 6-XIV, Paul Scherrer Institut Villigen, Swiss Centre for Life Cycle Inventories, Dübendorf, CH. Online: www.ecoinvent.ch.

[135] Heck T. (2007) Wärmepumpen. In: Dones, R. (Ed.) et al., Sachbilanzen von Energiesystemen: Grundlagen für den ökologischen Vergleich von Energiesystemen und den Einbezug von Energiesystemen in Ökobilanzen für die Schweiz. Final report ecoinvent No. 6-X, Paul Scherrer Institut Villigen, Swiss Centre for Life Cycle Inventories, Dübendorf, CH. Online: www.ecoinvent.ch

[136] Primas A. (2007) Life Cycle Inventories of new CHP systems. ecoinvent report No. 20. Swiss Centre for Life Cycle Inventories, B&H AG, Dübendorf and Zurich, 2007.

[137] Eicker U., Pietrushka D. Design and performance of solar powered absorption cooling system in office buildings. Energ Buildings, 41 (2009), pp. 81-91.

[138] Chiesa M., Monteleone B., Venuta M.L., Maffeis G., Greco S., Cherubini A., Schmidl C., Finco A., Gerosa G., Ballarin Denti A. Integrated study through LCA, ELCC analysis and air quality modelling related to the adoption of high efficiency small scale pellet boilers. Biomass and Bioenergy, 90 (2016), pp. 262-272.

[139] Cellura M., La Rocca V., Longo S., Mistretta M. Energy and environmental impacts of energy related products (ErP): a case study of biomass-fuelled systems. Journal of Cleaner Production, 85 (2014), pp. 359-370.

[140] Bauer, C. (2007) Holzenergie. In: Dones, R. (Ed.) et al., Sachbilanzen von Energiesystemen: Grundlagen für den ökologischen Vergleich von Energiesystemen und den Einbezug von Energiesystemen in Ökobilanzen für die Schweiz. Final report ecoinvent No. 6-IX, Paul Scherrer Institut Villigen, Swiss Centre for Life Cycle Inventories, Dübendorf, CH.

[141] Beccali M., Cellura M., Longo S., Nocke B., Finocchiaro P. LCA of a solar heating and cooling system equipped with a small water-ammonia absorption chiller. Solar Energy, 86 (2012), pp. 1491-1503.

[142] Beccali M., Cellura M., Longo S., Guarino F. Solar heating and cooling systems versus conventional systems assisted by photovoltaic: Application of a simplified LCA tool. Solar Energy Materials and Solar Cells, 92 (2016), pp. 92-100.

[143] Gurzenich D., Wagner H.J. Cumulative energy demand and cumulative emissions of photovoltaics production in Europe. Energy, 29 (2004), pp. 2297-2303.

[144] Ziviani, D., Beyene, A., Venturini, M., Advances and Challenges in ORC Systems Modeling for Low Grade Thermal Energy Recovery, Appl Energy, 121 (2014), pp. 79-95.

[145] Zamora M., Bourouis M., Caronas A., Vallès M. Part-load characteristics of a new ammonia/lithium nitrate absorption chiller. Int J Refrig, 56 (2015), pp. 43-51.

[146] Seo B.M., Lee K.H. Detailed analysis on part load ratio characteristics and cooling energy saving of chiller staging in an office building. Energ Buildings, 119 (2016), pp. 309-322.

[147] Ente Italiano di Normazione, UNI TS 11300, 2012, In Italian.

[148] Ente Italiano di Normazione, UNI 10349, 2016, In Italian.

[149] Vio M. Impianti di cogenerazione. Editoriale Delfino (2007).

Università degli Studi di Ferrara

Sezioni

Dottorati di ricerca

Il tuo indirizzo e-mail

> bhlhll@unife.it

Oggetto:

> Dichiarazione di conformità della tesi di Dottorato

Io sottoscritto Dott. (Cognome e Nome)

> Bahlawan Hilal

Nato a:

> Tripoli

Provincia:

> Libano

Il giorno:

> 18-12-1989

Avendo frequentato il Dottorato di Ricerca in:

> Scienze dell'Ingegneria

Ciclo di Dottorato

> 31

Titolo della tesi:

> OPTIMIZATION OF HYBRID ENERGY PLANTS BY ACCOUNTING FOR LIFE CYCLE ENERGY DEMAND

Titolo della tesi (traduzione):

> Ottimizzazione di sistemi energetici ibridi mediante la valutazione del consumo di energia primaria durante il ciclo di vita

Tutore: Prof. (Cognome e Nome)

> Spina Pier Ruggero

Settore Scientifico Disciplinare (S.S.D.)

> ING-IND/09

Parole chiave della tesi (max 10):

> Dynamic Programming; Energy consumption; GA optimization; Hybrid energy plant; LCA.

Consapevole, dichiara

> CONSAPEVOLE: (1) del fatto che in caso di dichiarazioni mendaci, oltre alle sanzioni previste dal codice penale e dalle Leggi speciali per l'ipotesi di falsità in atti ed uso di atti falsi, decade fin dall'inizio e senza necessità di alcuna formalità dai benefici conseguenti al provvedimento emanato sulla base di tali dichiarazioni; (2) dell'obbligo per l'Università di provvedere al deposito di legge delle tesi di dottorato al fine di assicurarne la conservazione e la consultabilità da parte di terzi; (3) della procedura adottata dall'Università di Ferrara ove si richiede che la tesi sia consegnata dal dottorando in 2 copie, di cui una in formato cartaceo e una in formato pdf non modificabile su idonei supporti (CD-ROM, DVD) secondo le istruzioni pubblicate sul sito : http://www.unife.it/studenti/dottorato alla voce ESAME FINALE – disposizioni e modulistica; (4) del fatto che l'Università, sulla base dei dati forniti, archivierà e renderà consultabile in rete il testo completo della tesi di dottorato di cui alla presente dichiarazione attraverso l'Archivio istituzionale ad accesso aperto "EPRINTS.unife.it" oltre che attraverso i Cataloghi delle Biblioteche Nazionali Centrali di Roma e Firenze. DICHIARO SOTTO LA MIA RESPONSABILITA': (1) che la copia

della tesi depositata presso l'Università di Ferrara in formato cartaceo è del tutto identica a quella presentata in formato elettronico (CD-ROM, DVD), a quelle da inviare ai Commissari di esame finale e alla copia che produrrà in seduta d'esame finale. Di conseguenza va esclusa qualsiasi responsabilità dell'Ateneo stesso per quanto riguarda eventuali errori, imprecisioni o omissioni nei contenuti della tesi; (2) di prendere atto che la tesi in formato cartaceo è l'unica alla quale farà riferimento l'Università per rilasciare, a mia richiesta, la dichiarazione di conformità di eventuali copie. PER ACCETTAZIONE DI QUANTO SOPRA RIPORTATO

Dichiarazione per embargo

12 mesi

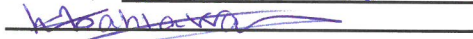Richiesta motivata embargo

1. Tesi in corso di pubblicazione

Liberatoria consultazione dati Eprints

Consapevole del fatto che attraverso l'Archivio istituzionale ad accesso aperto "EPRINTS.unife.it" saranno comunque accessibili i metadati relativi alla tesi (titolo, autore, abstract, ecc.)

Firma del dottorando

Ferrara, li 15-03-2019 _____ (data) Firma del Dottorando

Firma del Tutore

Visto: Il Tutore Si approva Firma del Tutore _____